universität wien

MASTERARBEIT / MASTER'S THESIS

Titel der Masterarbeit / Title of the Master's Thesis

„Response of phytoplankton and zooplankton to the Glacial – Interglacial cycles over the last 300 ka“

verfasst von / submitted by

Yaroslav Zechner, BSc

angestrebter akademischer Grad / in partial fulfilment of the requirements for the degree of

Master of Science (MSc)

Wien, 2024 / Vienna 2024

Studienkennzahl lt. Studienblatt / degree programme code as it appears on the student record sheet:	UA 066 815
Studienrichtung lt. Studienblatt / degree programme as it appears on the student record sheet:	Masterstudium Erdwissenschaften UG2002
Betreut von / Supervisor:	Univ.-Prof. Dr. Petra Heinz

Acknowledgements

This project would have been impossible without the support and help I was given during all these years. I would like to thank Univ.-Prof. Dr. Petra Heinz for many years of working together, from my bachelor thesis, study assistant and tutor in Micropaleontology class to my master thesis. I would also like to express my gratitude for introducing me into foraminifera world and all the support I gained working on this project.

I would also like to express my gratitude to Prof. Michal Kucera, who entrusted me this project, welcomed me at MARUM in Bremen, trained me and helped with identification of planktonic foraminifera species and supported me with interesting and insightful discussions and comments.

For helping me with core sampling, statistical analysis, coding in R, supporting the ongoing project through discussions, comments, and corrections, I would like to thank Dr. Lukas Jonkers. Without his support, this thesis would never come an end. Moreover, I would like to thank Dr. Tonke Strack, who helped me with core sampling, coding in R, literature research and helped me navigating through an Ocean of α- and β-diversity indices.

I would also like to thank Birgit Lübben, who helped me out in the lab and sample preparation. Without her help, it would have been impossible to obtain reasonable results.

For helping me with Keyence microscope I would also like to thank Dr. Michael Siccha, who gave me instructions on how to use it. Furthermore, I would like to thank Dr. Jeroen Groeneveld who provided updated $\delta^{18}O$ values. I would also like to thank Petra Witte for helping with Scanning Electron Microscope photographs and Dr. Deborah Tangunan for providing coccolith microphotographs. Many thanks to Dr. Kanchan Dasgupta, who reviewed and corrected my writing.

I would like to thank my university colleagues from Bremen and Vienna. I will never forget our field trips, *Stammtische*, legendary Barbara parties, lab classes, boring lectures, and the joy of passing difficult exams together.

Finally, and most importantly, I would like to thank my wife and love Alisa for all the given love and support during all these years. Thank you, I love you.

Abstract

The western Indian Ocean accommodates one of the largest concentrations of phytoplankton blooms, which is an essential part of the global marine food web and an important element in supporting local fisheries. Overfishing and the development of coastal areas have accelerated the long-term alterations in biological productivity, resulting in decreased abundance and biodiversity of marine organisms. In addition to significant overfishing, the western tropical Indian Ocean has experienced the most substantial long-term increase in sea surface temperatures over the last century, as a result of global warming. As a consequence, anthropogenic pressure and global climate change have resulted in the reduction of biological diversity, increasing threats to species, and altering ecosystem functions. Recent studies show that biodiversity across various ecosystems and organisms is already affected by climate change. Biodiversity change includes restructuring of species assemblages through local extinctions, colonizations, habitat tracking, and adaptations. However, the consequences of these shifts for community resilience and ecosystem functioning remain unclear and analysis of long-term data are required in order to improve our understanding of temporal α- and β-diversity changes.

The sediment core GeoB12613-1 provides extensive insights into the biodiversity dynamics of phyto- and zooplankton over the last two glacial – interglacial cycles in the western Indian Ocean. In this study we conducted micropaleontological and statistical analysis of the sediment core on temporal α- and β-diversities of coccolithophores and planktonic foraminifera: 1) We used principal components analysis in order to analyse species assemblages and their temporal changes. Subsequently, we correlated principal components with the highest explained variance with $\delta^{18}O$ and estimated paleoproductivity values, in order to understand the distribution pattern and distribution mechanisms of those assemblages in relation to global temperature changes and productivity. 2) We computed Hill – Shannon index, Pielou Evenness index and Morisita – Horn overlap measure to evaluate temporal α-diversity and temporal β-diversity respectively. Subsequently, we compared their rates of change through time based on the linear regression model and compared their trends with contemporary observations. 3) We compared temporal turnover rates of both functional groups in order to test the hypothesis that temporal turnover varies with the trophic level and the rate of life cycles.

Our study shows that planktonic foraminifera and coccolithophores species are affected by different environmental parameters. Planktonic foraminifera species indicate strong relationship with $\delta^{18}O$ values, indicating that they were predominantly influenced by global climate changes. Coccolithophores species indicate very weak relationship with $\delta^{18}O$ values, suggesting that species assemblages were not directly influenced by global climate changes. Instead, we found strong relationship with paleoproductivity estimates indicating that coccolithophores assemblages were predominantly influenced by productivity dynamics. Analysis of temporal α- and β-diversities revealed that coccolithophores species show almost stationary temporal α-diversity, with notable temporal compositional changes. On the other hand, temporal α- and β-diversities of planktonic foraminifera did not show substantial variations in their rates of change. One explanation could be, that contemporary temporal β-diversity is affected by anthropogenic forcing thus exhibiting higher rates of turnover. On the contrary, paleorecords are not affected by it exhibiting therefore lower rates of turnover. Analysis of temporal turnover between the two functional groups indicates that the rate of change of coccolithophores is higher than of planktonic foraminifera. This finding supports our hypothesis that the rate of temporal turnover throughout the last two glacial – interglacial cycles of coccolithophores was higher than of planktonic foraminifera. Difference in the rate of temporal turnover is probably associated with differences in the trophic level and the rate of life cycle of the studied microorganisms. Furthermore, temporal turnover of planktonic foraminifera is possibly related to habitat tracking, whereas temporal turnover of coccolithophores is related to adaptation and evolutionary replacement of *G. ericsonii* by *E. huxleyi*.

Zusammenfassung

Der westliche Indische Ozean weist eine der höchsten Konzentrationen von Phytoplankton auf, welches ein wesentlicher Bestandteil des globalen marinen Nahrungsnetzes und ein wichtiges Element für die lokale Fischerei ist. Überfischung und die Erschließung der Küstengebiete haben jedoch langfristige Veränderungen der letzten Jahrzehnte in der biologischen Produktivität verursacht, was bei den marinen Organismen zu einer verringerten Abundanz und Biodiversität geführt hat. Neben der erheblichen Überfischung hat der westliche tropische Indische Ozean im letzten Jahrhundert einen der stärkste Anstiege der Meerestemperaturen erfahren. Als Folge davon haben anthropogener Druck und der globale Klimawandel zu einer Verringerung und Bedrohung der Biodiversität, sowie zu Veränderungen der Funktionen des marinen Ökosystems geführt. Die Folgen der Biodiversität umfasst die Umstrukturierung von Artenzusammensetzungen durch lokales Aussterben, Migration, Habitat-Tracking und evolutionäre Anpassungen. Die Konsequenzen dieser Verschiebungen für die ökologische Resilienz und die Funktion des Ökosystems bleiben jedoch unklar. Langzeitbeobachtungen und Analysen sind deswegen notwendig um unser Verständnis der temporal α- and β-Diversitäten besser verstehen zu können.

Der Sedimentkern GeoB12613-1 bietet umfassende Einblicke in die Biodiversitätsdynamik von Phyto- und Zooplankton während der letzten zwei glazialen – interglazialen Zyklen im westlichen Indischen Ozean. In dieser Studie wurden mikropaläontologische und statistische Analysen des Sedimentkerns zu den temporalen α- und β-Diversitäten von Coccolithophoriden und planktonischen Foraminiferen in folgenden Schritten durchgeführt: 1) Eine Hauptkomponentenanalyse wurde angewendet, um Artenzusammensetzungen und ihre zeitlichen Veränderungen zu analysieren. Anschließend wurden die Hauptkomponenten mit der höchsten erklärten Varianz mit δ^{18}O-Werten und Paläoproduktivitätswerten korreliert, um das Verteilungsmuster und die Verteilungsmechanismen der Artengemeinschaften besser in Bezug zu globalen Temperaturveränderungen und Produktivität zu verstehen. 2) Der Hill-Shannon Index, der Pielou Äquität Index und der Morisita-Horn Index wurden berechnet, um die temporalen α- und β-Diversitäten zu bewerten. Anschließend wurden ihre Änderungsraten im Laufe der Zeit basierend auf dem linearen Regressionsmodell betrachtet und ihre Trends mit den gegenwärtigen Beobachtungen verglichen. 3) Die temporalen Artenwechselraten von planktonischen Foraminiferen und Coccolithophoriden wurden verglichen, um die Hypothese zu überprüfen, ob der temporale Artenwechsel je nach Trophiestufe und Lebenszyklusrate variiert.

Die Ergebnisse der Analysen zeigen, dass planktonische Foraminiferen und Coccolithophoriden von unterschiedlichen Umweltfaktoren beeinflusst werden. Planktonische Foraminiferen zeigen eine starke Korrelation mit δ^{18}O-Werten, was darauf hindeutet, dass sie hauptsächlich von globalen Klimaveränderungen beeinflusst wurden. Auf der anderen Seite zeigen Coccolithophoriden eine sehr schwache Korrelation zu den δ^{18}O-Werten und eine starke Korrelation zur Paläoproduktivität, was darauf hindeutet, dass Coccolithophoriden hauptsächlich von Produktivitätsdynamiken beeinflusst wurden. Die Analyse der temporalen α- und β-Diversitäten ergab, dass Coccolithophoriden fast stationäre temporale α-Diversität aufweisen, jedoch mit höheren Änderungsraten der temporale β-Diversität. Andererseits zeigten die temporalen α- und β-Diversitäten planktonischer Foraminiferen keine wesentlichen Variationen in ihren Änderungsraten. Eine Erklärung dafür könnte sein, dass die temporale β-Diversität der Gegenwart durch anthropogene Einflüsse beeinflusst wird und daher höhere Artenwechselraten aufweist. Im Gegensatz dazu sind Paläodaten davon nicht betroffen und weisen dadurch niedrigere Artenwechselraten auf. Die Analyse des temporalen Artenwechsels zwischen den beiden funktionalen Gruppen deutet darauf hin, dass die Änderungsrate von Coccolithophoriden höher ist als die von planktonischen Foraminiferen. Diese Beobachtung unterstützt unsere Hypothese, dass die Änderungsrate des temporalen Artenwechsels während der letzten beiden glazialen – interglazialen Zyklen von Coccolithophoriden höher war als von planktonischen Foraminiferen. Der Unterschied in der Änderungsrate des temporalen Artenwechsels ist wahrscheinlich mit den Unterschieden in der Trophiestufe und der Lebenszyklusrate der untersuchten funktionalen Gruppen verbunden. Darüber hinaus hängt der temporale Artenwechsel von planktonischen Foraminiferen möglicherweise mit dem Prozess des Habitat-Tracking zusammen, während der temporale Artenwechsel von Coccolithophoriden mit der Anpassung und evolutionären Ersetzung von *G. ericsonii* durch *E. huxleyi* zusammenhängt.

Table of contents

Abbreviations

AB	Andaman Ridge
AC	Agulhas Current
BBW	Bengal Bay Water
BR	Broken Ridge
CCD	Carbonate Compensation Depth
DCM	Deep Chlorophyll Maximum
DFZ	Diamantina Fracture Zone
DR	Dave Ridge
EACC	East African Coastal Current
EICC	East Indian Coastal Current
EIR	East Indian Ridge
ENSO	El Niño-Southern Oscillation
ENSO	El Niño – Southern Oscillation
GW	Great Whirl
ICW	Indian Central Water
IEW	Equatorial Westerlies
IO	Indian Ocean
IO	Indian Ocean
IOD	Indian Ocean Dipole
IR	Investigator Ridge
ITCZ	Intertropical Convergence Zone
ITF	Indonesian Throughflow
ka	Killoannus
LDG	Latitudinal Diversity Gradient
LL	Laccadive Low
Ma	Milleannus
MADP	Madagascar Plateau
MCE	Mozambique Current and anticyclonic eddies
MIS	Marine Isotope Stage
MOZP	Mozambique Plateau
MP	Mascarene Plain
NEMC	Northeast Madagascar Current
NIDW	North Indian Deep Water
NMB	The Northeast Monsoon Bloom

NMC	Northeast Monsoon Current
Nos	Number of species
PCA	Principal Component Analysis
PCs	Principal Components
PP	Primary Production
PSU	Practical Salinity Units
RHJ	Ras al Hadd Jet
RTJ	Rodriguez Triple Junction
SC	Somali Current
SD	Sri Lanka Dome
SE	Socotra Eddy
SEC	South Equatorial Current
SECC	South Equatorial Countercurrent
SG	Southern Gyre
SICC	South Indian Counter Current
SJC	South Java Current
SMB	Southwest Monsoon Bloom
SS	Sunda Ridge
SST	Sea Surface Temperature
STC	Subtropical Convergence
Sv	Sverdrup
T	Termination
WC	Walker Circulation
WC	Walker Circulation
WICC	West Indian Coastal Current

List of figures

List of tables

List of plates

1. Introduction

The Indian Ocean plays an important role in modulating interannual to decadal climate variability through an ocean – atmosphere coupling and feedback mechanisms on both regional and global scales. Atmospheric processes such as seasonally reversing monsoon winds and semi-annual intermonsoon trade winds influence oceanic circulation pattern, mixing of the surface waters, depth of the thermocline, and the intensity of the upwelling processes (Schott and McCreary 2001; Tangunan et al. 2017). The monsoon forcing is strongest in the western part of the Indian Ocean, resulting in a strong coastal and open ocean upwelling, supplying nutrients to the surface water masses, and enhancing primary productivity of marine organisms. Notably, the western Indian Ocean accommodates one of the largest concentrations of phytoplankton blooms – a crucial part of the global marine food web and an important element in supporting local fisheries.

Approximately 60 million people live along the coast of the southwestern Indian Ocean and many of them rely on seafood for their economic and social security, as well as a food source through fishing. However, rapid expansion of the population and economic growth over the last 50 years has significantly intensified the stress on coastal resources. Overfishing and the development of coastal areas have accelerated the long-term alterations in biological productivity, resulting in decreased abundance and biodiversity of marine organisms (Roxy et al. 2016; Groeneveld 2016). In addition to significant overfishing, the western tropical Indian Ocean has experienced the most substantial long-term increase in sea surface temperatures (SSTs) over the last century, as a result of global warming (Roxy et al. 2016). As a consequence, anthropogenic pressure and global climate change resulted in reductions in biological diversity. Recent studies on temporal biodiversity changes have reported that biodiversity across different ecosystems and organisms is already affected by global climate change (Parmesan 2006; Hillebrand et al. 2010; Dam 2013; Jonkers et al. 2019).

Temporal changes in assemblage composition encompass a wide range of species restructuring. Species assemblages could be replaced over time entirely or change in their composition through local colonisations/extinctions, habitat tracking or adaptations (Hillebrand et al. 2010). These processes lead to the creation of novel assemblages, with entirely different ecosystem structures. It is however unclear what the consequences of these shifts for community resilience and ecosystem functioning are (Magurran et al. 2019). Moreover, temporal turnover varies across different organisms and ecosystems. For instance, it is expected that organisms at lower trophic levels and with a high rate of life cycle exhibit higher turnover rates than organisms at higher trophic levels and with a slower rate of life cycle (Korhonen et al. 2010). Previous studies were primarily focused on contemporary temporal changes in species composition. However, long-term data and analysis are required in order to improve understanding of temporal α- and β-diversity changes (Thrush et al. 2009; Magurran and Henderson 2010; Magurran et al. 2019). For instance, paleorecords can be analysed by computing α- and β-diversity indices, such as Hill – Shannon index and Bray – Curtis dissimilarity metric respectively (Tomašových and Kidwell 2009; Magurran et al. 2010).

The sediment core GeoB12613-1 is located off the Tanzanian margin in East Africa and provides insights into the last two glacial – interglacial cycles in the western tropical Indian Ocean. The sediment core provides unbiased study material, with no signs of carbonate dissolution (Tangunan et al. 2017). Furthermore, tropical assemblages are of particular interest as they are less affected by seasonality and exhibit slow long-term turnover. As a consequence, tropical assemblages persist throughout the year and provide insights in their long-term adaptivity to environmental changes (Korhonen et al. 2010; Williams et al. 2017). In this study our primary objective is to investigate and analyse biodiversity changes and the response of coccolithophores and planktonic foraminifera to changing environmental conditions over the last two glacial – interglacial cycles. In particular we address and test the following hypotheses:

H1: Coccolithophores and planktonic foraminifera assemblages in the western tropical Indian Ocean will track changes in $\delta^{18}O$ values for the last two glacial – interglacial cycles. Marine plankton, in particular phytoplankton and zooplankton, is especially sensitive to environmental changes (Roxy et al. 2016; Jonkers et

al. 2019; Antão et al. 2020) and should indicate assemblage shifts with changing climatic conditions, comparable to $\delta^{18}O$ values which record global ice volume changes and sea surface temperatures (Schiebel and Hemleben 2017).

H2: The rate of change of temporal α-diversity is expected to be very low. On the other hand, we expect substantial changes in temporal β-diversity, as observed in contemporary observations.

H3: Coccolithophores have a shorter life cycle (days to weeks), whereas planktonic foraminifera have a longer life cycle (days to months). hypothesise that the rate of temporal turnover throughout the last two glacial – interglacial cycles of coccolithophores is higher than of planktonic foraminifera, as coccolithophores have shorter generation times and therefore they should have the potential to adapt faster in response to changing environmental conditions than planktonic foraminifera.

2. The Indian Ocean

2.1 Geography

The Indian Ocean (IO) covers ~73.6 million km^2 and is the world's third largest water body after the Pacific Ocean and the Atlantic Ocean respectively. The IO is bounded by Africa and Arabian Peninsula in the East, Asia and India in the North, borders Indonesia and Australia in the West and Antarctica in the South. Furthermore, the IO has no interconnection to the North Pole, which separates it from the Arctic polar water masses (Schlich 1982; Mukhopadhyay et al. 2008). The disconnection from the Arctic water masses and extensive orogenic belt in Asia contribute to unique oceanographic conditions in the Indian Ocean, such as extensive upwelling in the east African coast and formation of summer and winter monsoons (Mukhopadhyay et al. 2008). The IO can be further subdivided into the western and eastern parts (Fig. 1), which can approximately be delimited by the Ninetyeast Ridge (Schlich 1982).

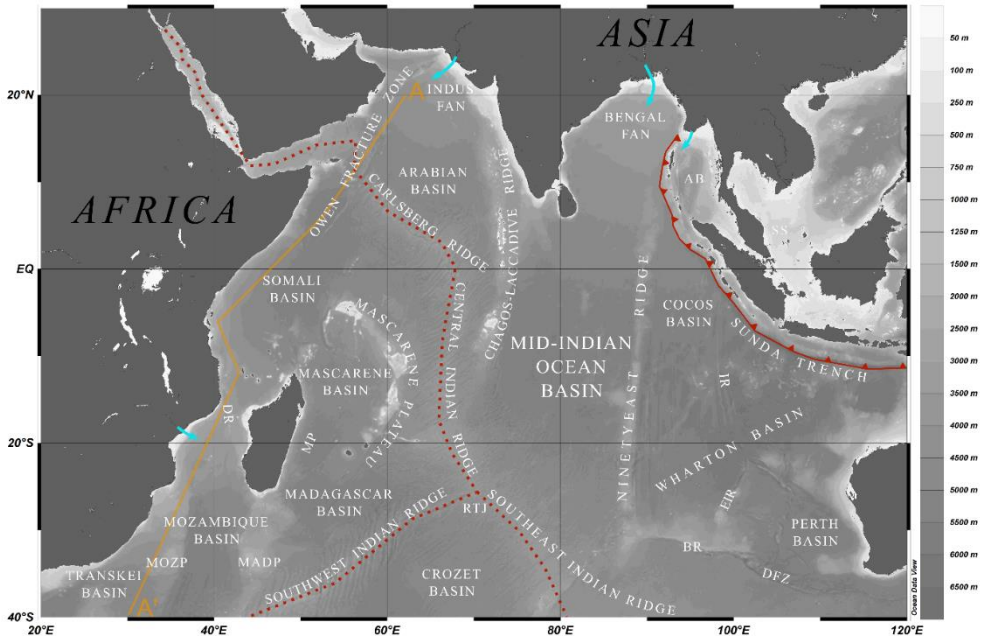

Fig. 1: Bathymetric map of the Indian Ocean with its major morphological and geological features. MOZP = Mozambique Plateau, MADP = Madagascar Plateau, MP = Mascarene Plain, DR = Davie Ridge, RTJ = Rodriguez Triple Junction, AB = Andaman Basin, SS = Sunda Shelf, IR = Investigator Ridge, EIR = East Indian Ridge, BR = Broken Ridge, DFZ = Diamantina Fracture Zone. Red punctuated lines indicate active mid-ocean ridges, red line with triangle symbols indicates the extension of the subduction zone along the Sunda Trench, light blue arrows indicate major freshwater and terrigenous material supply from the rivers, orange line represents A-A' transection. The map and bathymetry were compiled using Ocean Data View (Schlitzer 2022), topographic names were reproduced from (GEBCO 2014) and geological features after (Lemenkova 2020).

The Western Indian Ocean is dominated by deep abyssal plains: Arabian Basin, Somali Basin, Madagascar Basin, Mascarene Plain, Mozambique Basin, Transkei Basin, Crozet Basin, and Mid-Indian Ocean Basin. Deep-water basins are further bounded by a complex system of active mid-ocean ridges: Carlsberg Ridge, Southwest-, Southeast-, and Central Indian Ridges which form the Rodriguez Triple Junction at 25°S and 70°E (Mitchell and Parson 1993). Another important morphological feature of the Indian Ocean are the aseismic ridges, which are seismically inactive submarine structures, formed as a result of hot spot volcanism. In the Western Indian Ocean major aseismic ridges are the Chagos-Laccadive Ridge and the Ninetyeast Ridge. Further prominent morphological structures are (Fig. 1): Owen Fracture Zone, Mozambique, Madagascar and Mascarene Plateaus, continental shelves and thick sedimentary deposits of the Indus Fan and the Mozambique Fan (Schlich 1982; Parson and Evans 2005; Mukhopadhyay et al. 2008).

The Eastern Indian Ocean is characterized by an active subduction zone represented by the Sunda/Java Trench, which extends from the Burma and Andaman Islands in the North to the northwestern part of Australia in the southeast. The subduction zone corresponds to the Sunda-Banda arc system, which separates the Indo-Australian tectonic plate from the Eurasian/Sunda tectonic plates. Major deep-water basins are: Cocos Basin, Wharton Basin and Perth Basin, which are separated from each other through active ridges such as: Investigator Ridge, East Indian Ridge and through an aseismic structure of the Broken Ridge (Schlich 1982). Other important oceanic structures are (Fig. 1): Diamantina Fracture Zone and the Bengal Fan (Kolla and Kidd 1982).

2.2 Oceanography

The Indian Ocean forms the largest warm pool on Earth, modulating interannual to decadal climate variability through an ocean – atmosphere coupling and feedback mechanisms on both regional and global scales. In particular, the changes in sea surface temperatures influence hydrology, oceanic circulation, and the dynamics of the overlaying atmosphere. The IO has a unique set of oceanographic and climatic features, for instance, it is bounded to the north by the Asian continent preventing any heat transport northward with only weak ventilation of the thermocline from the north. Furthermore, the Asian continent exhibits strongest monsoon on Earth, with monsoonal winds generating large seasonal variations in ocean currents and their annual reversal which results in two mean states of the wind regime: the Northeast or Winter Monsoon and the Southwest or Summer Monsoon (Tomczak and Godfrey 1994; Schott et al. 2009; Felis 2020; Thompson 2022). Between the monsoon seasons (April – May and October – November), an equatorial wind regime is characterized by the Wyrtki Jets, which blow along the equator as a narrow band from west to east. The eastward direction of the jet acts as a surface current resulting in the uplift of the thermocline in the west and sinking in the east (Wyrtki 1973).

Another important climatological aspect of the ocean – atmosphere coupling in the Indian Ocean is the Walker Circulation (WC), which is referred to as large-scale atmospheric overturning cells along the equator. The neutral state of the WC consists of low-level westerlies over the Indian Ocean and low-level easterlies over the Pacific Ocean, with rising motions occurring over warm surface waters in the west of the Pacific Ocean and in the east of the Indian Ocean respectively. Subsequently, the return flow occurs in the opposite direction to low-level winds in the upper troposphere, with subsidence developing over the eastern Pacific Ocean and western Indian Ocean. Oscillations in WC impact thermocline depth, temperature gradient, sea level variations and precipitation. In the Pacific Ocean the WC oscillations are associated with the El Niño – Southern Oscillation (ENSO) climate system, whereas strengthening of the WC is correlated with the La Niña events and weakening of the WC is correlated with the El Niño events respectively (Lau and Yang 2003; Mohtadi et al. 2017). In the Indian Ocean oscillations in the WC are associated with the Indian Ocean Dipole (IOD), with positive IOD events related to the weakening of the WC and negative IOD events with the strengthening of the WC (Mohtadi et al. 2017).

2.2.1 Summer Monsoon circulation

The Summer Monsoon is characterized by low atmospheric pressure in Arabian Peninsula and north-western Asia and high atmospheric pressure in Australia and southern Africa during June – September. These south-north high pressure gradient result in reversal of the Trade Winds in the northern hemisphere and shifting of the Intertropical Convergence Zone (ITCZ) south of the Himalayas (Fig. 2), bringing moisture and rainfall to the region (Tomczak and Godfrey 1994; Schott and McCreary 2001; Phillips et al. 2021).

The circulation pattern of the surface currents during the Summer Monsoon is dominated by the wind field of the Southwest Trade Winds, where South Equatorial (SEC) and East African Coastal Currents supply the northward flowing Somali Current (SC), which occurs in form of circulating cells and gyres (Fig. 2). Before the onset of the Summer Monsoon (March – May) the Somali Current is an extension of the East African Coastal Current with northward flow direction. At 3 – 4°N the SC turns offshore, which initiates the development of a cold wedge and an upwelling regime further north (Fig. 2). During summer monsoon, (June

– July) the Somali Current recirculates as a set of multiple gyres in the form of the Southern Gyre (SG), the Great Whirl (GW) and the Socotra Eddy (SE). Further north at 10 – 12°N another cold wedge forms (Fig. 2). The cross-equatorial flow transports around 20 Sv and bifurcates into an eastward flow and a retroflected flow in form of the Southern Gyre. A fraction of the cross-equatorial flow migrates further north into the Arabian Sea, which is dominated by a northeastward coastal Ras al Hadd Jet (RHJ) and transports around 2 – 8 Sv of cold coastal upwelling waters into the warmer waters of the Gulf of Oman and into the interior of the Arabian Sea in form of filaments and eddies (Fig. 2) (Schott and McCreary 2001; Schott et al. 2009; Phillips et al. 2021).

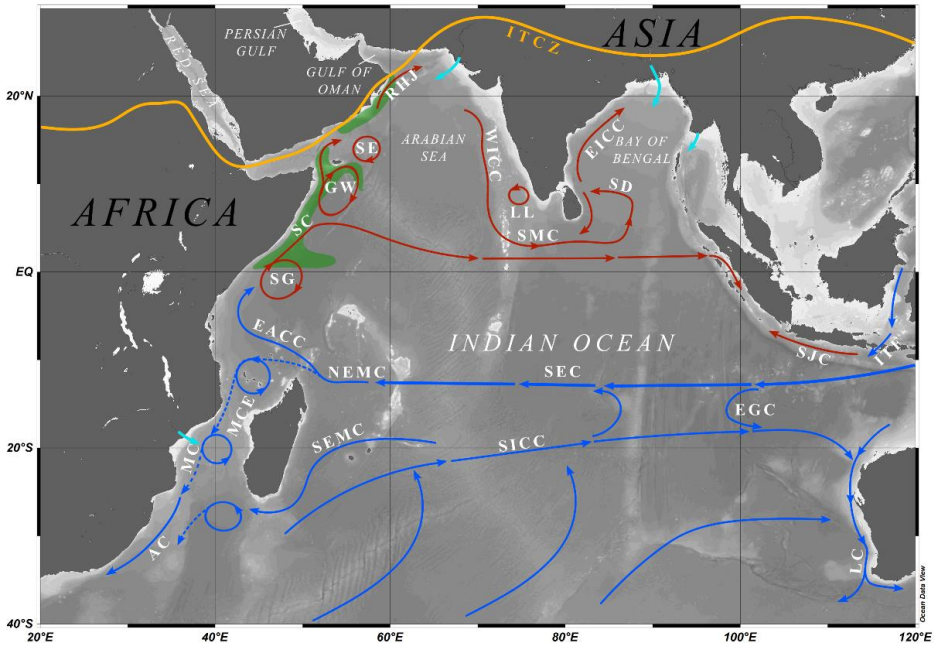

Fig. 2: Schematic representation of the major circulation patterns during northern hemisphere Summer (July/August) and the mean location of the Intertropical Convergence Zone (ITCZ) after (Yan 2005). In red indicated the Summer/Southwest Monsoon circulation: SJC = South Java Current, SG = Southern Gyre, GW = Great Whirl, SC = Somali Current, SE = Socotra Eddy, RHJ = Ras al Hadd Jet, WICC = West Indian Coastal Current, LL = Laccadive Low, SMC = Southwest Monsoon Current, SD = Sri Lanka Dome, EICC = East Indian Coastal Current. In blue indicated the Southern Indian Ocean circulation: ITF = Indonesian Throughflow, SEC = South Equatorial Current, NEMC = Northeast Madagascar Current, SEMC = Southeast Madagascar Current, EACC = East African Coastal Current, MCE = Mozambique Channel Eddies, MC = Mozambique Current, AC = Agulhas Current, SICC = South Indian Counter Current, EGC = East Gyral Current, LC = Leeuwin Current. Green shaded areas represent upwelling regions and light blue arrows indicate major riverine inflow. The map was compiled using Ocean Data View (Schlitzer 2022) and circulation patterns are modified after (Schott and McCreary 2001; Schouten et al. 2003; Schott et al. 2009; Phillips et al. 2021).

The surface circulation of the Arabian Sea is characterized in the east by the West Indian Coastal Current (WICC) (Fig. 2), which flows along the western coast of India and forms therefore the eastern boundary current system. The WICC transports warm, saline water masses during Summer Monsoon from Arabian Sea into the Bay of Bengal via the Southwest Monsoon Current and the East Indian Coastal Current (EICC) (Fig. 2). The EICC flows constantly only up to 10 – 18°N along the eastern coast of India as a weak and shallow (70 m) current transferring around 10 Sv (Schott and McCreary 2001), further north it extends in form of short pulses (Phillips et al. 2021). Another notable features during Summer Monsoon in the northern Indian Ocean are the anticyclonic Laccadive Low (LL) gyre (region of low sea level) and a closed anticyclonic Sri Lanka Dome (SD) (recurring region of upwelling of cold water) (Fig. 2) (Burns et al. 2017; Phillips et al. 2021).

2.2.2 Winter Monsoon circulation

The Winter Monsoon is characterized by high atmospheric pressure over the Asian land masses and low atmospheric pressure over the ocean in the northern hemisphere, with northeasterly wind circulation (Northeast

Trade Winds) over the tropics and northern subtropics during December – March, resulting in dry season in the southern Asia. In the southern hemisphere, low atmospheric pressure is located in the tropical region and high atmospheric pressure in the subtropical region, this pressure gradient results in the Southeast Trade Winds transporting moist air masses to northern Australia and the Indonesian region. During the Winter Monsoon, the ITCZ is located south of the equator (~5°S) (Fig. 3) (Tomczak and Godfrey 1994; Schott and McCreary 2001; Phillips et al. 2021).

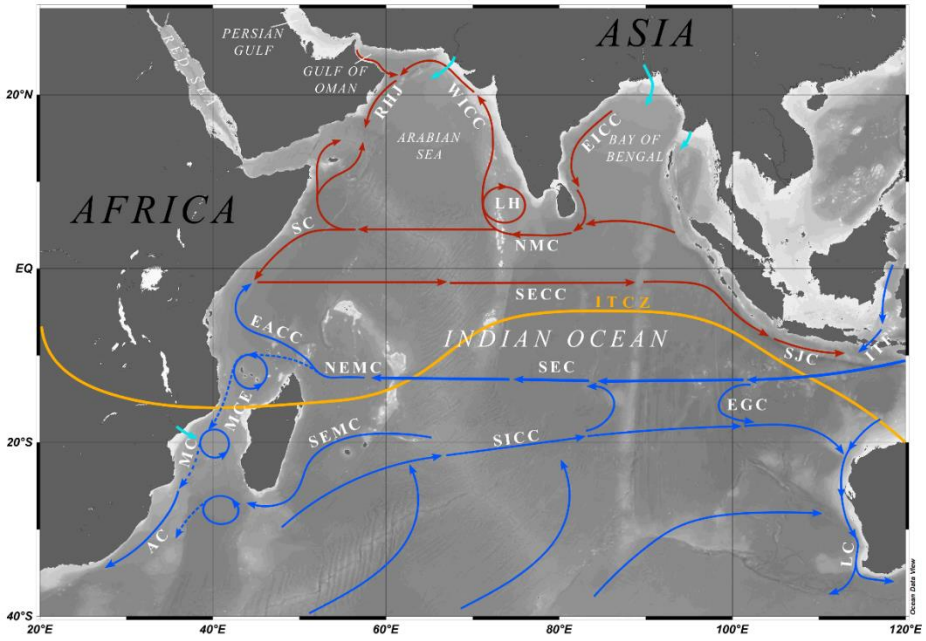

Fig. 3: Schematic representation of the major circulation patterns during northern hemisphere Winter (January/February) and the mean location of the Intertropical Convergence Zone (ITCZ) (Yan 2005). In red is indicated the Winter/Northeast Monsoon circulation: SJC = South Java Current, SECC = South Equatorial Countercurrent, SC = Somali Current, RHJ = Ras al Hadd Jet, WICC = West Indian Coastal Current, LH = Laccadive High, NMC = Northeast Monsoon Current, EICC = East Indian Coastal Current. In blue is indicated the Southern Indian Ocean circulation as in (Fig. 2). Light blue arrows indicate major riverine inflow. The map was compiled using Ocean Data View (Schlitzer 2022) and circulation patterns are modified after (Schott and McCreary 2001; Schouten et al. 2003; Schott et al. 2009; Phillips et al. 2021).

The circulation pattern of the surface currents during the winter monsoon is dominated by the wind field of the Southwest Trade Winds, with Somali Current (SC) flowing southward and transporting around 5 Sv during January – February, where it converges at 2 – 4°S with the northward flowing EACC (Fig. 3). Both currents supply the eastward flowing South Equatorial Countercurrent (SECC), which further supplies the southward flowing South Java Current (SJC). In the Bay of Bengal, the EICC transports low salinity and colder water masses along the anticyclonic Laccadive High gyre (region of sea-surface height anomaly) into the Arabian Sea via the seasonally reversing Northeast Monsoon Current (NMC). The West Indian Coastal Current also reverses during the winter monsoon and transports about 7 Sv of surface waters into the Arabian Sea and further south towards the Somali Current (Tomczak and Godfrey 1994; Schott and McCreary 2001; Schott et al. 2009; Phillips et al. 2021).

2.3 Primary and Secondary Production

Primary productivity in the marine environment is attributed to marine photosynthetic organisms. In the Indian Ocean major photosynthetic organisms are phytoplankton dominated by diatoms, dinoflagellates, and coccolithophores. The distribution of chlorophyll α is closely related to photosynthetic activity in the upper water layers of the oceans and can be used in assessing primary productivity (Fig. 4). Highest surface primary production (PP) values in the Indian Ocean can be found in the coastal areas, whereas the rest of the IO has low surface PP values (Fig. 4). High primary productivity areas are associated with seasonal phytoplankton blooms, due to the high abundance of nutrients in form of nitrogen and phosphorus. Nutrients are further

replenished in the upper water masses as a result of upwelling and riverine inflow (Krey 1973; Qasim 1977; McCreary et al. 2009).

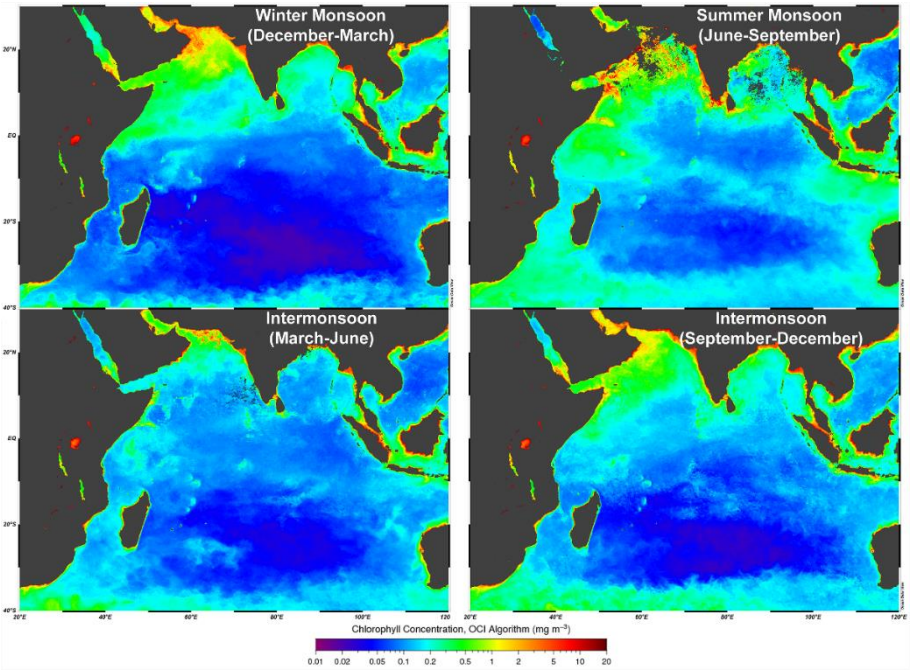

Fig. 4: Chlorophyll α distribution throughout the winter monsoon, summer monsoon and intermonsoon periods in 2018. Data has been generated using Aqua-MODIS instrument, with resolution of 4 km after (NASA Ocean Biology Processing Group 2022).

The northern Indian Ocean is characterized by two distinctive growing seasons. The Southwest Monsoon Bloom (SMB) is induced by intense upwelling along the coasts, lateral advective transport and Ekman pumping during the Summer Monsoon period (Fig. 4). The mixed layer depth during the SMB is shallowing along the coast and deepening in more distal areas. The Northeast Monsoon Bloom (NMB) is induced by entrainment of the nutrients into the surface layer, as a result of convective mixing during the Winter Monsoon period (Fig. 4). The intermonsoon periods are characterized by stratified waters, which are diminished in nutrients in the upper water layers and result in oligotrophic conditions and low primary productivity. Primary productivity of the equatorial Indian Ocean is strongly affected by the Wyrtki Jets during the intermonsoon periods. During this period the thermocline and the nutricline are deeper in the eastern part of the Indian Ocean, resulting in a lower primary productivity compared to the western part of the ocean (Lévy et al. 2007; Koné et al. 2009; McCreary et al. 2009).

Zooplankton plays an important role in marine food webs linking primary production to higher trophic levels and supplying minerals and carbon to deeper parts of the ocean. In the eutrophic environment large zooplankton, such as copepods and euphausiids, feed directly on phytoplankton, whereas in the oligotrophic environment a linkage between phytoplankton and larger zooplankton is utilized by microzooplankton (20 – 200 µm), such as foraminifera and radiolaria, which graze upon nanophytoplankton (2 – 20 µm) (Schmoker et al. 2013; Biard et al. 2016; Davies et al. 2022). Distribution of larger zooplankton and microzooplankton follows the distribution of phytoplankton and therefore of chlorophyll α, with highest abundances found during the Summer Monsoon period along the coasts of Somalia, Oman, western Indian and Arabian Peninsula (Fig. 4). During Winter Monsoon and intermonsoon periods secondary productivity values are lower compared to the Summer Monsoon period (Fig. 4). In the southern part of the Indian Ocean and in its central part, secondary productivity values are low (Rao 1973).

3. Ecology

3.1 Biodiversity

Biodiversity or biological diversity is referred to as the variety of life. It is used as a unifying concept to measure and characterize natural variability of species across different ecosystems. Biodiversity is also a multifaceted concept and there is no single universal measure of it. Instead, biodiversity is described by multiple measures of its different aspects, through the concepts of α-, β-, and γ- diversities (Magurran 2003; Magurran and McGill 2011; Magurran 2021).

3.1.1 Alpha Diversity

Alpha diversity is the diversity measured at the habitat level and used to characterize species communities. Specifically, α-diversity is the local diversity within a single sampling unit (Barwell et al. 2015). It consists of two components: species richness and equitability indices, which together represent two different aspects of species abundance distribution. Species richness measures the number of individuals per unit area or per sample and quantifies species content of the measured area/sample. Measures of evenness on the other hand characterize equitability of the relative abundances of different species in terms of their distribution. Species diversity and evenness can be expressed through richness, diversity, evenness, dominance, and rarity metrics (Magurran and McGill 2011; Thukral 2017).

3.1.2 Beta Diversity

Beta diversity is the measure of spatial and temporal variations in species composition and abundance between sampling units. In general, spatial changes in diversity are measured across environmental gradients or geographical transects, whereas temporal changes are measured over time. Temporal changes are also referred to as temporal turnover. Temporal β-diversity/temporal turnover quantifies differences in species composition between two samples separated in time. This can be measured either by comparing adjacent sampling periods or with reference to a single baseline sample or time period (Magurran and McGill 2011; Dornelas et al. 2014).

Temporal changes can occur either as directional change or non-directional change. Directional change of species composition can be associated with ecological succession of the species, pollution, invasive species, or catastrophic events. Non-directional change is the product of ongoing turnover, which affects all communities. It is associated with processes such as immigration, local extinction, and variation of species abundances. Moreover, temporal scaling is an important factor when analysing underlying processes of temporal change, as it has profound effect on species turnover. For instance, on longer timescales (multi-million-years) the magnitude of species turnover is high, with speciation and species extinctions acting as the main forcing factors. On the shorter timescales (multi-millennial to millennial years), the magnitude of species turnover decreases and the main forcing factors are changes in climatic conditions (Lewandowska et al. 2020). Moreover, temporal turnover varies between different organism types, latitude, and trophic level. Organisms in the tropics are affected by a higher energy input, therefore exhibiting a higher rate of life cycle. It is expected that temporal turnover is higher in the tropics. However, some studies suggest the opposite, as organisms in the tropics have higher stability because of their high diversity, thus lower turnover over time. Another important aspect is the body size and cell density. Small organisms such as microbial eukaryotes have a high rate of life cycle, high population dynamics and gene flow, therefore exhibiting higher rates of temporal turnover. Additionally, it is suggested that temporal turnover is related to trophic level, with temporal turnover decreasing with increasing trophic level (Korhonen et al. 2010).

Temporal turnover can be measured by using species-time curves, turnover indexes, evaluating changes in species abundance distribution or by plotting a diversity measure against time. Here we will focus only on turnover indexes, specifically on similarity/dissimilarity measures. Similarity measures can be incidence-based or abundance-based. Incidence-based measures are based only on presence or absence of species. An example

of incidence-based similarity measures are Jaccard and Sørensen indices. Abundance-based measures assess similarity on the differences in species frequencies among assemblages. An example of abundance-based measures are Morisita – Horn overlap measure and Bray – Curtis similarity measure (Jost 2006; Jost et al. 2011; Magurran and McGill 2011).

3.1.3 Gamma Diversity

Gamma diversity is a diversity measured between habitats within the landscape. It is a combined diversity of α- and β- diversities characterizing the diversity of the landscape. For true diversities (Hill numbers) the relationship between α-, β-, and γ-diversities is as follows:

$$\gamma = \alpha \times \beta$$

in which γ is diversity of all sites in the entire assemblage, α is diversity of a site and β is the compositional difference between spatial or temporal units. An important property of α- and β-diversities is their independence of each other (Jost 2006, 2007; Magurran 2021).

3.2 Adaptation, Migration and Evolution

In order to avoid extinction, natural populations respond to changing environment through plastic adaptation, migration, and evolutionary adaptation (Hoffmann and Sgrò 2011). In general, biological adaptation is a process by which organisms evolve and develop specific traits or characteristics that increase their survival and reproductive success in a specific environment or habitat. Adaptation is the result of natural selection and pressure on organisms from changing environment and biotic invasion. Over time, individuals with advantageous traits are more likely to survive, reproduce, and pass those traits on to their offspring. As a result, these traits become more prevalent in the population. Different types of adaptation can be distinguished: plastic adaptation and evolutionary adaptation (Parmesan and Yohe 2003; Parmesan 2006; Hoffmann and Sgrò 2011).

Plastic adaptation refers to phenotypic changes of the organisms, primarily as a response to environmental and seasonal changes. Evolutionary adaptation on the other hand refers to genetic changes in response to mutations and gene flows within the population. Another important process for species to avoid extinction in biotic or abiotic forcing is to migrate to their preferential habitat. This process is also referred to as habitat tracking. Habitat tracking is a spatial migration of species or biofacies in response to shifting environments. This process is especially widespread in marine plankton, due to the lack of geographical barriers and high dispersal potential through currents (Brett et al. 2007; Strack et al. 2022).

3.3 Effects of climate change on phytoplankton and zooplankton

Phytoplankton and zooplankton species, in particular coccolithophores and planktonic foraminifera species, are especially affected by evolutionary adaptation, as these microorganisms have large populations, large genetic diversity, short generation times and rapid reproduction. For instance, cultural experiments on *Emiliania huxleyi* in response to ocean acidification, revealed high potential of these organisms to a short-term adaptation (Lohbeck et al. 2012; Reusch and Boyd 2013; Poloczanska et al. 2013).

In addition to ocean acidification, global warming has a profound effect on biodiversity and reorganization of ecological communities, as species track temperature changes in order to stay in their respective thermal niches (Antão et al. 2020; Strack et al. 2022). Significant changes in species composition are expected particularly for tropical marine species due to their narrower thermal tolerances in comparison to temperate species. Furthermore, the spatial distribution and species turnover of marine microorganisms such as planktonic foraminifera and coccolithophores, are highly responsive to changes in SSTs and have resulted in a strong latitudinal diversity gradient (LDG) (Yasuhara et al. 2012; Yasuhara et al. 2020b; Strack et al. 2022).

Interestingly, the LDG pattern is bimodal, with a distinctive depression in the lower latitudes and the highest species richness in temperate regions. This pattern of species richness distribution and therefore diversity

decline in the lower latitudes possibly began to develop as a result of rapid warming after the Last Glacial Maximum, approximately 15.000 years ago. Nevertheless, warming trends during the Anthropocene are expected to accelerate the decline of tropical oceanic diversity (Yasuhara et al. 2020b). Indeed, the study by Jonkers et al. (2019) has reported that the anthropogenic climate change has already altered global composition of marine plankton communities. The Anthropocene species assemblages show significant differences compared to their pre-industrial counterparts, with the observed changes being consistent with current temperature changes (Jonkers et al. 2019; Yasuhara et al. 2020a).

3.4 Planktonic Foraminifera

Planktonic foraminifera are marine protozoans with chambered morphology and calcareous tests. First appearance of planktonic foraminifera is traced back into the mid-Jurassic (~170 Ma), with global distribution and populations in the oceans occurring since the mid-Cretaceous (~100 Ma). Planktonic foraminifera live their entire life cycle freely floating in the mixed layer and the upper thermocline (Kucera 2007; Schiebel and Hemleben 2017). The nutrition of planktonic foraminifera is diverse and based on phytoplankton, zooplankton, bacteria, organic matter, phytodetritus, symbiosis with algae and sequestered chloroplasts (Haynes 1981).

Planktonic foraminifera are extremely abundant in the modern oceans and many of the species have global distribution. Based on their test morphology ~50 living planktonic foraminifera species can be distinguished in the modern oceans, however, the number of genetic species is approximately one third higher (Kucera 2007; Morard et al. 2018). Most of their tests have a high preservation potential, which make them one of the most important microfossils for paleoceanographic reconstructions. Furthermore, planktonic foraminifera are one of the major producers of calcareous particles contributing to formation of the globigerina ooze and influence considerably marine carbonate and atmospheric CO_2 budgets (Schiebel et al. 2017).

The distribution of planktonic foraminifera, assemblage composition, diversity and test size are strongly influenced by sea surface temperature. However, at the regional scale, food availability, physical and chemical properties of the ambient seawater have major impact on the species distribution (Schiebel and Hemleben 2017). Specific planktonic foraminiferal assemblages define the tropical, subtropical, temperate, subpolar and polar provinces (Kucera 2007; Schiebel and Hemleben 2017; Schiebel et al. 2017).

3.4.1 Influence of monsoon circulation on planktonic foraminifera

Planktonic foraminifera in the northwestern Indian Ocean are strongly influenced by the monsoonal wind circulation. The summer monsoon circulation generates extensive coastal upwelling and eddy advection along the eastern African coast. In the Somali Basin, upwelling transports cold and nutrient rich waters to the surface, enhancing primary productivity from June to September. This period is characterized by the highest test flux of planktonic foraminifera and species assemblage is dominated by *Globigerina bulloides*, followed by *Neogloboquadrina pachyderma*, *Neogloboquadrina dutertrei*, *Pulleniatina obliquiloculata* and *Globigerinita glutinata*. Furthermore, summer monsoon assemblage is characterized by highest species richness and low diversity and equitability, as a result of the dominance of *G. bulloides* (Conan and Brummer 2000).

In October, at the end of the summer monsoon, coastal upwelling and eddy activity are reduced, and the highest test fluxes are produced by *Globoturborotalita rubescens*. During the autumn intermonsoon, the upper water column re-stratifies, and nutrients are depleted as a result of primary productivity. The intermonsoon period is characterized by a minimum test flux for all species. The assemblage is dominated by non-upwelling species, such as *Globigerinoides ruber*, *Globigerinoides tenella*, *Trilobatus trilobus*, *Trilobatus sacculifer*, *Globorotalia menardii* and *Globigerina falconensis*. On the other hand, the winter monsoon reverses the circulation pattern and transports nutrients from the nutricline to the euphotic zone, enhancing primary productivity between December and March. Species assemblage is dominated by the same species as during autumn intermonsoon period, but with a considerably higher test flux. The intermonsoon and the winter

monsoon assemblages are further characterized by low species richness and high diversity and equitability of the species (Conan and Brummer 2000).

3.5 Coccolithophores

Coccolithophores are a group of marine, unicellular algae, which belong to the phylum of Haptophyta, class Prymnesiophyceae. They are considered as one of the three main marine eukaryotic phytoplankton groups, together with diatoms and dinoflagellates. Coccolithophores are ubiquitous in the global ocean and form extensive blooms. Furthermore, coccolithophores produce and excrete two main types of microscopic calcite scales, called coccoliths: heterococcoliths, formed of individual crystal units of various size and shape and holococcoliths, formed of a single scale type. Coccolithophores inhabit various ecological niches, inhabiting marine environments ranging from oligotrophic to eutrophic, warm to cold, well illuminated to dim and stratified to mixed (Thierstein and Young 2004; Ziveri et al. 2004; Balch 2018).

Many coccolithophores have a haplodiplontic life cycle, with an alternation between a haploid motile form, which is covered predominantly with holococcoliths and a diploid non-motile form, which is covered with heterococcoliths. The heteromorphic life cycle results in ecological partitioning of the coccolithophores. Holococcolith forms flourish in low-nutrient surface waters and are more abundant during winter months, whereas heterococcoliths forms are predominant in low-light environments with high nutrient contents and are abundant during summer months (Balch 2018). The nutrition of coccolithophores is predominantly autotrophic, however, some coccolithophore species have a mixotrophic lifestyle and are able to digest micronutrients. Coccolithophores play an important role in modulating oceans biogeochemical processes through alkalinity pump and biological carbon pump. The alkalinity pump or the $CaCO_3$ pump lowers total alkalinity and dissolved inorganic carbon in the euphotic zone, which results in increased upper-ocean and atmospheric CO_2 contents. The biological carbon pump has an effect on sinking particulate organic carbon and results in decrease of surface CO_2 content. The balance between these biogeochemical pumps characterize the ocean as either a net source or as a sink for CO_2 (Thierstein and Young 2004; Balch 2018).

3.5.1 Influence of monsoon circulation on coccolithophores

Coccolithophores contribute significantly to the phytoplankton assemblages in the ocean and dominate the stratified waters of the subtropical and tropical regions. Recently upwelled waters are commonly dominated by diatoms. Nevertheless, blooms of coccolithophores occur during periods of upwelling relaxation, as the upper water column becomes stratified and depleted on silica. Coccolithophore export production increases during summer monsoon period. The species assemblage comprises lower- to upper- and middle-photic zone species, with low diversity. During upwelling relaxation, coccolithophore export production reaches its maximum and species diversity increases. The winter monsoon period is characterized by increased export production of shallow- and deep-living coccolithophore species, with similar fluxes to the summer monsoon period. The intermonsoon period is on the other hand characterized by low coccolithophore fluxes and high species diversity (Broerse et al. 2000).

4. Materials and Methods

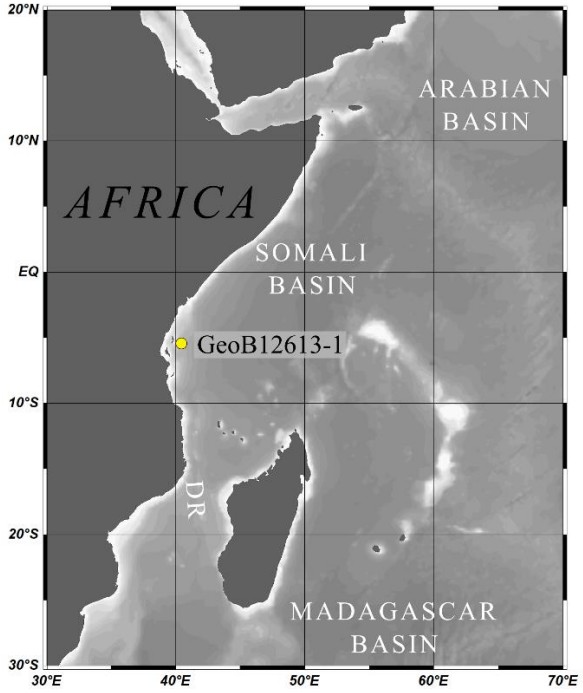

Fig. 5: Detailed map of the study area with the location of the studied core GeoB12613-1 (yellow dot). The map was compiled using Ocean Data View after (Schlitzer 2022). Core location after (Savoye et al. 2013).

The gravity core GeoB12613-1 was obtained from the Tanzanian margin in East Africa (05°29´S; 40°56´E, Fig. 5) at 2292 m water depth during the R/V Meteor cruise M75/2 in 2008 (Savoye et al. 2013). A previous study (Tangunan et al. 2017) has analysed the upper 7.54 m of the 11.7 m core, covering the last 300 ka, which represent the last two Glacial – Interglacial cycles. A total of 196 samples were collected at 4 cm intervals. The samples were thereafter analysed on coccolithophore assemblages. Stable oxygen isotopes were measured on planktonic foraminifera *Globigerinoides ruber* (white) and Sr/Ca ratios were obtained from coccolithophores tests (Tangunan, et al., 2017). The age model was based on accelerator mass spectrometry ^{14}C analyses measured on planktonic foraminifera *Globigerinoides sacculifer*. The $\delta^{18}O$ values (Fig. 6) were correlated to the benthic foraminifera $\delta^{18}O$ stack after (Lisiecki and Raymo 2005). In this project the working half of the core was sampled at the equivalent depths to the study after (Tangunan et al. 2017).

Sampling and further core investigations were conducted at MARUM in Bremen. The core was re-sampled in continues 4-cm intervals using 10 cm^3 syringes and the volumes were documented (Table 5). The samples were thereafter transferred into the plastic bags and wet weights were obtained. Subsequently the samples were frozen at ~ -20°C for one day and thereafter freeze-dried for another day. Freeze-dried samples were then wet sieved over 2 mm and 63 µm sieves. The residue was thereafter dried at ~60°C for one day. The dried residues were weighted and sieved over the 150 µm sieve. The acquired fractions of 63 – 150 µm and >150 µm were weighted and documented. Fraction >2 mm was not present in the studied samples.

Samples from the 2 – 62 cm sediment depth (cmsd), 302 – 386 cmsd and 574 – 658 cmsd intervals were considered for further analysis, as they cover the last three Termination events and last two glacial – interglacial cycles according to stratigraphy after (Tangunan et al. 2017). Furthermore, the warming periods are characterized by high biodiversity turnovers and therefore were considered for further analysis (Lewandowska et al. 2020). The age model was thereafter adjusted with the updated age values (pers. comm. Jeroen Groeneveld 2022).

Picking and counting of planktonic foraminifera were conducted only on >150 µm fraction. Samples were reduced in size by a microsplitter to an adequate fraction. The reduced fraction was then pre-counted, spread on a grid plate and studied under an optical microscope. At least 300 individuals of planktonic foraminifera were counted and identified in 60 samples. Each species has been extracted, documented, and transferred into an individual cell. The taxonomy for planktonic foraminifera was based on (Schiebel and Hemleben 2017; Siccha and Kucera 2017), whereas *Trilobatus sacculifer* was further differentiated into the morphotypes "with sac" for *Trilobatus sacculifer* and "without sac" for *Trilobatus trilobus*, as these species have different ecological preferences (Spezzaferri et al. 2015). Species *Globigerinoides ruber* was differentiated between *Globigerinoides ruber* (white), *Globigerinoides ruber* (pink) pink variety of *G. ruber* and *Globigerinoides elongatus*, distinguished by its slightly compressed or flattened chambers and a relatively small primary aperture (Wang 2000; Aurahs et al. 2009; Tapia et al. 2022).

Documentation of planktonic foraminifera species was done using optical microscope Keyence VHX 6000 with an integrated digital camera. Single images of planktonic foraminifera were stacked together with the provided software from Keyence. Additional documentation was conducted on Scanning Electron Microscope (SEM) at the University of Bremen (see appendix Plate V & Plate VI). In addition to obtained planktonic foraminifera data, data on coccolithophores after (Tangunan et al. 2017) were implemented into this study. The obtained datasets were further analysed on principal components and α- and β-diversity indices using software *R* (R Core Team 2021) and *RStudio* (Posit team 2022), with an ecology package *vegan* (Oksanen et al. 2020).

4.1 Stratigraphy

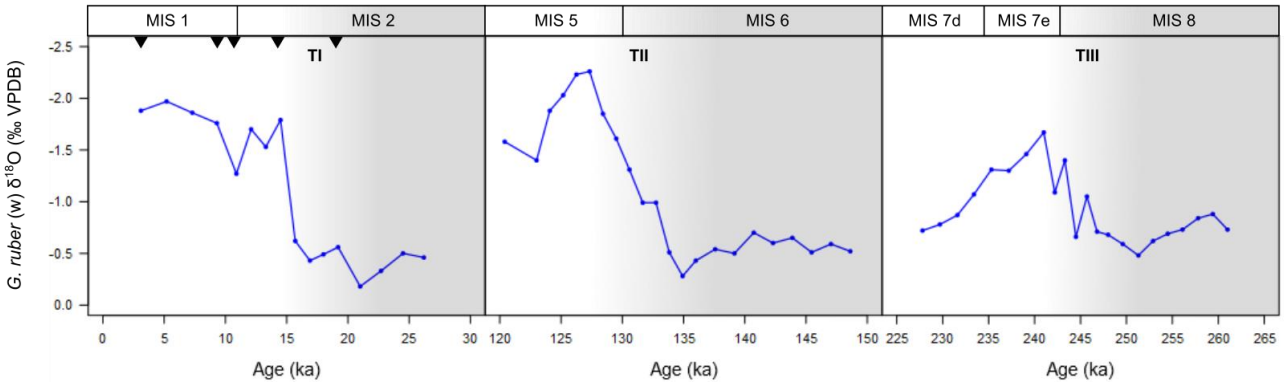

Fig. 6: Stratigraphic framework of GeoB12613-1 based on *Globigerinoides ruber* $\delta^{18}O$ record and *Globigerinoides sacculifer* ^{14}C accelerator mass spectrometry measurements after (Tangunan et al. 2017). Black triangles = accelerator mass spectrometry ^{14}C tie-points measured on planktonic foraminifera *Globigerinoides sacculifer*. MIS = Marine Isotopic Stage, light grey = glacial periods, white = interglacial periods, light grey gradient indicates deglaciations/Termination events TI, TII and TIII respectively.

The stratigraphy is based on updated *G. ruber* $\delta^{18}O$ values and ^{14}C tie-points (Fig. 6 & Table 7). The onset of MIS 1 was defined at ~11.7 ka after (Cohen et al. 2013). Stratigraphic boundaries between glacial and interglacial periods MIS 8/MIS 7 and MIS 6/MIS 5 were defined as temporal midpoints of the Terminations II and III at 130 ka and 243 ka respectively (Lisiecki and Raymo 2005). Terminations I, II and III were defined as rapid changes of *G. ruber* $\delta^{18}O$ values from maximum glacial value to minimum interglacial value (Fig. 6) (Lisiecki and Raymo 2005). MIS 7d is characterized by high *G. ruber* $\delta^{18}O$ values and the transition MIS 7e/MIS 7d was defined as midpoint between highest and lowest *G. ruber* $\delta^{18}O$ values (Lisiecki and Raymo 2005; Pang et al. 2021).

4.2 Principal Component Analysis

Principal Component Analysis was conducted in order to identify patterns and groupings in planktonic foraminifera and coccolithophores assemblages in response to Terminations and glacial – interglacial cycles. Principal Component Analysis (PCA) is a dimension-reducing, mathematical algorithm for analysing data, which reduces number of variables in a given dataset. The reduction is obtained through rotation of the original variables. New variables are the principal components (PCs) which represent linear functions of the original variables and explain maximum variance along a specific distance. Furthermore, PCs indicate coordinates of the variables in a rotated system. PCA is applied on a correlation matrix of the dataset, which is transformed into a covariance matrix and used as a measure of similarity, whereas the dissimilarity measure is the Euclidean distance between a pair of variables. The covariance matrix is thereafter used to calculate the eigenvectors and eigenvalues of the rotated variables. The eigenvectors represent the direction of maximum variance of the data in a rotated system and the eigenvalues are the measure of importance of the variance explained by a corresponding eigenvector or PCA axes (Nichols 1997; Jolliffe 2005; Ringnér 2008; Borcard et al. 2011b).

In this study we used *RStudio* package *vegan* to conduct principal components analysis on the relative abundances of planktonic foraminifera and coccolithophores. For choosing the principal components with most variance, Kaiser – Guttman criterion and the Broken Stick method were applied (see appendix: Fig. 25) using the *R* code provided in (Borcard et al. 2011b). In order to assess changes of biodiversity patterns over different timescales, principal component analyses were conducted on glacial – interglacial timescales covering individual Terminations and on multi-millennial timescale of around 300 ka covering Terminations I, II and III (Lewandowska et al. 2020). Principal components values were thereafter plotted against the age.

4.3 Alpha Diversity Indices

Alpha diversity is a diversity measured at the habitat level and used to characterize the communities (Thukral 2017). Planktonic foraminifera and coccolithophores assemblages were analysed on α-diversity where we used following indices: Species Richness, Gini – Simpson and Shannon – Wiener indices, and Evenness. Furthermore, Hill – Numbers were applied on Gini – Simpson and Shannon – Wiener indices. Major difference between species richness, Hill – Shannon and Hill – Simpson diversity metrics is the property of how rare species are characterized. Species richness is very sensitive to rare species, sample size and standardization method and can be effectively applied only if the community composition is completely known. Hill – Simpson index applies reciprocal scale, therefore the index is best applied to characterize relative abundances of the most common species in a given community. Hill – Shannon index is considered as a better index for characterizing biodiversity changes as species distributions can be described by log-normal distribution. Moreover, Hill – Shannon index is robust to under sampling and representation of the rare species (Mauerer and McGill 2011; Roswell et al. 2021).

We analysed samples on α-diversity in order to be able to characterize species community structure and community changes over multiple glacial – interglacial cycles. Furthermore, information on α-diversity provides insights into the changes of community structure over time. However, we used only Hill – Shannon and Pielou Evenness indices for further discussion and evaluation of α-diversity of planktonic foraminifera and coccolithophores assemblages, as they are robust to under sampling and do not under- or overrepresent rare species (Mauerer and McGill 2011; Roswell et al. 2021).

Species Richness is a measure of variety or diversity in a given community and represents number of total species in a specific sample or in our case age/depth.

Gini – Simpson Index is a measure of species diversity, which is based on dominance of the most common and dominant species. The index is not affected by rare species and considers number of species and their relative abundances in a sample. Mathematically it expresses the probability that any two individuals from the sample will belong to the same species. In *RStudio* package *vegan*, Simpson Index is calculated as follows:

$$1 - D = \sum_{i=1}^{s} p_i^2$$

where D is the calculated Simpson Index, p_i is the relative abundance of the i-th species and s is the number of species. Values of the resulted index range from 0 to 1, with higher values indicating low probability that two species belong to the same species and therefore resulting in higher biodiversity values (Fath 2019; Oksanen et al. 2020).

Shannon Entropy / Shannon – Wiener Index is a measure of entropy, which describes the uncertainty in the sampling process (Jost 2006, Roswell 2021). However, it is widely used as a measure of species diversity. Advantage of this index is that it is not affected by the sample size and facilitates considerable amount of information in one expression. In *RStudio* package *vegan* Shannon Index is calculated as follows:

$$H = -\sum_{i=1}^{n} p_i \ln p_i$$

where *H* is the index of species diversity, p_i is the relative abundance of the *i*-th species and *n* is the number of the *i*-th species. Shannon – Wiener index is widely used in detecting discriminability between different sites and samples. Low values indicate low biodiversity, with the index value equals 0 indicating that the sample has only one species (Spellerberg and Fedor 2003; Thukral 2017; Fath 2019).

Nevertheless, (Jost 2006) argues on the usability and interpretability of the Shannon and Gini – Simpson indices in this form, as they indicate entropy and not the actual diversity of the community in a given sample. Furthermore, Shannon and Gini – Simpson indices measure different types of entropies and in different units, which makes them difficult to compare with each other. Therefore, a conversation of these indices is needed, which is performed through Hill – Numbers described by (Hill 1973).

Hill – Shannon Index represents number of equally common species needed to attain specific value of a diversity index and does not exaggerate abundances of rare or common species. In general, it converts diversity index into number of species instead of values between 0 and 1. Advantage of converting indices like Shannon or Gini – Simpson is that it makes them more comparable with each other (Hill 1973; Jost 2006; Roswell et al. 2021). The conversion is performed in *RStudio* as follows:

$$H' = e^{H}$$

where *H'* is the Hill-Shannon index and *H* is the Shannon – Wiener entropy. Thereafter, values were rescaled through min-max normalization as follows:

$$x' = \frac{x - \min(x)}{\max(x) - \min(x)}$$

where *x'* is the normalized value and *x* is the original value. Subsequently, the rate of change was obtained as the slope of linear regression from the normalized Hill – Shannon values as % per ka.

Hill – Simpson Index is similar to Hill – Shannon index but utilizes reciprocal scale instead of logarithmic and emphasizes common species (Hill 1973; Jost 2006; Roswell et al. 2021). The conversion from entropy measure to diversity is performed in *RStudio* as follows:

$$D' = \frac{1}{1-D}$$

where *D'* is the Hill – Simpson index and *D* is the Gini – Simpson entropy.

Evenness / Pielou Evenness Index measures how well and evenly each species is represented in a sample. The values range from 0 to 1, where values closely to 0 indicate lowest equitability and dominance of only few species and values closely to 1 indicate highest equitability and even representation of the species in a sample (Fedor and Zvaríková 2019). Pielou Evenness Index was calculated in *RStudio* (Posit team 2022) as follows:

$$E_H = \frac{H}{\ln S}$$

where E_H is the evenness based on Shannon Index, *H* is the Shannon Index and *S* is species richness.

4.4 Beta Diversity Indices

Beta diversity is used to measure spatial and temporal variations or biological turnovers in species composition and abundances (Barwell et al. 2015). In this study we applied β-diversity indices to identify species turnovers at millennial and on multi-millennial timescales covering the last 300 ka. Planktonic foraminifera and coccolithophores assemblages were analysed on β-diversity using Jaccard and Morisita – Horn measures. The Jaccard index is based on the binary presence-absence data and does not consider relative abundances of the species. The index is therefore very susceptible to under sampling and rare species. Furthermore, the application of the Jaccard index requires complete knowledge of the species community and is therefore not suitable for identifying ecological trends and species turnovers in our case (Barwell et al. 2015). The results of

Jaccard index are provided in supplementary (see appendix: Fig. 26) but were not considered in further discussion. In order to adequately identify ecological patterns over time we used Morisita – Horn overlap measure, as the measure is very sensitive to detecting turnovers, abundance differences and species turnover (Jost et al. 2011; Barwell et al. 2015). Moreover, the index is easily applied by the statistical software *R* (R Core Team 2021) and is regarded as one of the most robust measures (Jost et al. 2011).

Jaccard dissimilarity/similarity measure is an incidence-based measure based on the presence or absence of the species. The index measures number of shared species that are common to both assemblages in relation to total number of species in both assemblages. The Jaccard index is defined as:

$$J = \frac{a}{a + b + c}$$

where *a* is the number of shared species, *b* is the number of unique species in the first assemblage and *c* is the number of unique species in the second assemblage (Jost et al. 2011; Barwell et al. 2015). For this study we used *RStudio* and the package *vegan* to compute Jaccard index (Oksanen et al. 2020; Posit team 2022). The dissimilarity matrix was plotted in two different ways: sequentially to identify biodiversity turnovers at millennial timescale and individual sample versus oldest sample to identify biodiversity turnovers at multi-millennial timescale covering the last two glacial – interglacial periods and recent deglaciation period. Sequential dissimilarity (further indicated as J_{seq}) values indicate the difference between two adjacent samples, whereas individual versus oldest (further indicated as J_{old}) indicate dissimilarity values between one sample versus the oldest sample.

Morisita – Horn overlap measure is an abundance-based dissimilarity index dominated by the most abundant species in the sample, with rare species having only little effect on the index and is robust against under-sampling. The index is based on the measurement of the squared differences of the relative abundances of the species and is calculated as follows:

$$S = 1 - \frac{\sum_{i=1}^{S}(p_{i1} - p_{i2})^2}{\sum_{i=1}^{S} {p_{i1}}^2 + \sum_{i=1}^{S} {p_{i2}}^2}$$

where p_{i1} is the relative abundance of the *i*-th species in the first assemblage and p_{i2} is the relative abundance of the *i*-th species in the second assemblage (Jost et al. 2011; Barwell et al. 2015). For this study we used *RStudio* and the package *vegan* to compute Morisita – Horn overlap measure (Oksanen et al. 2020; Posit team 2022). The dissimilarity matrix was measured in two different ways: sequentially and individual sample versus oldest sample. Sequential dissimilarity (further indicated as S_{seq}) values indicate the difference between two adjacent samples and cover dissimilarity indices at millennial timescale, whereas individual versus oldest (further indicated as S_{old}) indicate dissimilarity values between one sample versus the oldest sample. Thereafter, we obtained the rate of change as the slope linear regression line based on S_{old} plot.

5. Previous study after Tangunan et al. (2017)

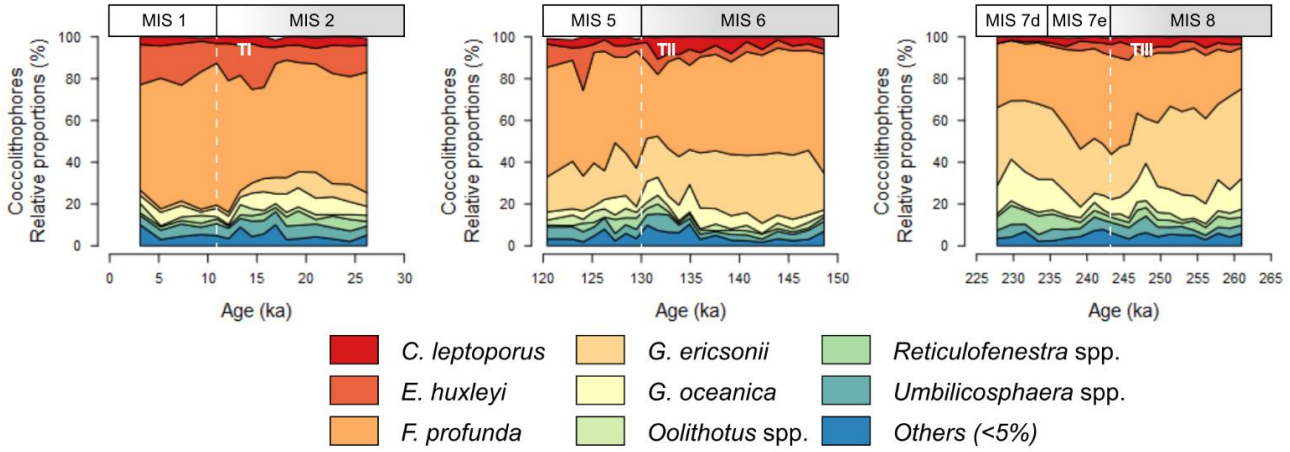

Fig. 7: Stacked relative abundances of most common coccolithophore species (relative abundance >5%) in GeoB12613-1. Species with relative abundances of <5% were summed together under *"Others"*. White dashed line represents the boundary between the glacial and interglacial periods. Upper panel indicates: MIS = Marine Isotopic Stage, light grey = Glacial periods, white = Interglacial periods, light grey gradient indicates deglaciations/Termination events TI, TII and TIII.

Coccolithophore assemblages have been analysed by (Tangunan et al. 2017) and 34 species in total were identified. Species composition is dominated by *F. profunda* with mean relative abundance of 42%, *G. ericsonii* (31.3%), *E. huxleyi* (14.9%) and *G. oceanica* (6.7%). Other important contributors to species composition are *C. leptoporus*, *Oolithotus* spp., *Reticulofenestra* spp. and *Umbilicosphaera* spp. General trends indicate increase in mean relative abundances of *F. profunda* and *E. huxleyi* and decrease in mean relative abundances of *G. ericsonii* and *G. oceanica* (Fig. 7) from MIS 8 to MIS 1.

5.1.1 Relative abundances of coccolithophores during MIS 8/MIS 7e-7d

The MIS 8 assemblage is dominated (species with relative abundance >5%) by *G. ericsonii*, followed by *F. profunda* and *G. oceanica*. During Termination III (TIII) a considerable decrease in relative abundance of *G. ericsonii* is observed, whereas relative abundance of *F. profunda* increases and the species becomes dominant throughout TIII and MIS 7e. The time period MIS 7e to MIS 7d is characterized by a further increase in relative abundance of *G. ericsonii* and decrease in relative abundance of *F. profunda* (Fig. 7).

5.1.2 Relative abundances of coccolithophores during MIS 6/MIS 5

The MIS 6 assemblage is dominated by *F. profunda*, followed by *G. ericsonii* and *G. oceanica*, which stay dominant throughout Termination II (TII) and MIS 5. Relative abundance of *F. profunda* decreases during TII but increases towards MIS 5, whereas relative abundance of *G. ericsonii* increase during TII but decreases towards MIS 5. Relative abundance of *G. oceanica* on the other hand decreases towards MIS 5 (Fig. 7).

5.1.3 Relative abundances of coccolithophores during MIS 2/MIS 1

The MIS 2 assemblage is dominated by *F. profunda*, *G. ericsonii*, *G. oceanica*, *C. leptoporus* and *E. huxleyi*. Relative abundance of *F. profunda* increase towards the MIS 1 and the species stays consistently dominant throughout the glacial – interglacial cycle. Relative abundance of *G. ericsonii* on the other hand decreases, especially towards the MIS 1. Another notable change in assemblage composition is an increase in relative abundance of *E. huxleyi* towards the MIS 1.

5.1.4 Coccolithophore species

In following, coccolithophores species with relative occurrence >5% in core GeoB12613-1 are listed.

Calcidiscus leptoporus (Murray & Blackman 1898) (**Plate I** - 1)

Ecology and environment: *C. leptoporus* coccolithophore assemblage is comprised of three morphotypes, with slightly different ecological preferences: large, intermediate, and small. Large morphotype is found predominantly in high productivity, mesotrophic environments (Ziveri et al. 2004). Intermediate morphotype is on the other hand predominantly found in cool, nutrient poor waters. Distribution of small morphotype is patchy and unclear, as noted by Ziveri et al. (2004). In general, intermediate morphotype dominates the *C. leptoporus* assemblage and has a broad geographical distribution. The large morphotype, is abundant in equatorial regions and is absent in higher latitudes. Furthermore, the assemblage exhibits differences in its life cycle phases in relation to nutrient availability (Ziveri et al. 2004). The haploid stage is adapted to more nutrient-depleted and stratified waters, whereas the diploid stage is more adapted to upwelling areas and therefore nutrient-rich environment, indicating that the distribution of *C. leptoporus* is of seasonal character (Renaud et al. 2002; Houdan et al. 2006).

Emiliania huxleyi (Lohman 1902) (**Plate I** - 2)

Ecology and environment: *E. huxleyi* is a cosmopolitan coccolithophore species and is only absent in higher latitudes. *Emiliania huxleyi* produces extensive blooms, which occur in eutrophic regions and are usually associated with low chlorophyll α concentrations. Nevertheless, the species is also highly abundant in permanently oligotrophic waters. *Emiliania huxleyi* blooms have a significant environmental impact on the regional scale. Excessive production of the coccoliths leads to an increased water albedo, dimethylsulfide (DMS) production, higher fluxes of $CaCO_3$ out of the surface waters and alteration in the uptake of CO_2 in the ocean. Main environmental factors affecting *E. huxleyi* blooms are increased light conditions, limited silicate content and high carbonate saturation of the surface waters (Tyrrell and Merico 2004). In general, *E. huxleyi* prefers stable, stratified, and nutrient rich water columns (Rogalla and Andruleit 2005).

Florisphaera profunda (Okada & Honjo, 1973) (**Plate I** - 3)

Ecology and environment: *F. profunda* is restricted to the lower euphotic zone in the tropical and subtropical regions of the ocean. As suggested by Molfino & McIntyre (1990), the species can be used to trace the variations in the depth of the nutricline. The species flourishes when the nutricline is deep and the upper euphotic zone is nutrient depleted (Molfino and McIntyre 1990; Rogalla and Andruleit 2005; Krumhardt et al. 2017). Furthermore, highest abundances of *F. profunda* are found during the onset of summer monsoon, when primary productivity is in general low. Subsequently, with the intensifying of the summer monsoon and therefore upwelling, *F. profunda* abundances decrease (Broerse et al. 2000).

Gephyrocapsa ericsonii (McIntyre & Bé, 1967) (**Plate I** - 4)

Ecology and environment: distribution of *G. ericsonii* is mostly independent of water temperature and depth of the thermocline. The species is very abundant in nutrient rich and stratified water columns. Ecological preferences are similar to *E. huxleyi*, however, *G. ericsonii* occurs only occasionally in extant coccolithophores assemblages. Paleorecords indicate decrease of *G. ericsonii* towards the Holocene/MIS 1 and an increase of *E. huxleyi*, which can be attributed to an evolutionary replacement of *G. ericsonii* (Rogalla and Andruleit 2005).

Gephyrocapsa oceanica (Kamptner, 1943) (**Plate I** - 5)

Ecology and environment: *G. oceanica* is associated with high nutrient supply in warm (temperature range between 12 and 30°C), tropical to subtropical regions of the ocean. Furthermore, the species is dominant during upwelling relaxation and upwelling maximum and therefore is dominant during summer monsoon conditions, especially in equatorial and coastal upwelling areas, and on continental shelves (Broerse et al. 2000; Ziveri et al. 2004; Rogalla and Andruleit 2005).

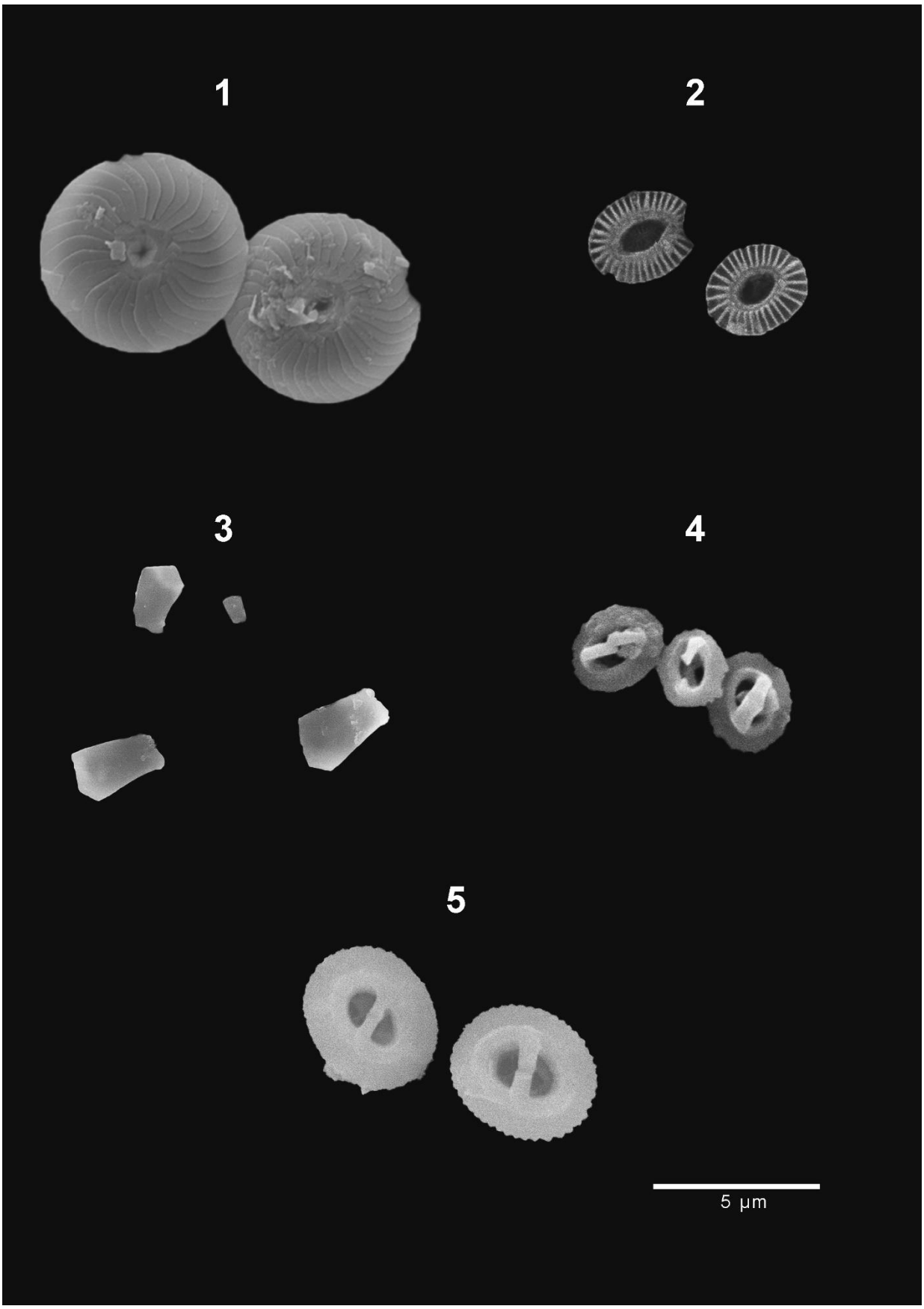

Plate I. Scanning electron microscope photographs of the most common and frequent coccoliths: 1) *Calcidiscus leptoporus*, 2) *Emiliania huxleyi*, 3) *Florisphaera profunda*, 4) *Gephyrocapsa ericsonii*, 5) *Gephyrocapsa oceanica* after (Tangunan et al. 2017).

5.1.5 Paleoceanographic interpretation based on coccolithophores record

The previous study on coccolithophores by Tangunan et al. (2017), suggest that a relatively stable and stratified water column prevailed over the last 300 ka in the studied area, as indicated by the relative abundance of *F. profunda*. Furthermore, this species is indicative of a deep nutricline, low total primary production and decreased turbidity. Coccolithophore species *G. oceanica* is regarded as an indicator for relatively high surface water productivity conditions. Consequently, high abundance of *G. oceanica* between 300 to 160 ka indicates high surface water productivity conditions and high nutrient availability (Fig. 7 & Fig. 8). Subsequently, Tangunan et al. (2017) observed a decline in *G. oceanica* abundance towards the MIS 1 suggesting a decrease in productivity and nutrient availability (Tangunan et al. 2017).

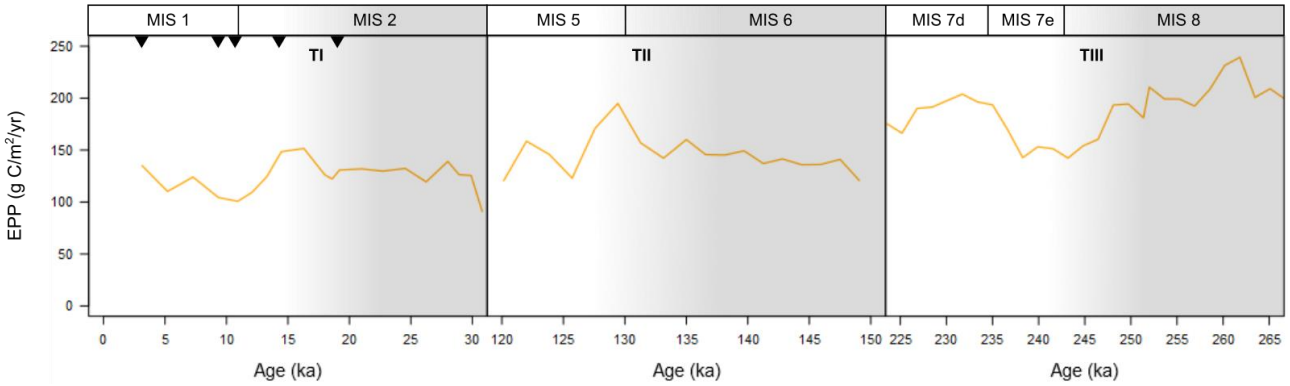

Fig. 8: Estimated primary productivity based on relative abundance of *F. profunda* after (Tangunan et al. 2017).

Productivity dynamics over the last two glacial – interglacial cycles are highly variable. The interval from MIS 8 to MIS 6 is characterized by relatively high productivity conditions. The period of high productivity is interrupted during TIII, due to highly stratified waters (Fig. 8 & Table 8). The period MIS 6 is characterized by predominantly oligotrophic conditions, with relatively high productivity but large amplitude in variability, as reported by the study after Tangunan et al. (2017). Subsequently, productivity decreased during MIS 5 and the water column became more stratified. Low surface water productivity and strong stratification characterize the interval between MIS 3 to Holocene, with oligotrophic and stratified conditions prevailing in the modern Indian Ocean. This findings imply, that coccolithophore communities in the studied area were not dependent on temperature but rather on nutrient availability (Tangunan et al. 2017).

The study by Tangunan et al. (2017), suggest that water column stratification and productivity dynamics are influenced by obliquity and precession cycles through atmospheric processes such as insolation intensity, Southern Oscillations, and monsoons. Furthermore, increase in nutrients in the equatorial IO during glacial periods is associated with global decrease in SST, subsequently weakening stratification and shoaling the thermocline. Possible mechanism for this process is a stronger summer monsoon and strengthening of the IO equatorial westerlies (IEW) during insolation maxima, which led to an intensified surface water circulation. These mechanisms might have shoaled the thermocline, delivering nutrients to the surface, subsequently increasing productivity. Another possible mechanism is a stronger NEMC, which could have transported surface waters northward, converging with EACC, thus resulting possible mixing, and shallowing of the mixed layer depth. Additionally, local perpetuations of the SC could carry nutrient-enriched waters from the upwelling regions (Tangunan et al. 2017).

6. Results

6.1 Relative abundances of planktonic foraminifera

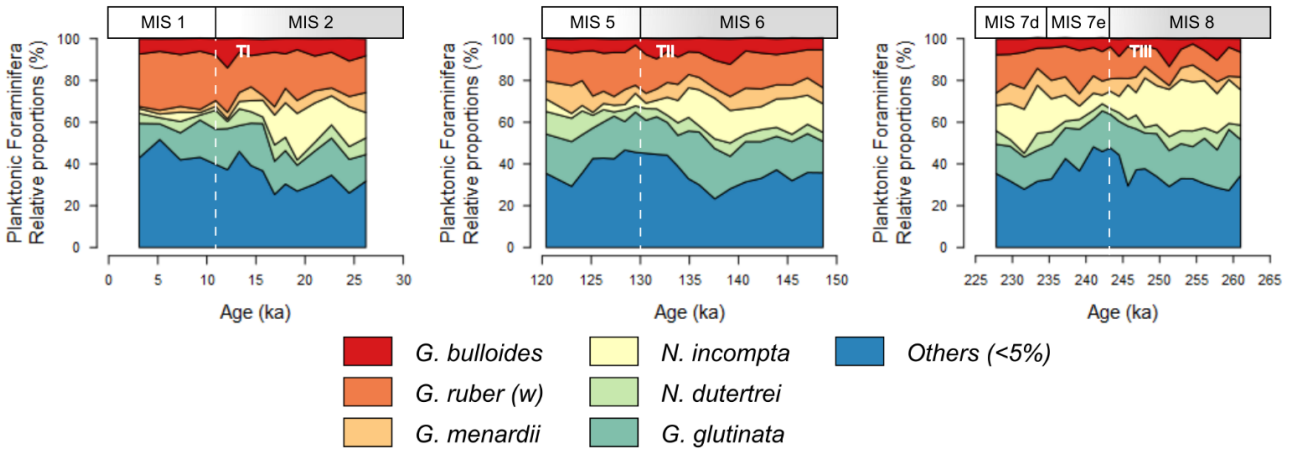

Fig. 9: Stacked relative abundances of most common planktonic foraminifera species (relative abundance >5%) in GeoB12613-1. Species with relative abundances of <5% were summed together under *"Others"*. White dashed line represents the boundary between the glacial and interglacial periods. Upper panel indicates: MIS = Marine Isotopic Stage, light grey = glacial periods, white = interglacial periods, light grey gradient indicates deglaciations/Termination events TI, TII and TIII.

We identified 36 planktonic foraminifera species (Table 6), which represent tropical to subtropical assemblages (Bé et al. 1977). Throughout the entire timescale species assemblage is dominated by *Globigerinita glutinata* with mean relative abundance of 17.55%, followed by *Globigerinoides ruber* (white) (16.34%), *Neogloboquadrina incompta* (11.73%), *Globigerina bulloides* (6.74%), *Globorotalia menardii* (6.10%) and *Neogloboquadrina dutertrei* (5.25%), comprising 63.71% of entire species composition (Fig. 9 & Table 6). Other important contributors to species composition are *G. falconensis*, *G. calida*, *G. siphonifera*, *G. trilobus*, *G. elongatus*, *G. ruber* (pink), *G. rubescens*, *G. tumida*, *G. ungulata* and *P. obliquiloculata*. General trends indicate considerable increase in relative abundance of *G. ruber* (white) and decrease of *N. incompta*. Minor increase in relative abundances is observed in *G. bulloides*, *G. siphonifera* and *P. obliquiloculata* (Fig. 9).

6.1.1 Relative abundances of planktonic foraminifera during MIS 8/MIS 7e-7d

The MIS 8 assemblage is dominated (species with relative abundance >5%) by *N. incompta*, followed by *G. glutinata* and *G. ruber* (white). During Termination III (TIII) species dominance shifts to *G. glutinata*, followed by *N. incompta* and *G. ruber* (white). Further changes in dominance are observed during MIS 7e, which is dominated by *G. glutinata*, *G. ruber* (white), *N. incompta* and *G. menardii*. During MIS 7d, dominance shifts to *N. incompta*, followed by *G. glutinata*, *G. ruber* (white) and *G. menardii*. Another notable change is increase in relative abundance of *G. menardii* from mean value of 5.17% during MIS 8 to mean value of 8.38% during MIS 7d. Other important contributors to species composition are *G. dutertrei*, *G. bulloides* and *G. trilobus* (Fig. 9, Table 6).

6.1.2 Relative abundances of planktonic foraminifera during MIS 6/MIS 5

The MIS 6 assemblage is dominated by *G. glutinata*, followed by *G. ruber* (white) and *N. incompta*. Species *G. glutinata* and *G. ruber* (white) stay consistently dominant throughout Termination II (TII) and MIS 5. Relative abundance of *N. incompta* on the other hand declines from mean value of 14.90% during MIS 6 to mean value of 3.07% during MIS 5. Other notable changes are decrease in relative abundance of *G. bulloides* and increase in relative abundances of *G. menardii* and *G. trilobus* (Fig. 9, Table 6).

6.1.3 Relative abundances of planktonic foraminifera during MIS 2/MIS 1

The MIS 2 assemblage is dominated by *G. ruber* (white), followed by *G. glutinata* and *N. incompta*. Species *G. ruber* (white) and *G. glutinata* stay consistently dominant throughout Termination I (TI) and the MIS 1, whereas relative abundance of *N. incompta* decreases from mean value of 15.63% during MIS 2 to mean value of 2.70% during the MIS 1. Another notable changes in species dominance are increase in relative abundances of *G. bulloides*, *G. trilobus* and *G. siphonifera* and decrease in relative abundance of *G. menardii* (Fig. 9, Table 6).

6.1.4 Planktonic foraminifera species

In following, planktonic foraminifera species with relative occurrence >5% in core GeoB12613-1 are listed.

Globigerina bulloides (d'Orbigny 1826) (**Plate II** - 1)

Ecology and environment: mainly dwells above the thermocline within the upper 60 m of the water column and bears no symbionts. The diet consists primarily of algae (Schiebel and Hemleben 2017). *Globigerina bulloides* is associated with temperate to sub-polar water masses and upwelling. Distribution pattern is related to hydrologic conditions and prey availability. *Globigerina bulloides* is regarded as an opportunistic species and often dominates the foraminifera fauna, test flux, and sediment assemblages. The species is an indicator of upwelling environments and of seasonally enhanced primary productivity (Bé et al. 1977; Ding et al. 2006; Schiebel and Hemleben 2017).

Neogloboquadrina dutertrei (d'Orbigny 1839) (**Plate III** - 6)

Ecology and environment: the species feeds exclusively herbivorous and ingests algae during phytoplankton blooms. The algae are thereafter being digested or used as symbionts. *Neogloboquadrina dutertrei* is a frequent species in tropical to subtropical waters and may be present in temperate waters during summer. The species is related to the initial phase of the summer monsoonal upwelling and enhanced concentration of prey in surface waters of the northwestern Indian Ocean. Furthermore, *N. dutertrei* may adopt an opportunistic behaviour, occurring in increased numbers between surface and thermocline waters, as a result of increased food availability (Bé et al. 1977; Ding et al. 2006; Schiebel and Hemleben 2017; Anbuselvan and Senthil Nathan 2021).

Pulleniatina obliquiloculata (Parker and Jones 1865) (**Plate IV** - 3)

Ecology and environment: the diet of *P. obliquiloculata* consists primarily of chrysophytes and diatoms. *Pulleniatina obliquiloculata* is a cosmopolitan species and is regarded as a rare species in tropical to subtropical environments. The species dwells between the upper and lower surface mixed layers near thermocline and Deep Chlorophyll Maximum (DCM). Furthermore, *P. obliquiloculata* has high preservation potential, therefore biasing its proportions in sediment assemblages (Schiebel and Hemleben 2017).

Globigerinita glutinata (Egger 1893) (**Plate II** - 5)

Ecology and environment: the species exhibits two population maxima. The first population maximun follows enhanced phytoplankton production in the surface waters, whereas the second seasonal maximum occurs in fall, during wind-driven nutrient enrichment of the surface waters, which results in enhanced phytoplankton production at the nutricline. *Globigerinita glutinata* is an abundant species in subtropical to temperate waters and decreases in frequency towards the high latitudes. Furthermore, this species is associated with upwelling conditions (Ding et al. 2006; Schiebel and Hemleben 2017).

Globorotalia tumida (Brady 1877) (**Plate IV** - 1)

Ecology and environment: *G. tumida* is a rare species of the tropical to subtropical ocean. The species dwells in low productive subsurface waters at around 40 to 80 m water depth (Schiebel and Hemleben 2017).

Globoturborotalita rubescens (Hofker 1956) (**Plate III** - 4)

Ecology and environment: *G. rubescens* occurs in tropical to temperate surface waters (Conan and Brummer 2000; Schiebel and Hemleben 2017).

Globigerina falconensis (Blow 1959) (**Plate II** - 2)

Ecology and environment: *G. falconensis* is a symbiont bearing species and less opportunistic compared to *G. bulloides*. The species occurs at maximum abundance in January and February during the winter monsoon period (Conan and Brummer 2000; Schiebel and Hemleben 2017).

Globigerinella calida (Parker 1962) (**Plate II** - 3)

Ecology and environment: *G. calida* occurs in mesotrophic waters of the tropical to temperate ocean. In the Arabian Sea, *G. calida* occurs throughout the upper 100 m of the water column in the marginal upwelling regions and during the intermonsoon and winter monsoon seasons (Schiebel and Hemleben 2017).

Trilobatus trilobus (Spezzaferri et al. 2015) (**Plate II** - 4)

Ecology and environment: *T. trilobus* is a symbiont bearing species, which dwells predominantly in a mixed-layer between 0 and 50 m water depth. The species is abundant in subtropical to tropical oceans and occurs under oligotrophic conditions, with habitat depth deepening during upwelling conditions (Schiebel and Hemleben 2017; Sosdian and Lear 2020; Anbuselvan and Senthil Nathan 2021; Tapia et al. 2022).

***Globigerinoides ruber* (white)** (d'Orbigny 1839) (**Plate III** - 1)

Ecology and environment: *G. ruber* is a symbiont bearing species and is very adaptable to changing ecological conditions. *Globigerinoides ruber* is the most frequent species in the tropical to subtropical waters and occurs in eutrophic and oligotrophic regions. The species dwells at a nutricline depth and is regarded as one of the shallowest dwelling planktonic foraminifera. Furthermore, *G. ruber* is the most tolerant species to low sea surface salinity and has a wide temperature range as well as salinity limits (Bé et al. 1977; Conan and Brummer 2000; Ding et al. 2006; Schiebel and Hemleben 2017).

Globorotalia menardii (Parker, Jones and Brady 1865) (**Plate IV** - 2)

Ecology and environment: *G. menardii* feeds predominantly on phytoplankton, consisting of diatoms and chrysophytes. Occasionally, the species feed on omnivorous diet and some of the ingested phytoplankton are used as symbionts. *Globorotalia menardii* dwells predominantly in the surface ocean, with highest abundances found at pycnocline/nutricline depths and depths of DCM (Schiebel and Hemleben 2017). Furthermore, *G. menardii* is a cosmopolitan species found mostly in tropical to subtropical waters, with preference for high SST. In addition, this species is associated with productive areas and upwelling (Bé et al. 1977; Ding et al. 2006).

Neogloboquadrina incompta (Cifelli 1961) (**Plate II** - 6)

Ecology and environment: *N. incompta* is a surface dwelling species of the temperate ocean. At periods of high food availability, the species is outnumbered by *G. bulloides* and *Turborotalita quinqueloba* as they are more opportunistic. At periods of low-productive conditions, as a result of a stratified surface water column, the species dominates the fauna with low standing stocks (Schiebel and Hemleben 2017). In addition, this species is usually associated with upwelling conditions (Bé et al. 1977; Ding et al. 2006).

Globigerinella siphonifera (d'Orbigny 1839) (**Plate II** - 7)

Ecology and environment: *G. siphonifera* is most frequent in the tropical to subtropical ocean (Schiebel and Hemleben 2017). Species abundance increases in nutrient rich areas and increased upwelling activity during summer monsoons (Anbuselvan and Senthil Nathan 2021).

Globorotalia ungulata (Bermudez 1960) (**Plate III** - 5)

Ecology and environment: *G. ungulata* is a rare species, with a similar distribution to *G. menardii*, and occurs sporadically in tropical and subtropical waters (Schiebel and Hemleben 2017).

***Globigerinoides elongatus* / *Globigerinoides ruber* s.l.** (d'Orbigny 1826) (**Plate III** - 2)

Ecology and environment: *G. elongatus* / *G. ruber* s.l. is a morphotype of *G. ruber*, with similar ecology. However, the species dwells below 30 m (Wang 2000; Schiebel and Hemleben 2017).

Globigerinoides ruber (pink) (d'Orbigny 1839) (**Plate III** - 3)

Ecology and environment: *G. ruber* (pink) is a pink variety of *G. ruber* stained by pink pigments. The pink variety is a shallow dwelling planktonic foraminifera and bears symbiotic zooxanthellae, which require the species to dwell in a near surface warm-water habitat (Thompson et al. 1979). Moreover, the species went extinct in the Red Sea and the Indo-Pacific region at the MIS 5e/6 transition (Thompson et al. 1979; Wang 2000). *Globigerinoides ruber* (pink) occurs in tropical areas of high surface temperature and topographically shallow regions, where carbonate dissolution is relatively low (Wang 2000; Schiebel and Hemleben 2017).

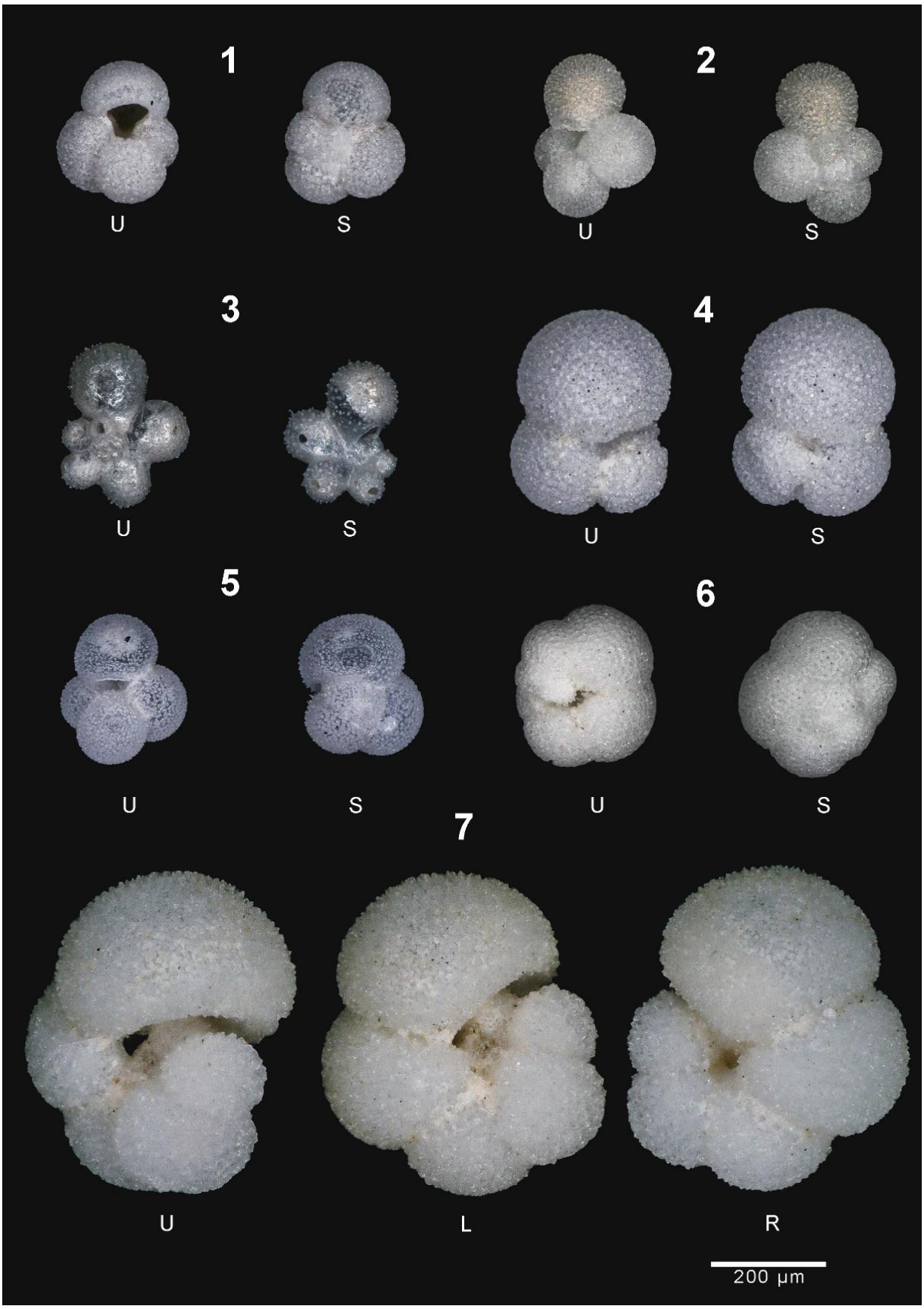

Plate II. Most common and relevant planktonic foraminifera species found in the analysed core section. U = ventral view, S = dorsal view, L = view of the left side of aperture, R = view of the right side of aperture: 1) *Globigerina bulloides*, 2) *Globigerina falconensis*, 3) *Globigerinella calida*, 4) *Trilobatus trilobus*, 5) *Globigerinita glutinata*, 6) *Neogloboquadrina incompta*, 7) *Globigerinella siphonifera*.

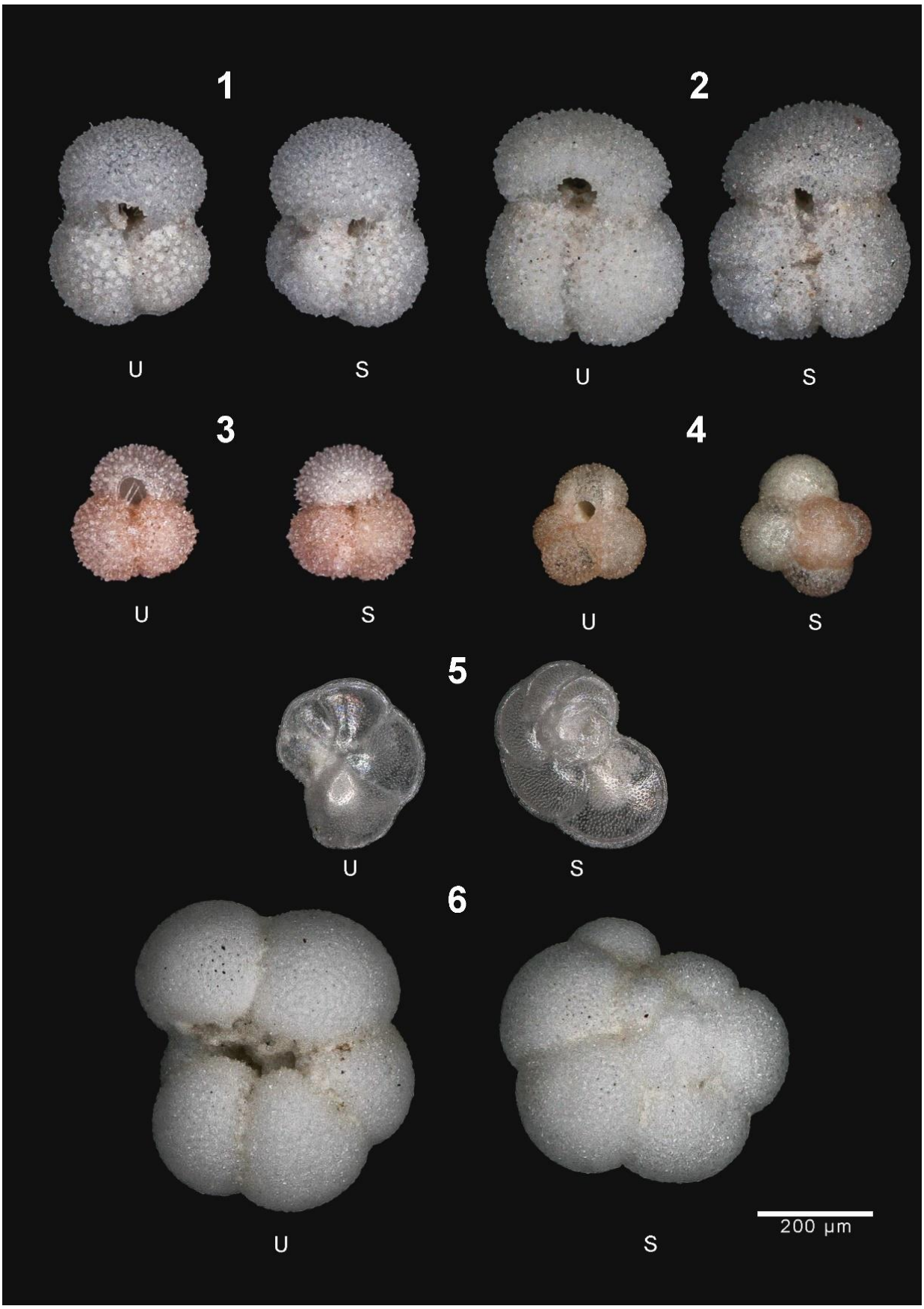

Plate III. Most common and relevant planktonic foraminifera species found in the analysed core section. U = ventral view, S = dorsal view: 1) *Globigerinoides ruber* (white), 2) *Globigerinoides elongatus*, 3) *Globigerinoides ruber* (pink), 4) *Globoturborotalita rubescens*, 5) *Globorotalia ungulata*, 6) *Neogloboquadrina dutertrei*.

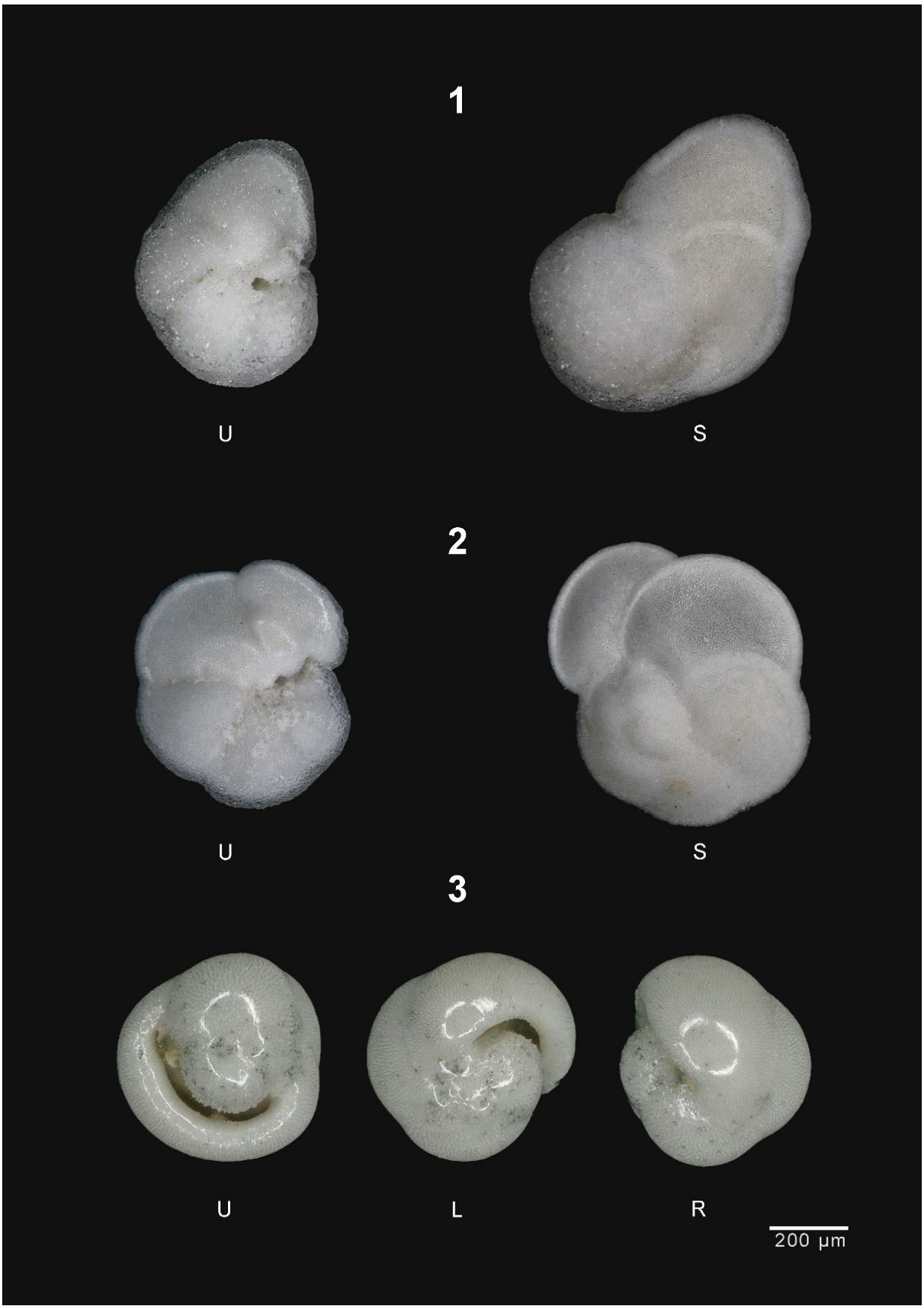

Plate IV. Most common and relevant planktonic foraminifera species found in the analysed core section. U = ventral view, S = dorsal view, L = view of the left side of aperture, R = view of the right side of aperture: 1) *Globorotalia tumida*, 2) *Globorotalia menardii*, 3) *Pulleniatina obliquiloculata*.

6.2 Principal components of planktonic foraminifera and coccolithophores

Principal components analysis of planktonic foraminifera and coccolithophores were performed on glacial – interglacial and on multi-glacial – interglacial timescales. First principal component values (PC1) or also indicated as species scores in *RStudio* package *vegan* were plotted against the age (Fig. 10 & Fig. 11).

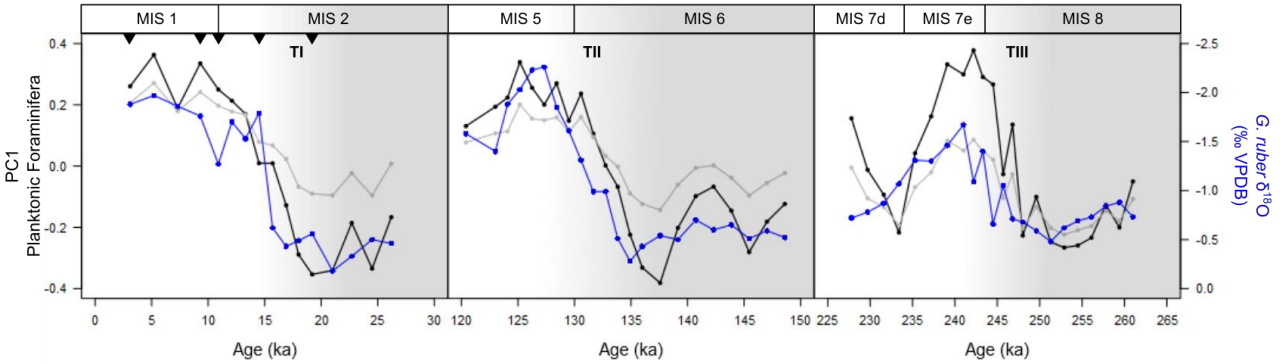

Fig. 10: First Principal Components (PC1) for planktonic foraminifera. Black solid line represents PCA analysis on glacial – interglacial timescales, grey solid line represents PCA analysis on multi-glacial – interglacial timescale and blue solid line represents *G. ruber* (white) $\delta^{18}O$ values.

The variance explained by PC1 of planktonic foraminifera for MIS 8/MIS 7 period is 56.58%, for MIS 6/MIS 5 period 52.45% and for MIS 2/MIS 1 56.58%. PC1 values are predominantly influenced by *N. incompta*, *G. ruber* (white), *G. trilobus*, *G. siphonifera*, *G. calida* and *G. glutinata*. On a multi-glacial – interglacial timescale the variance explained by PC1 equals 51.99%. PC1 values are in general low during glacial periods and increase rapidly during the Termination events. A notable increase in PC1 values is observed during MIS 7e with subsequent decrease during MIS 7d period. On a multi-glacial – interglacial timescale PC1 values follow similar trends as on glacial – interglacial timescales (Fig. 10).

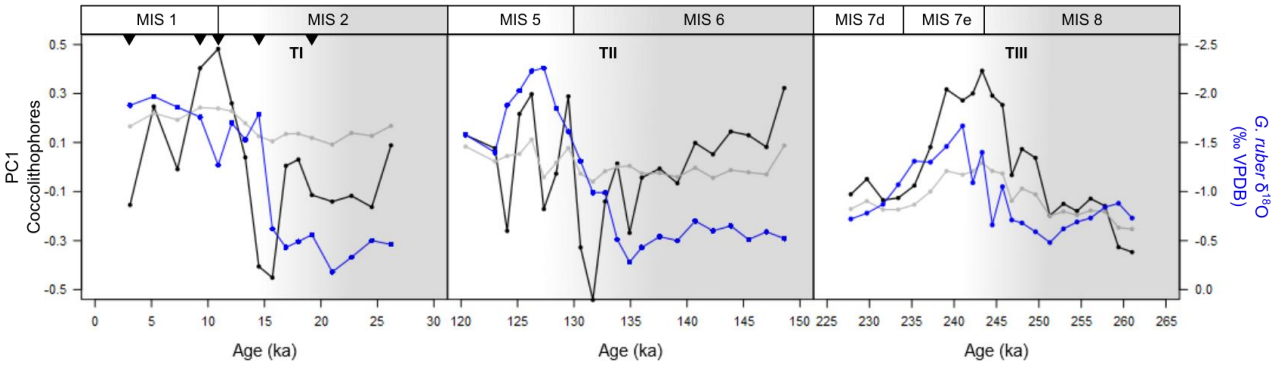

Fig. 11: First Principal Components (PC1) for coccolithophores. Black solid line represents PCA analysis on glacial – interglacial timescales, grey solid line represents PCA analysis on multi-glacial – interglacial timescale and blue solid line represents *G. ruber* (white) $\delta^{18}O$ values.

Variance explained by PC1 of coccolithophores for MIS 8/MIS7 period is 74.67%, for MIS 6/MIS 5 period 45.22% and for MIS 2/MIS 1 53.97%. PC1 values are predominantly influenced by *G. ericsonii*, *F. profunda*, *E. huxleyi* and *G. oceanica*. On a multi-glacial – interglacial timescale the variance explained by PC1 equals 80.06%. During MIS 8/MIS 7 the trend is similar to planktonic foraminifera. During MIS 6 PC1 values decrease with rapid decline during TII and show rapid increase during MIS 5. This trend is also observed during MIS 2/MIS 1 period. On a multi-glacial – interglacial timescale PC1 values do not follow glacial – interglacial trends (Fig. 11), instead a continuous increase in PC1 values is observed.

6.3 Alpha Diversity Indices

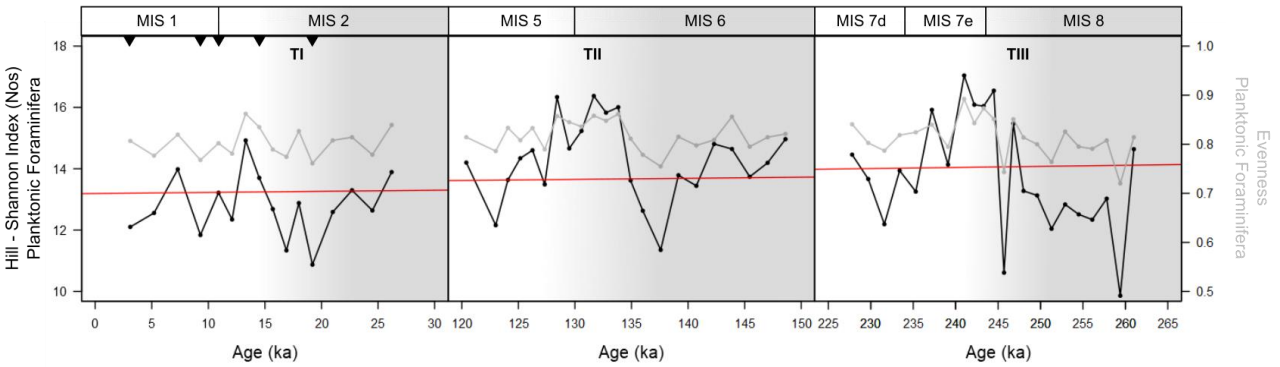

Fig. 12: Alpha diversity indices of planktonic foraminifera. Black solid line represents the Hill – Shannon index, grey solid line represents the Pielou Evenness index, red solid line represents linear regression model based on the entire dataset of the Hill – Shannon index.

Pielou Evenness Index (in following evenness) of planktonic foraminifera is higher than of coccolithophores. The index stays in general consistent throughout individual glacial – interglacial cycles and throughout multi-glacial – interglacial timescale (Fig. 12), with values ranging between 0.89 and 0.72. Evenness of coccolithophores on the other hand increases during Termination events and declines towards interglacial periods (Fig. 13), with evenness values ranging from 0.76 to 0.44. The slope of the linear regression model based on the entire dataset (Fig. 12) resulted in $s = 0.0035$, $R^2 = 0.03$, $p = 0.113$ (Table 1).

Table 1. Slope values, R^2 and *p*-values of the linear regression model of planktonic foraminifera based on the standard and normalized Hill – Shannon index.

Hill - Shannon	Slope (*s*)	R^2	*p*-value
Standard	0.0035	0.03	0.113
Normalized	0.0005	0.03	0.113

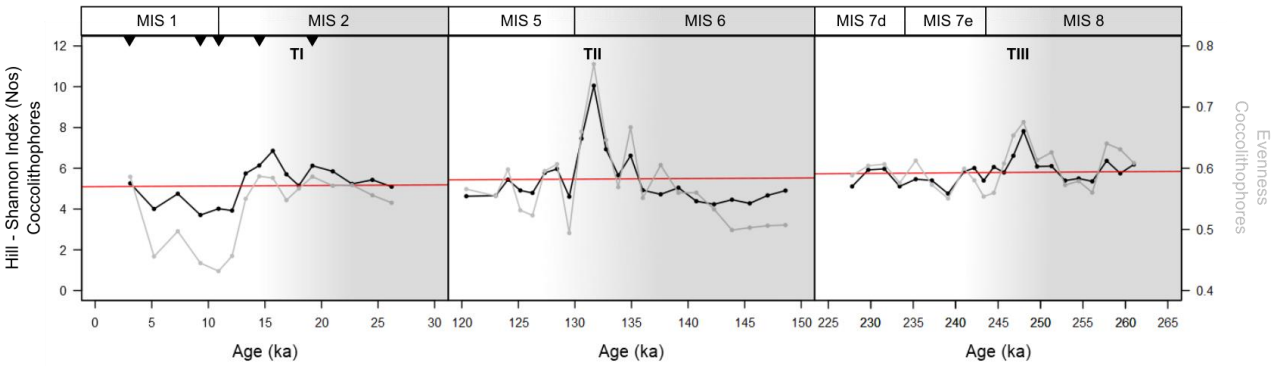

Fig. 13: Alpha diversity indices of coccolithophores. Black solid line represents Hill – Shannon index, grey solid line represents Pielou Evenness index, red solid line represents linear regression model based on the entire dataset of Hill – Shannon index and red dotted line represents linear regression model based on individual time intervals of Hill – Shannon index.

Hill-Shannon Index of planktonic foraminifera follows glacial – interglacial cycles, increasing during Termination events and exhibiting higher values during the interglacial periods. The index ranges between ~17 Nos (number of species) to ~10 Nos (Fig. 12). Hill – Shannon Index of coccolithophores is considerably lower than of planktonic foraminifera and ranges between ~11 Nos and ~4 Nos. The index is consistent throughout glacial and interglacial periods but increases during Termination events and declines to the lowest values during the MIS 1 with a mean of ~5 Nos (Fig. 13). Similar, to planktonic foraminifera, an overall slope of the linear regression model (Fig. 13) was obtained: $s = 0.0028$, $R^2 = 0.05$, $p = 0.054$ (Table 2).

Table 2. Slope values, R^2 and *p*-values of the linear regression model of coccolithophores based on the standard and normalized Hill – Shannon index.

Hill - Shannon	Slope (*s*)	R^2	*p*-value
Standard	0.0028	0.05	0.054
Normalized	0.0004	0.05	0.054

6.4 Beta Diversity Index

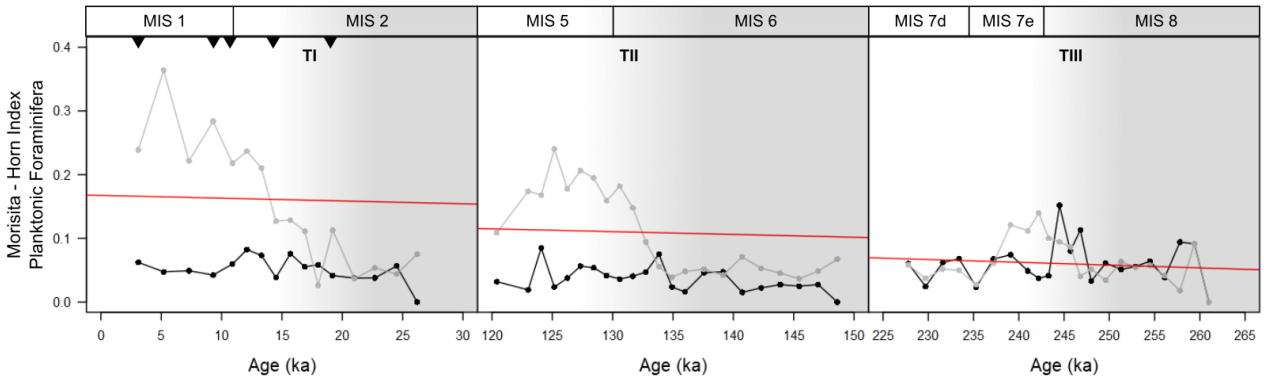

Fig. 14: Morisita – Horn overlap measure of planktonic foraminifera. Black solid line represents sequential dissimilarity (S_{seq}), grey solid line represents individual sample versus oldest sample dissimilarity (S_{old}), red solid line represents linear regression model based on the S_{old} on entire dataset.

Sequential Morisita – Horn values of planktonic foraminifera are relatively low and stay in general consistent throughout the studied intervals. However, a notable increase in S_{seq} values can be observed during Termination events. On multi-millennial timescales, S_{old} values are very low during glacial periods MIS 8, MIS 6, and MIS 2. However, S_{old} values increase significantly during Termination events and during interglacial periods, with considerably higher S_{old} values compared to glacial periods (Fig. 14). An overall slope of temporal β-diversity was obtained from the linear regression model: s = -0.00044, with R^2 = 0.26 and $p < 0.001$. As Morisita – Horn index ranges between 0 and 1, the slope can be expressed as a rate of change in %: 0.044 %/ka.

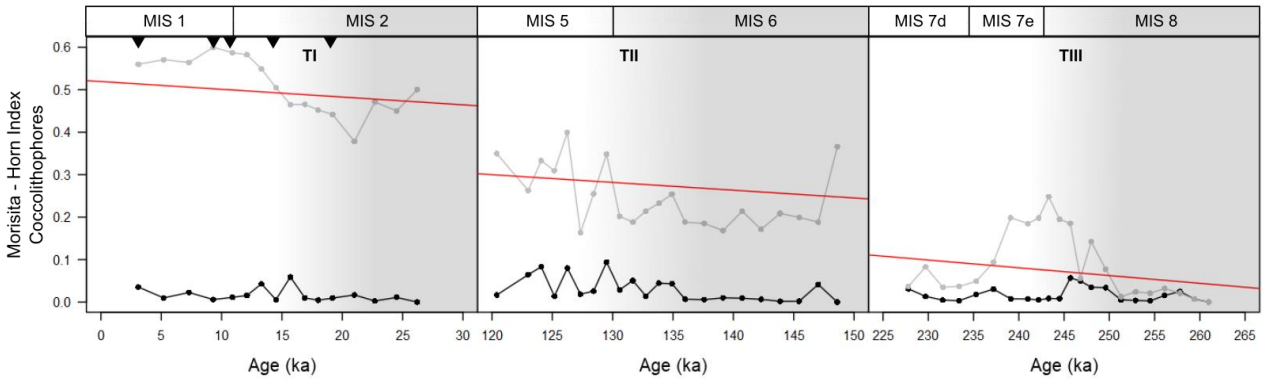

Fig. 15: Morisita – Horn overlap measure of coccolithophores. Black solid line represents sequential dissimilarity (S_{seq}), grey solid line represents individual sample versus oldest sample dissimilarity (S_{old}), red solid line represents linear regression model based on the S_{old} on entire dataset.

Sequential Morisita – Horn Index values of coccolithophores are low throughout glacial and interglacial periods, with short but notable increases during Termination events. Over multiple-glacial – interglacial cycles, S_{old} is very low during MIS 8 but increases with each subsequent glacial period. Furthermore, S_{old} values increase during Termination events and are considerably higher during interglacial periods of MIS 5 and MIS 1. The overall trend of Morisita – Horn index in coccolithophores is an increase of S_{old} values throughout multiple-glacial – interglacial cycles (Fig. 15). An overall slope of temporal β-diversity was obtained from

linear regression model: s = -0.00183, with R^2 = 0.85 and p < 0.001. Similar to planktonic foraminifera, the slope can be expressed as a rate of change in %: 0.183 %/ka, which is approximately four times higher compared to the rate of change in planktonic foraminifera.

In addition, based on the normalized Hill-Shannon index (Table 1 & Table 2) and Morisita – Horn dissimilarity index (Fig. 14 & Fig. 15) we obtained following slopes expressed as a rate of change in %/ka:

Table 3. Summary of the slopes expressed as a rate of change in %/ka obtained from the normalized Hill-Shannon index and Morisita – Horn dissimilarity index.

	α-diversity	β-diversity
Coccolithophores	0.04	0.18
Planktonic Foraminifera	0.05	0.04

6.4.1 Distribution of Morisita – Horn dissimilarity values

Table 4. Top depths in cm used for plotting boxplots of Morisita – Horn dissimilarity indices. Individual glacial and interglacial periods were defined based on the stratigraphic framework from (Fig. 6).

MIS 1	MIS 2	MIS 5	MIS 6	MIS 7e	MIS 8
2	46	302	346	590	622
6	50	306	350	594	626
10	54	310	354	598	630
14	58	314	358	602	634
18	62	318	362	606	638
-	-	322	366	610	642
-	-	326	370	-	646
-	-	330	374	-	650
-	-	-	378	-	654
-	-	-	382	-	658
-	-	-	386	-	-

Highest dissimilarity in planktonic foraminifera is observed between MIS 2 and MIS 1 periods (Mean: 0.19). Periods MIS 6/MIS 5 (Mean: 0.14) and MIS 8/MIS 7e (Mean: 0.15) show slightly lower dissimilarity values, with highest variability observed during MIS 8/MIS 7e periods. Dissimilarity values of coccolithophores are considerably lower, with highest variability observed between MIS 8 and MIS 7e periods. Interestingly, variability of dissimilarity values of coccolithophores decreases towards MIS 2/MIS 1 period (Fig. 16).

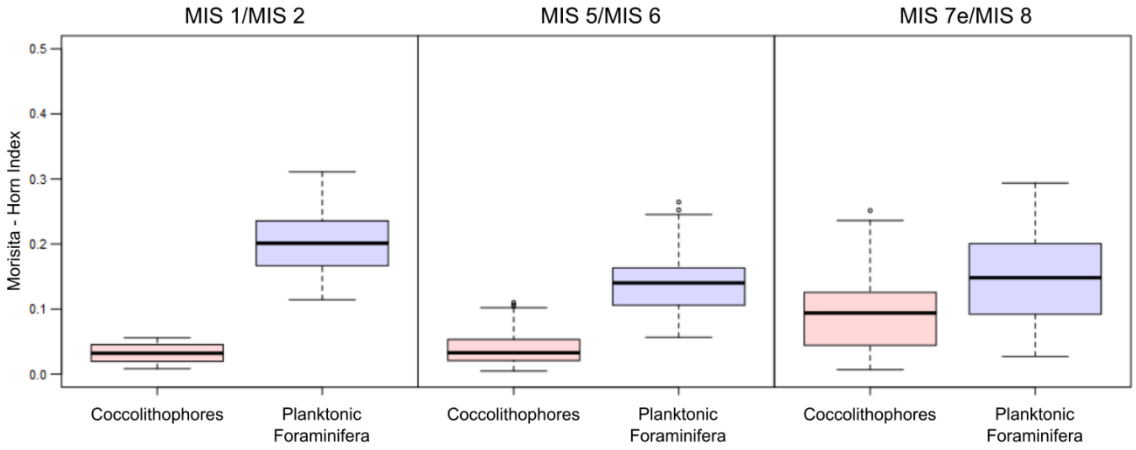

Fig. 16: Boxplots of Morisita – Horn dissimilarity indicating dissimilarities between glacial and interglacial periods based on (Table 4).

Planktonic foraminifera dissimilarity values of adjacent interglacial periods are relatively low (Fig. 17), with highest dissimilarity observed between MIS 1 and MIS 7e interglacial periods (Mean: 0.17). Similar trend is observed in dissimilarity values of coccolithophores, with highest variability and mean value observed between MIS 7e and MIS 1 periods (Fig. 17).

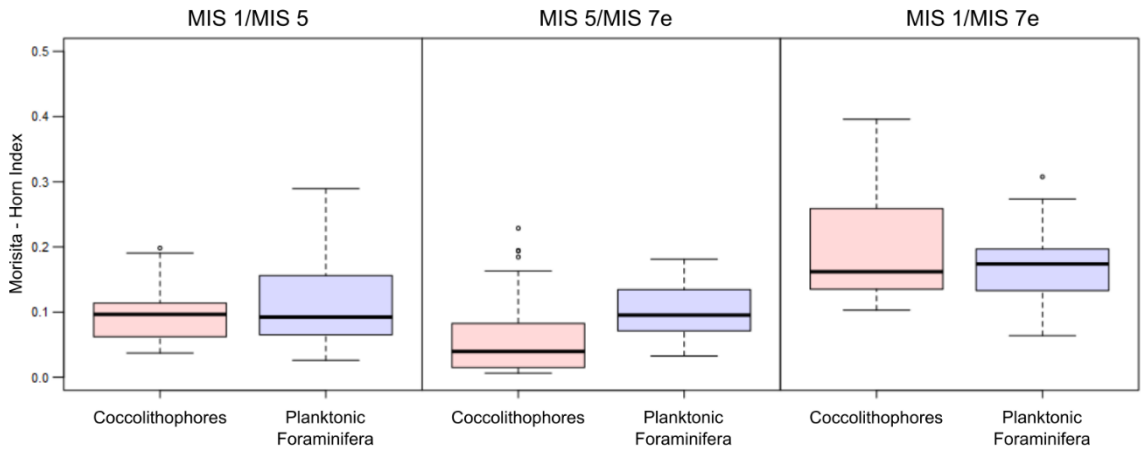

Fig. 17: Boxplots of Morisita – Horn dissimilarity indicating dissimilarities between individual interglacial periods based on (Table 4).

Dissimilarity values of planktonic foraminifera are consistently low throughout glacial periods. On the other hand, dissimilarity values of coccolithophores vary strongly between individual glacial periods. Highest values and variability are observed between MIS 2 and MIS 8 periods, with mean dissimilarity value of 0.30. Lowest dissimilarity values and variability are on the other hand observed between MIS 2 and MIS 6 periods (Fig. 18).

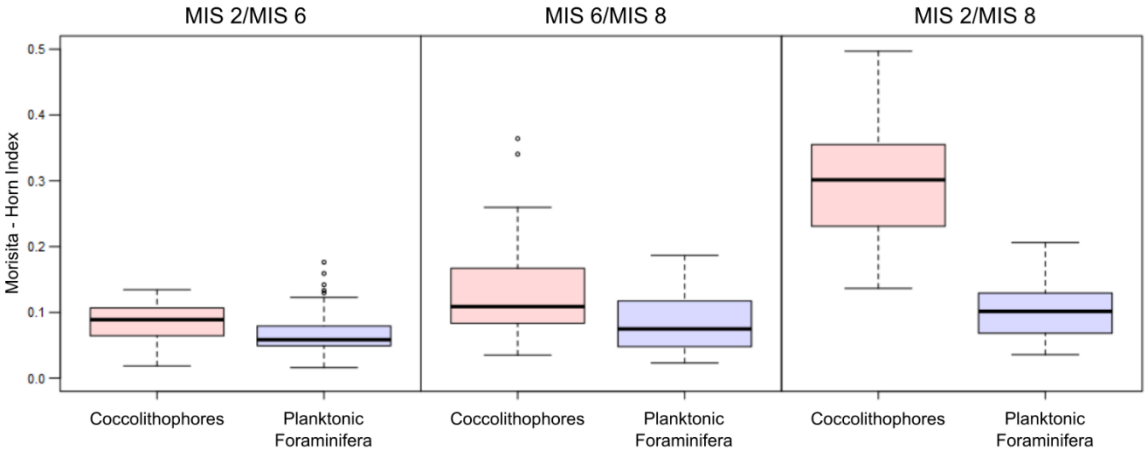

Fig. 18: Boxplots of Morisita – Horn dissimilarity indicating dissimilarities between individual glacial periods based on (Table 4).

7. Discussion

7.1 Composition and carbonate dissolution of planktonic foraminifera record

The studied sediment core GeoB12613-1 was obtained from ~2400 m water depth, between the Equator and 10S° latitude. The carbonate lysocline in equatorial regions is located at 3900 – 4000 m water depth, with CCD at >5000 m water depth (Kolla et al. 1976; Kidd and Davies 1978; Banakar et al. 1998; Yadav et al. 2022). Furthermore, in addition to coccolithophore record studied by Tangunan et al. (2017), who reported well to moderate preservation of coccoliths and occurrence of dissolution susceptible species, tests of planktonic foraminifera in our samples were well preserved with only minor fragmentation. Moreover, we also did not observe traces of carbonate dissolution on the tests. In addition, planktonic foraminifera samples contained well preserved dissolution susceptible species such as *G. anfracta*, *G. ruber* (white), *G. rubescens* and *G. tenella* (Parker and Berger 1971). The planktonic foraminifera record in core GeoB12613-1 is therefore not biased by carbonate dissolution.

In our study we identified 36 planktonic foraminifera species, with most common species being *G. glutinata*, *G. ruber* (white), *G. bulloides*, *N. incompta* and *G. dutertrei*. Other less common species, such as *G. falconensis*, *G. menardii*, *G. tumida* are also present. Species assemblage represents tropical to subtropical community structure, which is also supported by other studies from different areas of the Indian Ocean (Bé et al. 1977; Ding et al. 2006; Ishikawa and Oda 2007; Birch et al. 2013; Shen et al. 2023). Interestingly however, is the presence of subantarctic species of *N. incompta* (in older literature also right-coiling/dextral *N. pachyderma*). This species is most common during the glacial periods in the studied core and prefers waters with SSTs between 10 and 18°C (Bé et al. 1977). The appearance of *N. incompta* in the fossil assemblage of GeoB12613-1 close to equator is possibly related to upwelling of cold waters during glacial periods (Ding et al. 2006). Moreover, relative abundance of *N. incompta* is reduced during Terminations and during interglacial periods. It is therefore possible, that *N. incompta* follows its preferential ecological niche through habitat tracking and could be regarded as a migratory species (Strack et al. 2022). In addition, species *G. ruber* (pink) is absent in the MIS 2/MIS 1 sediments, which is consistent with previous observations that the species went extinct at ~120 ka (Thompson et al. 1979; Schiebel and Hemleben 2017).

7.2 Species dynamics

7.2.1 Species dynamics of planktonic foraminifera

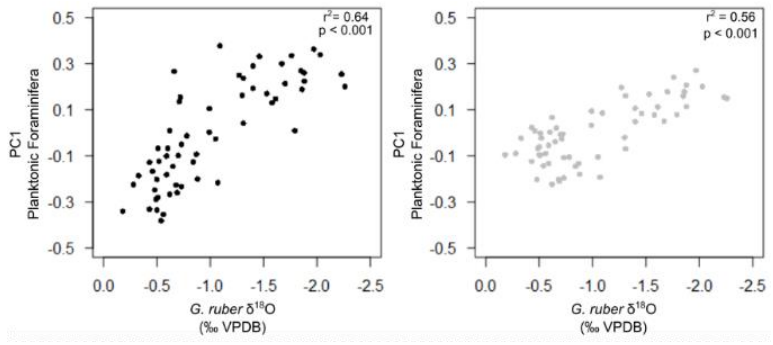

Fig. 19: Crossplots of PC1 and *G. ruber* (white) $\delta^{18}O$ values of planktonic foraminifera. Black dots represent PC1 analysis on glacial – interglacial timescale, whereas grey dots represent PC1 analysis on multi-glacial – interglacial timescales.

Assemblage composition of most common planktonic foraminifera remains consistent throughout glacial – interglacial cycles, indicating that there is no loss and gain in most common species. PC1 values are predominantly influenced by *N. incompta*, *G. ruber* (white), *G. trilobus*, *G. siphonifera*, *G. calida* and *G. glutinata*. In line with our H1, that marine plankton is sensitive to environmental changes (Roxy et al. 2016; Jonkers et al. 2019; Antão et al. 2020), PC1 values of planktonic foraminifera follow an identical trend as $\delta^{18}O$

values at every studied time period and timescale. PC1 values are low during glacial periods and increase during Termination events, with highest values found during interglacial periods (Fig. 10). Furthermore, we found strong correlation between PC1 and $\delta^{18}O$ values (Fig. 19; Pearson correlation: $r^2 = 0.56$, $p < 0.001$). This observation indicates that the assemblage composition of planktonic foraminifera followed global climate changes. The response is similar in both performed PCA analysis, with PC1 values showing slightly higher correlation on glacial – interglacial timescales (Fig. 19; Pearson correlation: $r^2 = 0.64$, $p < 0.001$). Our results indicate that environmental changes in the region were the main forcing factor on distribution and changes of planktonic foraminifera assemblages both on short and long time intervals. Regional environmental changes could be attributed to changes in upwelling intensity, with glacial periods being dominated by summer monsoon and increased upwelling. Increased upwelling of cold bottom waters, might have shoaled the thermocline, increased vertical mixing, and possibly reduced SST (Zelle et al. 2004; Tangunan et al. 2017). Importance of SST on the distribution of planktonic foraminifera has been previously noted by other studies, where authors found that planktonic foraminifera species are highly responsive to SST variations (Jonkers et al. 2019; Antão et al. 2020; Rillo et al. 2022; Strack et al. 2022).

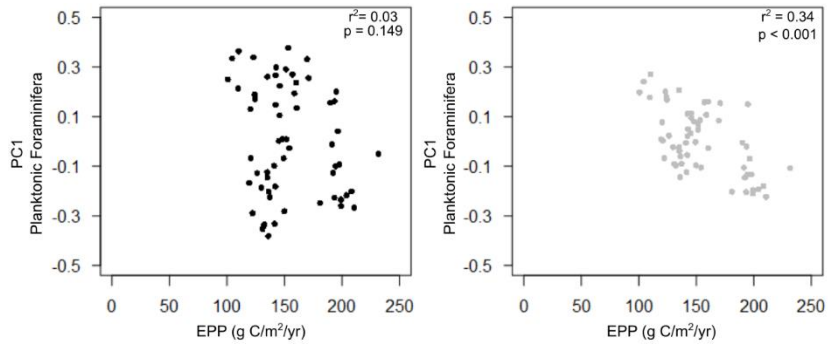

Fig. 20: Crossplots of PC1 and Estimated Paleoproductivity values of planktonic foraminifera. Black dots represent PC1 analysis on glacial – interglacial timescale, whereas grey dots represent PC1 analysis on multi-glacial – interglacial timescales.

In addition to $\delta^{18}O$, we correlated PC1 values with EPP values. Here we found a moderate correlation on the longer timescale (Fig. 20; Pearson correlation: $r^2 = 0.34$, $p < 0.001$). However, on the shorter timescales, we did not observe significant correlation between PC1 and EPP values (Fig. 20). It seems therefore, that variations in productivity does not affect planktonic foraminifera assemblages on short time intervals. However, on longer time scale primary productivity has minor influence on distribution and changes of planktonic foraminifera assemblages (Fig. 20).

7.2.2 Species dynamics of coccolithophores

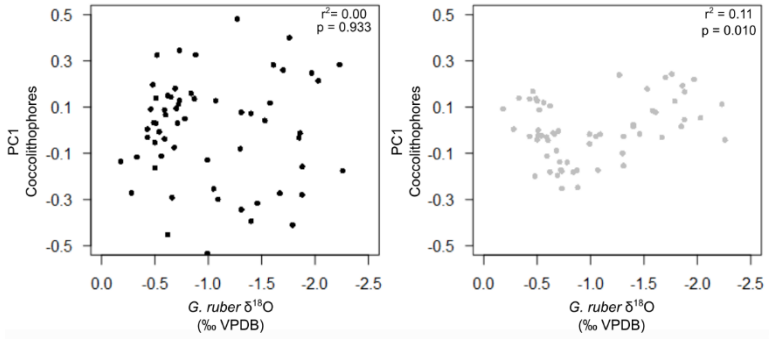

Fig. 21: Crossplots of PC1 and *G. ruber* (white) $\delta^{18}O$ values of coccolithophores. Black dots represent PC1 analysis on glacial – interglacial timescale, whereas grey dots represent PC1 analysis on multi-glacial – interglacial timescales.

Species composition of coccolithophores has been previously studied and analysed by Tangunan et al. (2017). In general, the assemblage is dominated by four species: *F. profunda*, *G. ericsonii*, *E. huxleyi* and *G. oceanica* (Tangunan et al. 2017). Species composition of coccolithophore assemblage stays consistent throughout the

studied intervals. However, there is a notable decline in relative abundance of *G. ericsonii* throughout glacial-interglacial cycles (Fig. 7), which is possibly related to an evolutionary replacement of *G. ericsonii* by *E. huxleyi* (Rogalla and Andruleit 2005).

Principal components of coccolithophores are predominantly influenced by the four dominating species. Furthermore, PC1 values show glacial – interglacial trends, with distinctive changes in PC1 values observed during Termination events (Fig. 11). This is especially evident during MIS 8/MIS 7 time period. Our observation suggests that coccolithophore species responded to rapid changes in climatic conditions. Nevertheless, a study by Tangunan et al. (2017) observed no clear glacial – interglacial pattern in the individual coccolith records and suggested that coccolithophore species distribution is primarily dependent on nutrient availability. Indeed, we did not observe significant correlation between PC1 and $\delta^{18}O$ values at both analysed timescales (Fig. 21).

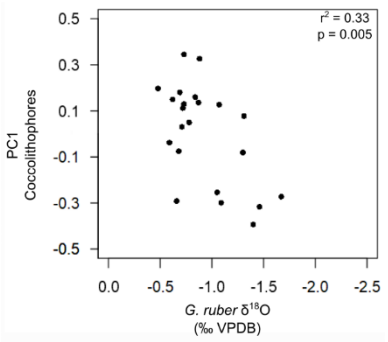

Fig. 22: Crossplots of PC1 and *G. ruber* (white) $\delta^{18}O$ values of coccolithophores during MIS 8/MIS 7 period.

However, we observed moderate correlation between PC1 and $\delta^{18}O$ values (Fig. 22; Pearson correlation: r^2 = 0.33, p = 0.005) during MIS 8/MIS 7 period (Fig. 11 & Fig. 22). This observation indicates that at least during MIS 8/MIS 7 period, coccolithophore assemblages were influenced by global climate changes. Furthermore, the general trend in PC1 values exhibits continues increase (Fig. 11), which is possibly associated with evolutionary replacement of *G. ericsonii* by *E. huxleyi* (Tangunan et al. 2017).

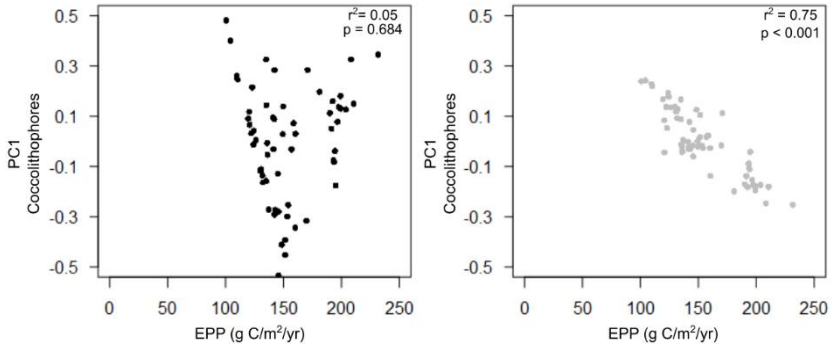

Fig. 23: Crossplots of PC1 and Estimated Paleoproductivity values of coccolithophores. Black dots represent PC1 analysis on glacial – interglacial timescale, whereas grey dots represent PC1 analysis on multi-glacial – interglacial timescales.

In addition, we found strong correlation between EPP and PC1 values of coccolithophores on longer timescale (Fig. 23; Pearson correlation: r^2 = 0.75, p < 0.001). This finding indicates that coccolithophores assemblages were predominantly influenced by productivity dynamics, as has been previously noted by (Tangunan et al. 2017). However, this correlation is very weak and insignificant on shorter timescales (Fig. 23; Pearson correlation: r^2 = 0.05, p < 0.684). Furthermore, it has to be noted, that EPP values are based on relative abundance of *F. profunda* (Tangunan et al. 2017), which is also the highest contributor to species loadings of PC1 values. It is therefore possible that correlation between PC1 and EPP values does not represent the relationship between coccolithophores species assemblage and paleoproductivity but rather a correlation between two variables derived from the same variable.

7.2.3 Summary species dynamics

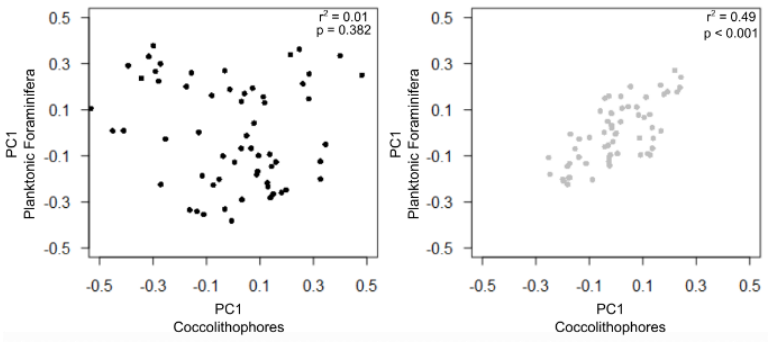

Fig. 24: Crossplots of PC1 values of coccolithophores and planktonic foraminifera. Black dots represent PC1 analysis on glacial – interglacial timescale, whereas grey dots represent PC1 analysis on multi-glacial – interglacial timescales.

In addition, we found a strong correlation between PC1 values of coccolithophores and planktonic foraminifera on the longer timescale (Fig. 24; Pearson correlation: $r^2 = 0.49$, $p < 0.001$). This observation suggests that planktonic foraminifera and coccolithophore assemblages respond in a similar way on the longer timescales. However, on the shorter timescales, species assemblages of both functional groups responded differently to changing environmental conditions. We also found that, planktonic foraminifera and coccolithophores species are affected by different environmental drivers.

Planktonic foraminifera species indicate strong relationship with $\delta^{18}O$ values, indicating that they were predominantly influenced by global climate changes at both analysed timescales, possibly attributed to variations in upwelling intensity throughout glacial – interglacial cylces in the region (Tangunan et al. 2017). Paleoproductivity estimate based on *F. profunda*, showed moderate correlation on a longer timescale. Coccolithophores species indicate very weak relationship with $\delta^{18}O$ values, suggesting that species assemblages were not influenced by global climate changes at both analysed timescales. On the other hand, paleoproductivity estimates showed strong correlation with PC1 values of coccolithophores only on the longer timescale.

7.3 Temporal α- and β-diversities trends

A study by Magurran et al. (2018) found that temporal α-diversity remained stable throughout the studied time interval. On the contrary, temporal β-diversity indicated more evident compositional changes. Their findings suggest that temporal α-diversity is decoupled from temporal β-diversity. It is however also possible that temporal α- and β-diversities occur on different timescales. Another possible explanation for differences in trends of α- and β-diversities, is that substantial temporal compositional changes and stationary temporal α-diversity represent a general pattern in ecology (Magurran et al. 2018). According to our H2, we expect to see no substantial changes in α-diversity through time. On the other hand, we expect substantial changes in temporal β-diversity.

Based on the normalized Hill-Shannon index (Fig. 12 & Fig. 13) and Morisita – Horn dissimilarity index (Fig. 14 & Fig. 15) we obtained slopes expressed as a rate of change in %/ka (Table 3). Our results indicate very low changes in temporal α-diversity in both functional groups (0.04 %/ka for coccolithophores and 0.05 %/ka for planktonic foraminifera). However, prominent changes were observed in temporal β-diversity in coccolithophores (0.18 %/ka). Nevertheless, temporal β-diversity of planktonic foraminifera was similar to temporal α-diversity. It is difficult to draw concise conclusions from our observations in relation to contemporary observations.

Coccolithophores species show almost stationary temporal α-diversity and notable temporal compositional changes, thus aligning with observations of Magurran et al. (2018). On the contrary, temporal α- and β-diversities of planktonic foraminifera did not show substantial variations in their rates of change.

One explanation for the deviation in observations, is that our results were obtained from marine organisms, thus temporal α- and β-diversities can show different trends than in terrestrial or freshwater organisms (Magurran et al. 2018; Hillebrand et al. 2018). Another explanation could be that temporal α- and β-diversities trends vary across organisms, ecosystems, and latitudes. It is also possible that contemporary temporal β-diversity is affected by anthropogenic forcing thus exhibiting higher rates of turnover (Magurran et al. 2018). On the contrary, paleorecords are not affected by it, therefore the rates of turnover are low and do not differ considerably from the temporal α-diversity rates. Finally, it is also possible that temporal scaling affects the rates of change of temporal α- and β-diversities.

7.4 Temporal β-diversity of coccolithophores and planktonic foraminifera

Temporal β-diversity is affected by ecological, physical, and geographical variables. In particular, temporal turnover of organisms at lower trophic levels, smaller in size and with a high rate of life cycle is expected to be higher than of organisms at higher trophic levels, larger in size and slower rate of life cycle (Korhonen et al. 2010). Our results of temporal turnover (Morisita – Horn index) indicate that the rate of change of coccolithophores (Fig. 15; 0.18 %/ka) is higher than of planktonic foraminifera (Fig. 14; 0.04 %/ka). This finding supports our H3 that the rate of temporal turnover throughout the last two glacial – interglacial cycles of coccolithophores was higher than of planktonic foraminifera. This difference in temporal turnover is probably associated with differences in the trophic level and the rate of life cycle of both functional groups (Korhonen et al. 2010). Coccolithophores are primary producers and have shorter generation times (days to weeks), thus increasing their potential to adapt faster in response to changing environmental conditions (Rogalla and Andruleit 2005; Balch 2018). Planktonic foraminifera on the other hand have longer generation times (days to months), thus reducing their potential to adapt. On the other hand, longer generation times imply higher dispersal potential for the organisms to the preferred ecological and thermal niche (Vargas et al. 2004; Schiebel and Hemleben 2017).

Temporal turnover is associated with migration and local extinction of the species as well as their ability to adapt (Hillebrand et al. 2010; Magurran et al. 2019). Differences in the rate and trends of temporal turnover might represent different driving mechanisms. Dissimilarity of planktonic foraminifera species is highest between glacial – interglacial periods (Fig. 16) and relatively low between adjacent interglacial and glacial periods (Fig. 17 & Fig. 18). In addition, Morisita – Horn values follow glacial – interglacial trends (Fig. 14) and our principal components analysis showed strong correlation between PC1 and $\delta^{18}O$ values (Fig. 10 & Fig. 19). These results suggest that species composition of planktonic foraminifera changed on shorter timescales in response to environmental changes, possibly through habitat tracking (Brett et al. 2007). On a regional scale, environmental changes in the study area could be attributed to changes in upwelling intensity, with glacial periods dominated by summer monsoon and interglacial periods dominated by winter monsoon (Tangunan et al. 2017).

Temporal turnover of coccolithophores on the other hand, tends to be predominantly influenced by adaptation of the species. Dissimilarity of coccolithophores assemblages is very low to absent between glacial – interglacial cycles (Fig. 16) and between adjacent glacial and interglacial periods (Fig. 17 & Fig. 18). This observation suggests, that coccolithophore assemblages are not affected by intermediate temporal turnover processes such as local colonization and extinction or immigration (Korhonen et al. 2010). On the other hand, dissimilarity is more pronounced on longer timescales (Fig. 17 & Fig. 18), thus implying that coccolithophore assemblages are predominantly influenced by evolutionary processes, in particular by adaptation. Long term adaptation of coccolithophores is possibly driven by nutrient supply and productivity of oceanic water masses. However, other abiotic and biotic processes, such as environmental changes and competition with other organisms, might have driven evolutionary processes in coccolithophores over the last two glacial – interglacial cycles (Bown et al. 2004; Vargas et al. 2007).

8. Conclusion

The sediment core GeoB12613-1 provides extensive insights into the biodiversity dynamics of phyto- and zooplankton over the last two glacial – interglacial cycles in the western Indian Ocean. In this study we analysed the sediment core on temporal α- and β-diversities of coccolithophores and planktonic foraminifera. According to research questions posed in the introduction part, our study revealed following:

1) Marine plankton, in particular phytoplankton and zooplankton are especially sensitive to environmental changes. We found a strong correlation between PC1 values of coccolithophores and planktonic foraminifera on the longer timescale. This observation suggests that planktonic foraminifera and coccolithophore assemblages respond in a similar way on the longer timescales. However, on the shorter timescales, species assemblages of both functional groups responded differently to changing environmental conditions. We also found that, planktonic foraminifera and coccolithophores species are affected by different environmental drivers. Planktonic foraminifera species indicate strong relationship with $\delta^{18}O$ values, indicating that they were predominantly influenced by global climate changes at both analysed timescales. Coccolithophores species indicate very weak relationship with $\delta^{18}O$ values, suggesting that species assemblages were not influenced by global climate changes at both analysed timescales. Instead, we found strong relationship with paleoproductivity estimates indicating that coccolithophores assemblages were predominantly influenced by productivity dynamics.
2) Analysis of temporal α- and β-diversities revealed that coccolithophores species show almost stationary temporal α-diversity and notable temporal compositional changes. On the other hand, temporal α- and β-diversities of planktonic foraminifera did not show substantial variations in their rates of change. One explanation for the deviation in observations, is that our results were obtained from marine organisms, thus temporal α- and β-diversities can show different trends than in terrestrial or freshwater organisms. Another explanation could be that contemporary temporal β-diversity of organisms is affected by anthropogenic forcing thus exhibiting higher rates of turnover. On the contrary, paleorecords are not affected by anthropogenic forcing, therefore the rates of turnover are low and do not differ considerably from the temporal α-diversity rates.
3) Analysis of temporal turnover between the two functional groups, indicate that the rate of change of coccolithophores (0.18 %/ka) is higher than of planktonic foraminifera (0.04 %/ka). This finding supports our hypothesis that the rate of temporal turnover throughout the last two glacial – interglacial cycles of coccolithophores was higher than of planktonic foraminifera. Difference in the rate of temporal turnover is probably associated with differences in the trophic level and the rate of life cycle of the studied functional groups. Furthermore, temporal turnover of planktonic foraminifera is possibly related to habitat tracking, whereas temporal turnover of coccolithophores is related to adaptation and evolutionary replacement of *G. ericsonii* by *E. huxleyi.*

9. References

Anbuselvan, N.; Senthil Nathan, D. (2021): Distribution and environmental implications of planktonic foraminifera in the surface sediments of southwestern part of Bay of Bengal, India. In *J. Sediment. Environ.* 6 (2), pp. 213–235. DOI: 10.1007/s43217-021-00053-8.

Antão, Laura H.; Bates, Amanda E.; Blowes, Shane A.; Waldock, Conor; Supp, Sarah R.; Magurran, Anne E. et al. (2020): Temperature-related biodiversity change across temperate marine and terrestrial systems. In *Nature ecology & evolution* 4 (7), pp. 927–933. DOI: 10.1038/s41559-020-1185-7.

Aurahs, Ralf; Grimm, Guido W.; Hemleben, Vera; Hemleben, Christoph; Kucera, Michal (2009): Geographical distribution of cryptic genetic types in the planktonic foraminifer Globigerinoides ruber. In *Molecular ecology* 18 (8), pp. 1692–1706. DOI: 10.1111/j.1365-294X.2009.04136.x.

Balch, William M. (2018): The Ecology, Biogeochemistry, and Optical Properties of Coccolithophores. In *Annual review of marine science* 10, pp. 71–98. DOI: 10.1146/annurev-marine-121916-063319.

Banakar, V.K; Parthiban, G.; Pattan, J.N; Jauhari, P. (1998): Chemistry of surface sediment along a north–south transect across the equator in the Central Indian Basin: an assessment of biogenic and detrital influences on elemental burial on the seafloor. In *Chemical Geology* 147 (3-4), pp. 217–232. DOI: 10.1016/S0009-2541(98)00015-1.

Barwell, Louise J.; Isaac, Nick J. B.; Kunin, William E. (2015): Measuring β-diversity with species abundance data. In *The Journal of animal ecology* 84 (4), pp. 1112–1122. DOI: 10.1111/1365-2656.12362.

Bé, Allan W. H.; Hutson, William H.; Be, Allan W. H. (1977): Ecology of Planktonic Foraminifera and Biogeographic Patterns of Life and Fossil Assemblages in the Indian Ocean. In *Micropaleontology* 23 (4), p. 369. DOI: 10.2307/1485406.

Biard, Tristan; Stemmann, Lars; Picheral, Marc; Mayot, Nicolas; Vandromme, Pieter; Hauss, Helena et al. (2016): In situ imaging reveals the biomass of giant protists in the global ocean. In *Nature* 532 (7600), pp. 504–507. DOI: 10.1038/nature17652.

Birch, Heather; Coxall, Helen K.; Pearson, Paul N.; Kroon, Dick; O'Regan, Matthew (2013): Planktonic foraminifera stable isotopes and water column structure: Disentangling ecological signals. In *Marine Micropaleontology* 101, pp. 127–145. DOI: 10.1016/j.marmicro.2013.02.002.

Borcard, Daniel; Gillet, Francois; Legendre, Pierre (2011a): Numerical Ecology with R. New York, NY: Springer New York.

Borcard, Daniel; Gillet, François; Legendre, Pierre (2011b): Numerical ecology with R. 1. ed. New York, Heidelberg: Springer (Use R!). Available online at http://www.loc.gov/catdir/enhancements/fy1108/2011280876-d.html.

Bown, Paul R.; Lees, Jackie A.; Young, Jeremy R. (2004): Calcareous nannoplankton evolution and diversity through time. In Hans R. Thierstein, Jeremy R. Young (Eds.): Coccolithophores. Berlin, Heidelberg: Springer Berlin Heidelberg, pp. 481–508.

Brett, C. E.; Hendy, A. J.W.; Bartholomew, A. J.; Bonelli, J. R.; McLaughlin, P. I. (2007): Response of shallow marine biotas to sea-level fluctuations: a review of faunal replacement and the process of habitat tracking. In *PALAIOS* 22 (3), pp. 228–244. DOI: 10.2110/palo.2005.p05-028r.

Broerse, A.T.C.; Brummer, G.-J.A.; Hinte, J.E.Van (2000): Coccolithophore export production in response to monsoonal upwelling off Somalia (northwestern Indian Ocean). In *Deep Sea Research Part II: Topical Studies in Oceanography* 47 (9-11), pp. 2179–2205. DOI: 10.1016/S0967-0645(00)00021-7.

Burns, Jessica M.; Subrahmanyam, Bulusu; Murty, V. S. N. (2017): On the dynamics of the S ri L anka D ome in the B ay of B engal. In *J. Geophys. Res. Oceans* 122 (9), pp. 7737–7750. DOI: 10.1002/2017JC012986.

Cohen, K. M.; Finney, S. C.; Gibbard, P. L.; Fan, J.-X. (2013): The ICS International Chronostratigraphic Chart (Episodes 36), pp. 199–204.

Conan, S.M.-H.; Brummer, G.J.A. (2000): Fluxes of planktic foraminifera in response to monsoonal upwelling on the Somalia Basin margin. In *Deep Sea Research Part II: Topical Studies in Oceanography* 47 (9-11), pp. 2207–2227. DOI: 10.1016/S0967-0645(00)00022-9.

Dam, Hans G. (2013): Evolutionary adaptation of marine zooplankton to global change. In *Annual review of marine science* 5, pp. 349–370. DOI: 10.1146/annurev-marine-121211-172229.

Davies, Claire H.; Beckley, Lynnath E.; Richardson, Anthony J. (2022): Copepods and mixotrophic Rhizaria dominate zooplankton abundances in the oligotrophic Indian Ocean. In *Deep Sea Research Part II: Topical Studies in Oceanography* 202, p. 105136. DOI: 10.1016/j.dsr2.2022.105136.

Ding, X.; Bassinot, F.; Guichard, F.; Li, Q. Y.; Fang, N. Q.; Labeyrie, L. et al. (2006): Distribution and ecology of planktonic foraminifera from the seas around the Indonesian Archipelago. In *Marine Micropaleontology* 58 (2), pp. 114–134. DOI: 10.1016/j.marmicro.2005.10.003.

Dornelas, Maria; Gotelli, Nicholas J.; McGill, Brian; Shimadzu, Hideyasu; Moyes, Faye; Sievers, Caya; Magurran, Anne E. (2014): Assemblage time series reveal biodiversity change but not systematic loss. In *Science (New York, N.Y.)* 344 (6181), pp. 296–299. DOI: 10.1126/science.1248484.

Fath, Brian (2019): Encyclopedia of ecology. Second edition. Amsterdam, Boston, Heidelberg, London, New York, Oxford: Elsevier.

Fedor, Peter; Zvaríková, Martina (2019): Biodiversity Indices. In : Encyclopedia of Ecology: Elsevier, pp. 337–346.

Felis, Thomas (2020): Extending the Instrumental Record of Ocean-Atmosphere Variability into the Last Interglacial Using Tropical Corals. In *Oceanog* 33 (2). DOI: 10.5670/oceanog.2020.209.

GEBCO (2014): General Bathymetric Chart of the Ocean (GEBCO). World Ocean Bathymetry. Available online at https://www.gebco.net, checked on 10/25/2022.

Groeneveld, Johan (2016): The Western Indian Ocean as a source of food.

Haynes, John R. (1981): Foraminifera. London: Palgrave Macmillan UK.

Hill, M. O. (1973): Diversity and Evenness: A Unifying Notation and Its Consequences. In *Ecology* 54 (2), pp. 427–432. DOI: 10.2307/1934352.

Hillebrand, Helmut; Blasius, Bernd; Borer, Elizabeth T.; Chase, Jonathan M.; Downing, John A.; Eriksson, Britas Klemens et al. (2018): Biodiversity change is uncoupled from species richness trends: Consequences for conservation and monitoring. In *J Appl Ecol* 55 (1), pp. 169–184. DOI: 10.1111/1365-2664.12959.

Hillebrand, Helmut; Soininen, Janne; SNOEIJS, PAULINE (2010): Warming leads to higher species turnover in a coastal ecosystem. In *Global Change Biology* 16 (4), pp. 1181–1193. DOI: 10.1111/j.1365-2486.2009.02045.x.

Hoffmann, Ary A.; Sgrò, Carla M. (2011): Climate change and evolutionary adaptation. In *Nature* 470 (7335), pp. 479–485. DOI: 10.1038/nature09670.

Houdan, A.; Probert, I.; Zatylny, C.; Véron, B.; Billard, C. (2006): Ecology of oceanic coccolithophores. I. Nutritional preferences of the two stages in the life cycle of Coccolithus braarudii and Calcidiscus leptoporus. In *Aquat. Microb. Ecol.* 44, pp. 291–301. DOI: 10.3354/ame044291.

Ishikawa, Satoko; Oda, Motoyoshi (2007): Reconstruction of Indian monsoon variability over the past 230,000 years: Planktic foraminiferal evidence from the NW Arabian Sea open-ocean upwelling area. In *Marine Micropaleontology* 63 (3-4), pp. 143–154. DOI: 10.1016/j.marmicro.2006.11.004.

Jolliffe, Ian (2005): Principal Component Analysis. In Brian S. Everitt, David C. Howell (Eds.): Encyclopedia of Statistics in Behavioral Science. Chichester, UK: John Wiley & Sons, Ltd.

Jonkers, Lukas; Hillebrand, Helmut; Kucera, Michal (2019): Global change drives modern plankton communities away from the pre-industrial state. In *Nature* 570 (7761), pp. 372–375. DOI: 10.1038/s41586-019-1230-3.

Jost, L.; Chao, A.; Chazdon, R. L. (2011): Compositional similarity and beta diversity. In A. Magurran, B. McGill (Eds.): Biological Diversity: Frontiers in Measurement and Assessment. Oxford: Oxford University Press, pp. 66–84.

Jost, Lou (2006): Entropy and diversity. In *Oikos* 113 (2), pp. 363–375. DOI: 10.1111/j.2006.0030-1299.14714.x.

Jost, Lou (2007): Partitioning diversity into independent alpha and beta components. In *Ecology* 88 (10), pp. 2427–2439. DOI: 10.1890/06-1736.1.

Kidd, Robert B.; Davies, Thomas A. (1978): Indian Ocean sediment distribution since the Late Jurassic. In *Marine Geology* 26 (1-2), pp. 49–70. DOI: 10.1016/0025-3227(78)90045-2.

Kolla, Venkatarathnam; Bé, Allan W. H.; Biscaye, Pierre E. (1976): Calcium carbonate distribution in the surface sediments of the Indian Ocean. In *J. Geophys. Res.* 81 (15), pp. 2605–2616. DOI: 10.1029/JC081i015p02605.

Kolla, Venkatarathnam; Kidd, Robert B. (1982): Sedimentation and Sedimentary Processes in the Indian Ocean. In Alan E. M. Nairn, Francis G. Stehli (Eds.): The Ocean Basins and Margins. Boston, MA: Springer US, pp. 1–50.

Koné, Vamara; Aumont, Olivier; Lévy, Marina; Resplandy, Laure (2009): Physical and biogeochemical controls of the phytoplankton seasonal cycle in the Indian Ocean: A modeling study. In Jerry D. Wiggert, Raleigh R. Hood, S. Wajih A. Naqvi, Kenneth H. Brink, Sharon L. Smith (Eds.): Indian Ocean Biogeochemical Processes and Ecological Variability, vol. 185. Washington, D. C.: American Geophysical Union (Geophysical Monograph Series), pp. 147–166.

Korhonen, Jenni J.; Soininen, Janne; Hillebrand, Helmut (2010): A quantitative analysis of temporal turnover in aquatic species assemblages across ecosystems. In *Ecology* 91 (2), pp. 508–517. DOI: 10.1890/09-0392.1.

Krey, J. (1973): Primary Production in the Indian Ocean I. In J. Jacobs, O. L. Lange, J. S. Olson, W. Wieser, Bernt Zeitzschel, Sebastian A. Gerlach (Eds.): The Biology of the Indian Ocean, vol. 3. Berlin, Heidelberg: Springer Berlin Heidelberg (Ecological Studies), pp. 115–126.

Krumhardt, Kristen M.; Lovenduski, Nicole S.; Iglesias-Rodriguez, M. Debora; Kleypas, Joan A. (2017): Coccolithophore growth and calcification in a changing ocean. In *Progress in Oceanography* 159, pp. 276–295. DOI: 10.1016/j.pocean.2017.10.007.

Kucera, Michal (2007): Chapter Six Planktonic Foraminifera as Tracers of Past Oceanic Environments. In : Proxies in Late Cenozoic Paleoceanography, vol. 1: Elsevier (Developments in Marine Geology), pp. 213–262.

Lau, K.-M.; Yang, S. (2003): Walker Circulation. In : Encyclopedia of Atmospheric Sciences: Elsevier, pp. 2505–2510.

Lemenkova, Polina (2020): Insights on the Indian Ocean Tectonics and Geophysics Supported by GMT. In *RCJ* 27 (2), pp. 67–83. DOI: 10.24193/RCJ2020_12.

Lévy, M.; Shankar, D.; André, J.-M.; Shenoi, S. S. C.; Durand, F.; Boyer Montégut, C. de (2007): Basin-wide seasonal evolution of the Indian Ocean's phytoplankton blooms. In *J. Geophys. Res.* 112 (C12). DOI: 10.1029/2007JC004090.

Lewandowska, Aleksandra M.; Jonkers, Lukas; Auel, Holger; Freund, Jan A.; Hagen, Wilhelm; Kucera, Michal; Hillebrand, Helmut (2020): Scale dependence of temporal biodiversity change in modern and fossil marine plankton. In *Global Ecology and Biogeography* 29 (6), pp. 1008–1019. DOI: 10.1111/geb.13078.

Lisiecki, Lorraine E.; Raymo, Maureen E. (2005): A Pliocene-Pleistocene stack of 57 globally distributed benthic δ 18 O records. In *Paleoceanography* 20 (1), n/a-n/a. DOI: 10.1029/2004PA001071.

Lohbeck, Kai T.; Riebesell, Ulf; Reusch, Thorsten B. H. (2012): Adaptive evolution of a key phytoplankton species to ocean acidification. In *Nature Geosci* 5 (5), pp. 346–351. DOI: 10.1038/NGEO1441.

Magurran, A.; McGill, B. (Eds.) (2011): Biological Diversity: Frontiers in Measurement and Assessment. Oxford: Oxford University Press.

Magurran, Anne E. (2003): Measuring biological diversity. 9 [Nachdr.]. Malden, Mass.: Wiley-Blackwell.

Magurran, Anne E. (2021): Measuring biological diversity. In *Current biology : CB* 31 (19), R1174-R1177. DOI: 10.1016/j.cub.2021.07.049.

Magurran, Anne E.; Baillie, Stephen R.; Buckland, Stephen T.; Dick, Jan McP; Elston, David A.; Scott, E. Marian et al. (2010): Long-term datasets in biodiversity research and monitoring: assessing change in ecological communities through time. In *Trends in ecology & evolution* 25 (10), pp. 574–582. DOI: 10.1016/j.tree.2010.06.016.

Magurran, Anne E.; Deacon, Amy E.; Moyes, Faye; Shimadzu, Hideyasu; Dornelas, Maria; Phillip, Dawn A. T.; Ramnarine, Indar W. (2018): Divergent biodiversity change within ecosystems. In *Proceedings of the National Academy of Sciences of the United States of America* 115 (8), pp. 1843–1847. DOI: 10.1073/pnas.1712594115.

Magurran, Anne E.; Dornelas, Maria; Moyes, Faye; Henderson, Peter A. (2019): Temporal β diversity—A macroecological perspective. In *Global Ecol Biogeogr* 28 (12), pp. 1949–1960. DOI: 10.1111/geb.13026.

Magurran, Anne E.; Henderson, Peter A. (2010): Temporal turnover and the maintenance of diversity in ecological assemblages. In *Philosophical transactions of the Royal Society of London. Series B, Biological sciences* 365 (1558), pp. 3611–3620. DOI: 10.1098/rstb.2010.0285.

Mauerer, B. A.; McGill, B. J. (2011): Measurement of species diversity. In A. Magurran, B. McGill (Eds.): Biological Diversity: Frontiers in Measurement and Assessment. Oxford: Oxford University Press, pp. 55–65.

McCreary, J. P.; Murtugudde, R.; Vialard, J.; Vinayachandran, P. N.; Wiggert, J. D.; Hood, R. R. et al. (2009): Biophysical processes in the Indian Ocean. In Jerry D. Wiggert, Raleigh R. Hood, S. Wajih A. Naqvi, Kenneth H. Brink, Sharon L. Smith (Eds.): Indian Ocean Biogeochemical Processes and Ecological Variability, vol. 185. Washington, D. C.: American Geophysical Union (Geophysical Monograph Series), pp. 9–32.

Mitchell, Neil C.; Parson, Lindsay M. (1993): The tectonic evolution of the Indian Ocean Triple Junction, anomaly 6 to present. In *J. Geophys. Res.* 98 (B2), pp. 1793–1812. DOI: 10.1029/92JB00582.

Mohtadi, Mahyar; Prange, Matthias; Schefuß, Enno; Jennerjahn, Tim C. (2017): Late Holocene slowdown of the Indian Ocean Walker circulation. In *Nature communications* 8 (1), p. 1015. DOI: 10.1038/s41467-017-00855-3.

Molfino, B.; McIntyre, A. (1990): Precessional forcing of nutricline dynamics in the equatorial atlantic. In *Science (New York, N.Y.)* 249 (4970), pp. 766–769. DOI: 10.1126/science.249.4970.766.

Morard, Raphaël; Garet-Delmas, Marie-José; Mahé, Frédéric; Romac, Sarah; Poulain, Julie; Kucera, Michal; Vargas, Colomban de (2018): Surface ocean metabarcoding confirms limited diversity in planktonic foraminifera but reveals unknown hyper-abundant lineages. In *Scientific reports* 8 (1), p. 2539. DOI: 10.1038/s41598-018-20833-z.

Mukhopadhyay, Ranadhir; Ghosh, Anil K.; Iyer, Sridhar D. (2008): The Indian Ocean nodule field. Geology and resource potential. 1. ed. Amsterdam: Elsevier (Handbook of exploration and environmental geochemistry, 10). Available online at http://www.sciencedirect.com/science/publication?issn=18742734&volume=10.

NASA Ocean Biology Processing Group (2022): Aqua MODIS Level 3 Binned Chlorophyll Data, Version R2022.0, checked on 8/12/2022.

Nichols, Scott (1997): On the interpretation of principal components analysis in ecological contexts. In *Vegetatio* 34 (3), pp. 191–197. DOI: 10.1007/BF00055215.

Oksanen, J.; Blanchet, Guillaume, F.; Michael Friendly; Roeland Kindt; Pierre Legendre; Dan McGlinn; Peter R. Minchin (2020): vegan: Community Ecology Package. Version R package version 2.5-7. Available online at https://CRAN.R-project.org/package=vegan.

Pang, Xiaolei; Bassinot, Franck; Sepulcre, Sophie (2021): Indonesian Throughflow variability over the last two glacial-interglacial cycles: Evidence from the eastern Indian Ocean. In *Quaternary Science Reviews* 256, p. 106839. DOI: 10.1016/j.quascirev.2021.106839.

Parker, Frances L.; Berger, Wolfgang H. (1971): Faunal and solution patterns of planktonic Foraminifera in surface sediments of the South Pacific. In *Deep Sea Research and Oceanographic Abstracts* 18 (1), pp. 73–107. DOI: 10.1016/0011-7471(71)90017-9.

Parmesan, Camille (2006): Ecological and Evolutionary Responses to Recent Climate Change. In *Annu. Rev. Ecol. Evol. Syst.* 37 (1), pp. 637–669. DOI: 10.1146/annurev.ecolsys.37.091305.110100.

Parmesan, Camille; Yohe, Gary (2003): A globally coherent fingerprint of climate change impacts across natural systems. In *Nature* 421 (6918), pp. 37–42. DOI: 10.1038/nature01286.

Parson, Lindsay M.; Evans, Alan J. (2005): Seafloor topography and tectonic elements of the Western Indian Ocean. In *Philosophical transactions. Series A, Mathematical, physical, and engineering sciences* 363 (1826), pp. 15–24. DOI: 10.1098/rsta.2004.1472.

Phillips, Helen E.; Tandon, Amit; Furue, Ryo; Hood, Raleigh; Ummenhofer, Caroline C.; Benthuysen, Jessica A. et al. (2021): Progress in understanding of Indian Ocean circulation, variability, air–sea exchange, and impacts on biogeochemistry. In *Ocean Sci.* 17 (6), pp. 1677–1751. DOI: 10.5194/os-17-1677-2021.

Poloczanska, Elvira S.; Brown, Christopher J.; Sydeman, William J.; Kiessling, Wolfgang; Schoeman, David S.; Moore, Pippa J. et al. (2013): Global imprint of climate change on marine life. In *Nature Clim Change* 3 (10), pp. 919–925. DOI: 10.1038/NCLIMATE1958.

Posit team (2022): RStudio: Integrated Development Environment for R. Boston, MA: Posit Software, PBC. Available online at http://www.posit.co/.

Qasim, Syed Zahoor (1977): Biological Productivity of the Indian Ocean. In *Indian Journal of Marine Sciences* 6, pp. 122–137.

R Core Team (2021): R: A language and environment for statistical. Vienna, Austria: R Foundation for Statistical Computing. Available online at https://www.R-project.org/.

Rao, T. S. S. (1973): Zooplankton Studies in the Indian Ocean. In J. Jacobs, O. L. Lange, J. S. Olson, W. Wieser, Bernt Zeitzschel, Sebastian A. Gerlach (Eds.): The Biology of the Indian Ocean, vol. 3. Berlin, Heidelberg: Springer Berlin Heidelberg (Ecological Studies), pp. 243–255.

Renaud, Sabrina; Ziveri, Patrizia; Broerse, Alexandra T.C. (2002): Geographical and seasonal differences in morphology and dynamics of the coccolithophore Calcidiscus leptoporus. In *Marine Micropaleontology* 46 (3-4), pp. 363–385. DOI: 10.1016/S0377-8398(02)00081-6.

Reusch, Thorsten B. H.; Boyd, Philip W. (2013): Experimental evolution meets marine phytoplankton. In *Evolution; international journal of organic evolution* 67 (7), pp. 1849–1859. DOI: 10.1111/evo.12035.

Rillo, Marina C.; Woolley, Skipton; Hillebrand, Helmut (2022): Drivers of global pre-industrial patterns of species turnover in planktonic foraminifera. In *Ecography* 2022 (1), Article ecog.05892. DOI: 10.1111/ecog.05892.

Ringnér, Markus (2008): What is principal component analysis? In *Nature biotechnology* 26 (3), pp. 303–304. DOI: 10.1038/nbt0308-303.

Rogalla, U.; Andruleit, H. (2005): Precessional forcing of coccolithophore assemblages in the northern Arabian Sea: Implications for monsoonal dynamics during the last 200,000 years. In *Marine Geology* 217 (1-2), pp. 31–48. DOI: 10.1016/j.margeo.2005.02.028.

Roswell, Michael; Dushoff, Jonathan; Winfree, Rachael (2021): A conceptual guide to measuring species diversity. In *Oikos* 130 (3), pp. 321–338. DOI: 10.1111/oik.07202.

Roxy, Mathew Koll; Modi, Aditi; Murtugudde, Raghu; Valsala, Vinu; Panickal, Swapna; Prasanna Kumar, S. et al. (2016): A reduction in marine primary productivity driven by rapid warming over the tropical Indian Ocean. In *Geophys. Res. Lett.* 43 (2), pp. 826–833. DOI: 10.1002/2015GL066979.

Savoye, Bruno; Ridderinkhof, Herman; Pätzold, Jürgen; Schneider, Ralph (2013): Western Indian Ocean Climate and Sedimentation - Cruise No. M75 - December 29, 2007 - April 08, 2008 - Port Louis (Mauritius) - Cape Town (South Africa). In *METEOR-Berichte* M75. DOI: 10.2312/cr_m75.

Schiebel, Ralf; Hemleben, Christoph (2017): Planktic Foraminifers in the Modern Ocean. Berlin, Heidelberg: Springer Berlin Heidelberg.

Schiebel, Ralf; Spielhagen, Robert F.; Garnier, Julie; Hagemann, Julia; Howa, Hélène; Jentzen, Anna et al. (2017): Modern planktic foraminifers in the high-latitude ocean. In *Marine Micropaleontology* 136, pp. 1–13. DOI: 10.1016/j.marmicro.2017.08.004.

Schlich, R. (1982): The Indian Ocean: Aseismic Ridges, Spreading Centers, and Oceanic Basins. In Alan E. M. Nairn, Francis G. Stehli (Eds.): The Ocean Basins and Margins. Boston, MA: Springer US, pp. 51–147.

Schlitzer, Reiner (2022): Ocean Data View. Version 5.6.3. Available online at https://odv.awi.de.

Schmoker, Claire; Hernández-León, Santiago; Calbet, Albert (2013): Microzooplankton grazing in the oceans: impacts, data variability, knowledge gaps and future directions. In *Journal of Plankton Research* 35 (4), pp. 691–706. DOI: 10.1093/plankt/fbt023.

Schott, Friedrich A.; McCreary, Julian P. (2001): The monsoon circulation of the Indian Ocean. In *Progress in Oceanography* 51 (1), pp. 1–123. DOI: 10.1016/S0079-6611(01)00083-0.

Schott, Friedrich A.; Xie, Shang-Ping; McCreary, Julian P. (2009): Indian Ocean circulation and climate variability. In *Rev. Geophys.* 47 (1). DOI: 10.1029/2007RG000245.

Schouten, Mathijs W.; Ruijter, Wilhelmus P.M. de; van Leeuwen, Peter Jan; Ridderinkhof, Herman (2003): Eddies and variability in the Mozambique Channel. In *Deep Sea Research Part II: Topical Studies in Oceanography* 50 (12-13), pp. 1987–2003. DOI: 10.1016/S0967-0645(03)00042-0.

Shen, Wei; Qiao, Shuqing; Sun, Rongtao; He, Zhoutian; Wu, Bin; Jin, Lina et al. (2023): Distribution pattern of planktonic and benthic foraminifera in surface sediments near the equatorial western Indian Ocean and its indications of paleo-environment and productivity. In *Journal of Asian Earth Sciences* 250, p. 105635. DOI: 10.1016/j.jseaes.2023.105635.

Siccha, Michael; Kucera, Michal (2017): ForCenS, a curated database of planktonic foraminifera census counts in marine surface sediment samples. In *Scientific data* 4, p. 170109. DOI: 10.1038/sdata.2017.109.

Sosdian, S. M.; Lear, C. H. (2020): Initiation of the Western Pacific Warm Pool at the Middle Miocene Climate Transition? In *Paleoceanography and Paleoclimatology* 35 (12). DOI: 10.1029/2020PA003920.

Spellerberg, Ian F.; Fedor, Peter J. (2003): A tribute to Claude Shannon (1916-2001) and a plea for more rigorous use of species richness, species diversity and the 'Shannon-Wiener' Index. In *Global Ecology and Biogeography* 12 (3), pp. 177–179. DOI: 10.1046/j.1466-822X.2003.00015.x.

Spezzaferri, Silvia; Kucera, Michal; Pearson, Paul Nicholas; Wade, Bridget Susan; Rappo, Sacha; Poole, Christopher Robert et al. (2015): Fossil and genetic evidence for the polyphyletic nature of the planktonic foraminifera "Globigerinoides", and description of the new genus Trilobatus. In *PloS one* 10 (5), e0128108. DOI: 10.1371/journal.pone.0128108.

Strack, Tonke; Jonkers, Lukas; C Rillo, Marina; Hillebrand, Helmut; Kucera, Michal (2022): Plankton response to global warming is characterized by non-uniform shifts in assemblage composition since the last ice age. In *Nature ecology & evolution* 6 (12), pp. 1871–1880. DOI: 10.1038/s41559-022-01888-8.

Tangunan, Deborah; Baumann, Karl-Heinz; Pätzold, Jürgen; Henrich, Rüdiger; Kucera, Michal; Pol-Holz, Ricardo de; Groeneveld, Jeroen (2017): Insolation forcing of coccolithophore productivity in the western tropical Indian Ocean over the last two glacial-interglacial cycles. In *Paleoceanography* 32 (7), pp. 692–709. DOI: 10.1002/2017PA003102.

Tapia, Raúl; Ho, Sze Ling; Wang, Hui-Yu; Groeneveld, Jeroen; Mohtadi, Mahyar (2022): Contrasting vertical distributions of recent planktic foraminifera off Indonesia during the southeast monsoon: implications for paleoceanographic reconstructions. In *Biogeosciences* 19 (13), pp. 3185–3208. DOI: 10.5194/bg-19-3185-2022.

Thierstein, Hans R.; Young, Jeremy R. (Eds.) (2004): Coccolithophores. Berlin, Heidelberg: Springer Berlin Heidelberg.

Thompson, Diane M. (2022): Environmental records from coral skeletons: A decade of novel insights and innovation. In *WIREs Climate Change* 13 (1). DOI: 10.1002/wcc.745.

Thompson, Peter R.; Bé, Allan W. H.; Duplessy, Jean-Claude; Shackleton, Nicholas J. (1979): Disappearance of pink-pigmented Globigerinoides ruber at 120,000 yr BP in the Indian and Pacific Oceans. In *Nature* 280 (5723), pp. 554–558. DOI: 10.1038/280554a0.

Thrush, Simon F.; Hewitt, Judi E.; Dayton, Paul K.; Coco, Giovanni; Lohrer, Andrew M.; Norkko, Alf et al. (2009): Forecasting the limits of resilience: integrating empirical research with theory. In *Proceedings. Biological sciences* 276 (1671), pp. 3209–3217. DOI: 10.1098/rspb.2009.0661.

Thukral, Ashwani K. (2017): A review on measurement of Alpha diversity in biology. In *Intern. Jour. Contemp. Microbiol.* 54 (1), p. 1. DOI: 10.5958/2395-146X.2017.00001.1.

Tomašových, Adam; Kidwell, Susan M. (2009): Fidelity of variation in species composition and diversity partitioning by death assemblages: time-averaging transfers diversity from beta to alpha levels. In *Paleobiology* 35 (1), pp. 94–118. DOI: 10.1666/08024.1.

Tomczak, Matthias; Godfrey, J. Stuart (1994): The Indian Ocean. In : Regional Oceanography: Elsevier, pp. 193–220.

Tyrrell, Toby; Merico, Agostino (2004): Emiliania huxleyi: bloom observations and the conditions that induce them. In Hans R. Thierstein, Jeremy R. Young (Eds.): Coccolithophores. Berlin, Heidelberg: Springer Berlin Heidelberg, pp. 75–97.

Vargas, Colomban de; AUBRY, MARIE-PIERRE; PROBERT, I. A.N.; YOUNG, JEREMY (2007): Origin and Evolution of Coccolithophores: From Coastal Hunters to Oceanic Farmers. In : Evolution of Primary Producers in the Sea: Elsevier, pp. 251–285.

Vargas, Colomban de; Sáez, Alberto G.; Medlin, Linda K.; Thierstein, Hans R. (2004): Super-Species in the calcareous plankton. In Hans R. Thierstein, Jeremy R. Young (Eds.): Coccolithophores. Berlin, Heidelberg: Springer Berlin Heidelberg, pp. 271–298.

Wang, Luejiang (2000): Isotopic signals in two morphotypes of Globigerinoides ruber (white) from the South China Sea: implications for monsoon climate change during the last glacial cycle. In *Palaeogeography, Palaeoclimatology, Palaeoecology* 161 (3-4), pp. 381–394. DOI: 10.1016/S0031-0182(00)00094-8.

Williams, Caroline M.; Ragland, Gregory J.; Betini, Gustavo; Buckley, Lauren B.; Cheviron, Zachary A.; Donohue, Kathleen et al. (2017): Understanding Evolutionary Impacts of Seasonality: An Introduction to the Symposium. In *Integrative and comparative biology* 57 (5), pp. 921–933. DOI: 10.1093/icb/icx122.

Wyrtki, K. (1973): An equatorial jet in the Indian ocean. In *Science (New York, N.Y.)* 181 (4096), pp. 262–264. DOI: 10.1126/science.181.4096.262.

Yadav, Ramanand; Naik, Sushant S.; Naidu, Pothuri Divakar (2022): Contrasts in calcium carbonate dissolution above the lysocline in the equatorial Indian Ocean over the last ~40 ka. In *Marine Geology* 444, p. 106717. DOI: 10.1016/j.margeo.2021.106717.

Yan, Yuk Yee (2005): Intertropical Convergence Zone (ITCZ). In John E. Oliver (Ed.): Encyclopedia of World Climatology: Springer Netherlands (Encyclopedia of Earth Sciences Series), pp. 429–432.

Yasuhara, Moriaki; Huang, Huai-Hsuan; Hull, Pincelli; Rillo, Marina; Condamine, Fabien; Tittensor, Derek et al. (2020a): Time Machine Biology: Cross-Timescale Integration of Ecology, Evolution, and Oceanography. In *Oceanog* 33 (2). DOI: 10.5670/oceanog.2020.225.

Yasuhara, Moriaki; Hunt, Gene; Dowsett, Harry J.; Robinson, Marci M.; Stoll, Danielle K. (2012): Latitudinal species diversity gradient of marine zooplankton for the last three million years. In *Ecology letters* 15 (10), pp. 1174–1179. DOI: 10.1111/j.1461-0248.2012.01828.x.

Yasuhara, Moriaki; Wei, Chih-Lin; Kucera, Michal; Costello, Mark J.; Tittensor, Derek P.; Kiessling, Wolfgang et al. (2020b): Past and future decline of tropical pelagic biodiversity. In *Proceedings of the National Academy of Sciences of the United States of America* 117 (23), pp. 12891–12896. DOI: 10.1073/pnas.1916923117.

Zelle, Hein; Appeldoorn, Gerrian; Burgers, Gerrit; van Oldenborgh, Geert Jan (2004): The Relationship between Sea Surface Temperature and Thermocline Depth in the Eastern Equatorial Pacific. In *Journal of Physical Oceanography* 34 (3), pp. 643–655. DOI: 10.1175/2523.1.

Ziveri, Patrizia; Baumann, Karl-Heinz; Böckel, Babette; Bollmann, Jörg; Young, Jeremy R. (2004): Biogeography of selected Holocene coccoliths in the Atlantic Ocean. In Hans R. Thierstein, Jeremy R. Young (Eds.): Coccolithophores. Berlin, Heidelberg: Springer Berlin Heidelberg, pp. 403–428.

Appendix

Table 5. GeoB12613-1 sedimentological data and split fractions used for faunistic analysis.

Latitude (deg)	Longitude (deg)	Depth Top (cm)	Depth Bottom (cm)	Volume (ml)	Volume Quality	Wet Weight (g)	Wet Bulk Density (g/cm³)	Dry Weight (g)	Dry Weight 63 µm (g)	Dry Weight 63-150 µm (g)	Dry Weight >150 µm (g)	Split
-5.488	40.934	2	3	3.5	Good	5.01	1.4	2.67	1.68	0.29	0.70	0.01171875
-5.488	40.934	6	7	3.5	Good	5.93	1.7	3.22	2.16	0.34	0.72	0.015625
-5.488	40.934	10	11	4.5	Moderate	5.69	1.3	3.08	1.89	0.39	0.80	0.0078125
-5.488	40.934	14	15	3.5	Moderate	5.21	1.5	2.83	1.87	0.25	0.71	0.0078125
-5.488	40.934	18	19	2.0	Uncertain	4.09	2.0	2.25	1.63	0.18	0.43	0.015625
-5.488	40.934	22	23	3.5	Good	5.34	1.5	2.87	2.22	0.20	0.45	0.0234375
-5.488	40.934	26	27	3.5	Good	5.41	1.6	2.98	2.00	0.23	0.76	0.01171875
-5.488	40.934	30	31	4.0	Good	5.10	1.3	2.78	2.01	0.21	0.57	0.015625
-5.488	40.934	34	35	3.6	Moderate	5.87	1.6	3.19	2.62	0.23	0.33	0.0234375
-5.488	40.934	38	39	3.5	Good	4.97	1.4	2.72	1.96	0.20	0.57	0.0078125
-5.488	40.934	42	43	4.0	Good	4.75	1.2	2.54	1.68	0.19	0.67	0.01171875
-5.488	40.934	46	47	3.6	Good	5.58	1.6	2.98	2.17	0.20	0.61	0.0078125
-5.488	40.934	50	51	5.5	Good	7.75	1.4	4.07	2.88	0.27	0.92	0.0078125
-5.488	40.934	54	55	2.4	Moderate	2.76	1.2	1.53	1.14	0.09	0.31	0.015625
-5.488	40.934	58	59	5.0	Good	7.33	1.5	3.91	2.80	0.26	0.85	0.0078125
-5.488	40.934	62	63	3.5	Good	4.87	1.4	2.66	1.81	0.14	0.71	0.0078125
-5.488	40.934	302	303	4.5	Moderate	5.87	1.3	3.11	2.13	0.26	0.73	0.01171875
-5.488	40.934	306	307	4.5	Good	6.55	1.5	3.41	2.55	0.23	0.62	0.01171875
-5.488	40.934	310	311	5.0	Good	5.48	1.1	2.82	1.95	0.21	0.66	0.015625
-5.488	40.934	314	315	5.3	Good	7.66	1.4	3.97	2.95	0.33	0.68	0.0078125
-5.488	40.934	318	319	7.5	Uncertain	10.38	1.4	5.35	3.70	0.51	1.14	0.00585938
-5.488	40.934	322	323	4.0	Good	5.16	1.3	2.65	2.01	0.20	0.43	0.015625
-5.488	40.934	326	327	5.0	Good	6.75	1.4	3.55	2.55	0.27	0.72	0.0078125
-5.488	40.934	330	331	5.3	Moderate	8.35	1.6	4.48	3.36	0.36	0.76	0.0078125
-5.488	40.934	334	335	4.1	Good	6.12	1.5	3.22	2.53	0.21	0.47	0.01171875
-5.488	40.934	338	339	4.0	Moderate	6.18	1.5	3.31	2.33	0.25	0.73	0.0078125
-5.488	40.934	342	343	4.3	Good	6.57	1.5	3.55	2.67	0.27	0.61	0.01171875
-5.488	40.934	346	347	4.3	Good	5.01	1.2	2.74	2.09	0.21	0.43	0.015625
-5.488	40.934	350	351	4.0	Good	5.85	1.5	3.08	2.26	0.27	0.54	0.0078125
-5.488	40.934	354	355	4.5	Good	5.95	1.3	3.08	2.06	0.31	0.71	0.0078125
-5.488	40.934	358	359	4.5	Good	6.23	1.4	3.24	2.24	0.33	0.67	0.0078125
-5.488	40.934	362	363	4.2	Good	6.14	1.5	3.30	2.35	0.24	0.71	0.0078125
-5.488	40.934	366	367	4.5	Moderate	6.61	1.5	3.53	2.43	0.33	0.77	0.0078125
-5.488	40.934	370	371	6.5	Moderate	7.06	1.1	3.95	2.88	0.28	0.79	0.0078125
-5.488	40.934	374	375	3.0	Moderate	4.57	1.5	2.56	1.71	0.23	0.62	0.0078125
-5.488	40.934	378	379	3.5	Good	4.53	1.3	2.55	1.67	0.25	0.63	0.0078125
-5.488	40.934	382	383	3.5	Good	5.07	1.5	2.86	1.99	0.28	0.60	0.0078125
-5.488	40.934	386	387	4.6	Good	7.16	1.6	4.08	2.78	0.35	0.95	0.0078125
-5.488	40.934	574	575	3.0	Good	5.16	1.7	3.01	2.11	0.26	0.64	0.0078125

Table 5 *(continued)*

-5.488	40.934	578	579	5.0	Good	7.71	1.5	4.44	3.25	0.34	0.85	0.0078125
-5.488	40.934	582	583	4.3	Good	6.09	1.4	3.45	2.68	0.24	0.54	0.01171875
-5.488	40.934	586	587	4.0	Good	5.98	1.5	3.24	2.53	0.18	0.53	0.015625
-5.488	40.934	590	591	3.9	Good	6.13	1.6	3.35	2.22	0.28	0.85	0.0078125
-5.488	40.934	594	595	4.0	Good	6.38	1.6	3.48	2.27	0.29	0.92	0.0078125
-5.488	40.934	598	599	4.5	Good	6.51	1.5	3.53	2.33	0.31	0.89	0.0078125
-5.488	40.934	602	603	4.0	Good	5.83	1.5	3.12	2.13	0.24	0.75	0.0078125
-5.488	40.934	606	607	4.0	Good	6.01	1.5	3.30	2.20	0.25	0.85	0.0078125
-5.488	40.934	610	611	4.3	Good	6.74	1.6	3.67	2.74	0.27	0.66	0.0078125
-5.488	40.934	614	615	3.5	Good	5.23	1.5	2.83	2.01	0.23	0.59	0.01171875
-5.488	40.934	618	619	3.5	Good	5.17	1.5	2.82	2.13	0.22	0.46	0.0078125
-5.488	40.934	622	623	4.0	Good	6.07	1.5	3.35	2.36	0.27	0.73	0.01171875
-5.488	40.934	626	627	4.5	Good	5.61	1.3	3.05	1.96	0.30	0.79	0.0078125
-5.488	40.934	630	631	4.5	Good	6.81	1.5	3.73	2.63	0.31	0.79	0.0078125
-5.488	40.934	634	635	3.5	Good	5.45	1.6	2.98	2.16	0.25	0.57	0.0078125
-5.488	40.934	638	639	4.5	Good	7.11	1.6	3.86	2.61	0.32	0.94	0.0078125
-5.488	40.934	642	643	4.5	Good	7.27	1.6	4.01	2.52	0.40	1.09	0.0078125
-5.488	40.934	646	647	4.5	Good	6.92	1.5	3.75	2.52	0.29	0.94	0.0078125
-5.488	40.934	650	651	3.5	Good	5.10	1.5	2.84	1.87	0.20	0.76	0.0078125
-5.488	40.934	654	655	3.5	Good	5.55	1.6	3.05	2.13	0.29	0.63	0.0078125
-5.488	40.934	658	659	3.5	Good	5.49	1.6	3.08	2.26	0.23	0.59	0.0078125

Table 6. GeoB12613-1 planktonic foraminifera count. Note that the table is subdivided into four parts due to size.

Depth Top (cm)	*G. glutinata*	*G. ruber* (white)	*G. elongatus*	*N. incompta*	*G. bulloides*	*G. menardii*	*N. dutertrei*	*G. falconensis*	*G. adamsi*	*G. calida*	*G. siphonifera*	*G. sacculifer*	*G. trilobus*	*G. ruber* (pink)	*G. conglobatus*	*G. tenella*	*G. rubescens*
2	79	120	40	11	35	5	23	6	0	19	19	16	33	0	16	3	12
6	34	128	29	8	27	8	13	7	0	11	40	12	49	0	15	5	10
10	43	83	14	15	25	9	18	4	3	8	18	9	18	0	10	1	7
14	60	94	11	4	21	5	8	15	0	20	20	7	29	0	6	2	5
18	65	84	11	7	30	11	35	7	0	21	17	10	35	0	8	2	4
22	98	106	8	6	69	16	17	16	0	23	36	15	18	0	5	2	13
26	67	104	21	19	36	23	43	17	0	37	35	12	35	0	2	4	7
30	92	68	29	24	36	30	25	16	0	26	11	4	17	0	2	5	5
34	107	94	22	38	32	11	15	21	0	30	12	3	13	0	3	12	12
38	79	130	16	71	32	20	39	14	0	7	9	4	10	0	3	0	9
42	63	65	24	65	29	27	25	8	0	0	9	3	9	0	4	3	8
46	44	86	14	79	19	22	9	9	0	0	12	2	3	0	2	1	8
50	52	55	16	62	27	19	14	10	0	3	5	2	6	0	1	0	7
54	74	71	29	58	27	16	26	5	0	21	11	2	8	0	4	2	14
58	92	97	19	109	62	28	35	12	0	13	12	3	8	0	3	6	10
62	41	57	15	39	26	31	26	1	0	10	7	3	10	0	1	0	6
302	82	67	19	26	22	37	47	3	0	5	14	10	31	0	8	2	3
306	101	74	25	11	31	63	53	2	0	11	9	10	22	1	4	4	3
310	71	54	18	10	24	46	44	1	0	9	14	5	31	0	4	4	3
314	62	92	13	6	25	33	26	5	0	35	16	6	36	0	5	4	3
318	79	83	15	13	31	27	27	1	0	26	21	11	43	2	8	7	9
322	82	85	11	13	25	17	8	5	0	29	12	4	26	1	7	18	12
326	49	64	17	9	23	26	20	7	0	20	13	6	27	1	12	13	5
330	83	83	9	26	13	17	13	10	0	31	15	11	34	7	12	12	10
334	68	80	18	11	33	20	24	20	0	23	18	14	29	4	17	6	6
338	66	53	23	15	35	20	14	17	0	21	10	9	14	7	6	10	3
342	73	69	36	40	27	33	16	24	0	19	6	3	19	15	2	14	5
346	69	61	14	50	41	36	28	24	0	8	15	7	23	12	9	5	3
350	84	40	20	52	23	23	24	7	0	15	3	4	10	13	2	5	9
354	95	45	12	65	26	22	11	15	0	7	6	2	12	4	1	4	10
358	100	55	5	81	43	20	19	6	0	7	6	3	12	10	0	3	8
362	65	64	5	65	50	28	26	8	0	10	10	5	10	10	6	6	6
366	65	60	4	41	21	33	12	14	0	17	9	2	9	4	3	4	3
370	89	87	13	56	37	43	29	17	0	13	3	4	18	11	8	4	9
374	52	47	7	44	24	22	14	9	0	13	8	4	15	15	3	2	4
378	65	54	10	60	24	22	12	15	0	12	4	1	3	10	2	7	6
382	83	60	7	62	24	37	20	28	0	16	10	4	15	6	5	3	7
386	70	85	8	64	26	36	20	14	0	12	7	8	14	11	3	4	9
574	45	59	15	39	24	19	21	9	0	0	4	2	10	15	3	3	2
578	68	57	8	70	30	39	13	5	0	11	2	7	12	14	5	5	14
582	70	79	15	96	29	45	8	8	0	2	2	8	12	9	4	3	9
586	59	38	9	91	20	32	32	1	0	15	5	2	11	11	9	3	2

Table 6 *(continued)*

Depth Top (cm)	*G. glutinata*	*G. ruber* (white)	*G. elongatus*	*N. incompta*	*G. bulloides*	*G. menardii*	*N. dutertrei*	*G. falconensis*	*G. adamsi*	*G. calida*	*G. siphonifera*	*G. sacculifer*	*G. trilobus*	*G. ruber* (pink)	*G. conglobatus*	*G. tenella*	*G. rubescens*
590	73	69	25	69	20	39	28	6	0	6	1	10	18	22	3	5	5
594	74	74	28	63	20	44	16	9	0	13	9	12	30	31	6	4	10
598	136	141	12	44	39	41	32	13	0	19	8	13	42	35	10	6	16
602	61	62	12	38	20	38	19	16	0	17	14	9	43	19	16	9	6
606	103	75	12	22	35	36	18	23	0	22	17	11	37	23	10	4	13
610	78	74	21	40	19	29	13	31	0	26	13	10	32	25	8	6	8
614	75	49	17	37	38	40	19	34	0	17	12	10	28	16	8	3	3
618	160	86	10	93	22	17	18	39	0	12	0	2	21	16	2	6	15
622	80	52	11	44	23	30	27	12	0	12	10	9	15	15	3	2	14
626	75	44	23	104	14	24	12	7	0	8	5	7	18	18	6	6	25
630	105	65	19	96	27	24	22	11	0	24	4	2	14	21	1	4	26
634	77	41	21	101	59	8	30	8	0	6	1	1	8	19	8	7	18
638	83	44	6	122	24	28	31	10	0	17	9	2	11	21	7	6	22
642	64	42	14	97	10	34	31	5	0	2	4	6	11	6	5	0	14
646	127	61	14	132	35	22	29	4	0	17	5	6	18	17	8	4	25
650	70	39	14	72	40	22	31	18	0	5	3	2	10	7	4	4	11
654	143	68	17	103	20	8	14	8	0	4	1	4	13	17	2	0	27
658	62	43	16	61	23	22	25	12	0	1	5	3	15	9	7	2	12

Table 6 *(continued)*

Depth Top (cm)	*O. universa*	*S. dehiscens*	*T. quinqueloba*	*T. clarkei*	*T. humilis*	*B. digitata*	*G. inflata*	*G. truncatulinoides*	*G. crassaformis*	*G. hirsuta*	*G. scitula*	*G. theyeri*	*G. tumida*	*G. ungulata*	*D. anfracta*	*P. obliquiloculata*	*G. conglomerata*	*G. hexagonus*	*C. nitida*	*T. parkerae*
2	5	0	0	0	0	0	0	0	0	0	0	1	3	2	0	25	1	5	0	0
6	1	1	0	0	1	1	0	0	0	0	1	0	9	1	0	34	1	6	2	0
10	3	1	0	0	1	1	0	0	0	0	0	0	4	3	0	24	1	10	0	0
14	3	2	0	0	1	1	0	0	0	0	1	5	1	4	0	11	0	1	0	0
18	1	0	0	0	2	2	0	0	2	0	1	2	2	5	0	14	0	8	0	0
22	4	0	0	0	1	3	0	0	0	0	3	2	5	18	0	12	1	1	0	0
26	3	0	0	0	0	1	0	0	0	0	6	5	6	22	0	29	0	6	0	0
30	0	0	0	0	1	0	0	0	2	0	1	2	4	25	0	23	0	6	0	0
34	2	0	0	0	2	0	0	1	1	0	4	1	4	13	0	18	0	2	0	0
38	5	0	0	0	2	1	0	0	5	0	0	5	6	7	0	23	0	1	0	0
42	1	0	0	0	0	1	0	0	13	0	4	0	7	8	0	16	0	1	0	0
46	0	0	0	0	2	1	0	0	4	0	2	2	7	10	0	15	0	1	0	0
50	2	0	0	0	2	0	0	0	9	0	3	1	5	11	0	17	0	1	0	0
54	4	0	0	0	3	0	0	3	3	0	0	1	4	17	0	12	0	1	0	0
58	4	0	0	0	1	0	0	5	10	0	0	6	2	13	1	14	1	4	0	0
62	3	0	0	0	0	0	0	7	1	0	3	3	8	11	1	13	0	0	0	0
302	1	0	0	0	0	1	0	5	10	0	1	3	4	9	0	20	2	4	0	0
306	0	0	0	0	1	0	0	0	4	0	1	11	3	12	0	14	3	0	0	0
310	3	0	0	0	0	0	0	7	11	0	0	4	3	6	0	13	2	0	0	0
314	2	0	0	0	2	2	0	2	4	0	0	2	3	14	0	14	5	4	0	3
318	11	1	0	0	0	0	0	0	4	0	0	4	6	12	0	12	2	1	0	0
322	5	0	0	0	2	1	0	3	0	0	0	2	1	22	1	6	2	2	0	0
326	1	0	0	0	1	0	0	6	0	0	0	1	5	12	0	13	1	4	0	3
330	6	0	0	0	0	1	0	0	3	0	0	0	1	16	0	10	5	4	0	0
334	4	0	0	0	0	3	0	1	2	0	0	1	0	11	1	14	0	1	1	0
338	3	1	0	0	0	4	0	0	1	0	0	4	0	14	5	7	2	3	0	0
342	2	0	0	0	0	1	0	9	0	0	0	6	2	21	0	14	1	1	0	6
346	1	0	0	0	0	2	0	7	11	0	0	1	0	21	0	11	0	2	6	0
350	1	0	0	0	1	0	0	4	4	0	0	3	4	13	0	2	0	1	0	0
354	2	0	0	0	1	0	0	5	5	0	0	4	2	10	1	7	0	2	0	0
358	0	0	0	0	0	1	0	5	2	0	2	1	2	9	4	9	0	2	0	0
362	1	0	0	0	0	0	0	5	6	0	2	0	5	9	0	11	0	2	0	1
366	1	0	0	0	2	0	0	2	6	0	0	1	2	11	1	8	0	2	0	0
370	3	0	0	0	0	1	0	7	9	0	2	6	1	19	1	14	0	1	0	2
374	2	0	0	0	0	0	0	6	9	0	0	1	0	17	0	5	0	0	0	1
378	2	0	0	0	1	1	0	4	4	0	0	3	2	13	1	7	0	2	0	0
382	3	0	0	0	0	0	0	3	8	0	1	1	0	29	1	7	0	5	0	1
386	7	0	0	0	0	1	0	6	6	0	1	5	0	33	2	8	0	7	0	1
574	1	0	0	0	0	0	0	8	9	0	0	2	5	14	1	9	0	2	0	0
578	1	0	0	0	0	0	0	3	7	0	1	2	6	23	1	2	0	2	0	0
582	0	0	0	1	0	0	0	2	5	0	0	5	15	15	0	5	0	7	0	0
586	5	0	0	0	0	0	0	9	8	0	1	5	12	8	0	3	0	5	0	0
590	1	0	0	0	0	0	0	1	10	0	0	0	9	12	0	10	0	1	0	0

Table 6 *(continued)*

Depth Top (cm)	*O. universa*	*S. dehiscens*	*T. quinqueloba*	*T. clarkei*	*T. humilis*	*B. digitata*	*G. inflata*	*G. truncatulinoides*	*G. crassaformis*	*G. hirsuta*	*G. scitula*	*G. theyeri*	*G. tumida*	*G. ungulata*	*D. anfracta*	*P. obliquiloculata*	*G. conglomerata*	*G. hexagonus*	*C. nitida*	*T. parkerae*
594	2	0	0	0	2	1	0	4	4	0	0	3	4	23	0	11	4	3	0	0
598	4	0	0	0	2	2	0	3	4	0	0	7	6	30	0	15	1	2	1	0
602	6	0	0	0	0	0	0	7	2	0	0	1	5	22	0	13	0	4	0	0
606	3	0	0	0	1	2	0	3	4	0	0	3	5	34	0	12	1	3	0	0
610	3	0	0	0	0	0	0	2	7	0	4	0	4	15	0	14	0	2	0	0
614	1	0	3	0	0	0	0	1	4	0	0	5	5	22	0	14	3	1	0	1
618	2	0	0	0	0	0	0	1	6	0	1	1	4	14	0	10	0	0	0	1
622	2	0	0	0	0	0	0	6	9	0	0	1	4	16	0	6	0	2	0	3
626	1	0	0	0	0	0	0	1	4	0	0	4	4	15	0	12	0	2	0	0
630	2	0	0	0	0	0	0	0	11	0	2	8	1	11	0	8	2	3	0	0
634	1	0	0	0	0	0	0	4	2	0	2	3	3	14	1	3	0	0	0	1
638	0	0	0	0	0	0	0	3	12	0	1	0	4	18	0	16	0	0	0	0
642	3	0	0	0	1	0	0	5	5	0	1	0	39	8	0	5	3	0	0	0
646	4	0	0	0	0	0	0	3	8	0	1	1	10	17	0	15	0	0	0	0
650	0	0	0	0	0	1	0	2	7	0	0	0	9	5	1	6	0	1	0	0
654	0	0	0	0	0	1	0	4	5	0	0	2	5	15	1	7	0	1	0	0
658	2	0	1	0	0	0	0	0	9	0	1	0	12	7	1	6	1	1	0	1

Table 7. *Globigerinoides ruber* (white) $\delta^{18}O$ record of GeoB12613-1 after Tangunan et al. (2017).

Age (ka)	*G. ruber* (white) $\delta^{18}O$ (‰ VPDB)	Age (ka)	*G. ruber* (white) $\delta^{18}O$ (‰ VPDB)
3.1	-1.88	137.6	-0.54
5.2	-1.97	139.2	-0.50
7.3	-1.86	140.7	-0.70
9.3	-1.76	142.3	-0.60
10.9	-1.27	143.9	-0.65
12.1	-1.70	145.5	-0.51
13.3	-1.53	147.0	-0.59
14.5	-1.79	148.6	-0.52
15.7	-0.62	227.8	-0.72
16.9	-0.43	229.7	-0.78
18.0	-0.49	231.6	-0.87
19.2	-0.56	233.4	-1.07
21.0	-0.18	235.3	-1.31
22.7	-0.33	237.2	-1.30
24.5	-0.50	239.1	-1.46
26.2	-0.46	241.0	-1.67
120.4	-1.58	242.2	-1.09
123.0	-1.40	243.3	-1.40
124.1	-1.88	244.5	-0.66
125.2	-2.03	245.7	-1.05
126.3	-2.23	246.8	-0.71
127.3	-2.26	248.0	-0.68
128.4	-1.85	249.6	-0.59
129.5	-1.61	251.3	-0.48
130.6	-1.31	252.9	-0.62
131.7	-0.99	254.5	-0.69
132.8	-0.99	256.1	-0.73
133.8	-0.51	257.8	-0.84
134.9	-0.28	259.4	-0.88
136.0	-0.43	261.0	-0.73

Table 8. Estimated primary productivity after Tangunan et al. (2017).

Age (ka)	EPP (g C/m^2/yr)	Age (ka)	EPP (g C/m^2/yr)
3.1	135.04	142.8	141.48
5.2	110.19	144.4	135.93
7.3	124.06	145.9	136.15
9.3	104.37	147.5	141.08
10.9	100.65	149.1	120.72
12.1	109.56	150.6	135.28
13.3	124.46	225.2	166.24
14.5	148.49	226.8	190.09
16.3	151.57	228.5	191.41
18.0	126.14	230.1	197.72
18.6	122.23	231.7	203.93
19.2	130.86	233.4	196.43
21.0	131.90	235.0	193.56
22.7	129.76	236.6	169.66
24.5	132.33	238.3	142.73
26.2	119.43	239.9	153.16
28.0	139.04	241.5	151.35
28.9	126.38	243.2	142.29
29.9	125.47	244.8	154.09
30.8	90.94	246.5	160.51
120.1	120.51	248.1	193.34
122.0	158.56	249.7	194.42
123.9	145.81	251.4	181.04
125.7	123.01	252.0	210.58
127.6	170.86	253.6	199.24
129.4	194.96	255.3	199.13
131.3	156.94	256.9	192.40
133.1	142.22	258.5	208.35
135.0	160.13	260.2	231.55
136.6	145.69	261.8	239.39
138.1	145.19	263.5	200.70
139.7	149.34	265.1	209.09
141.3	137.09	-	-

Additional plots and figures

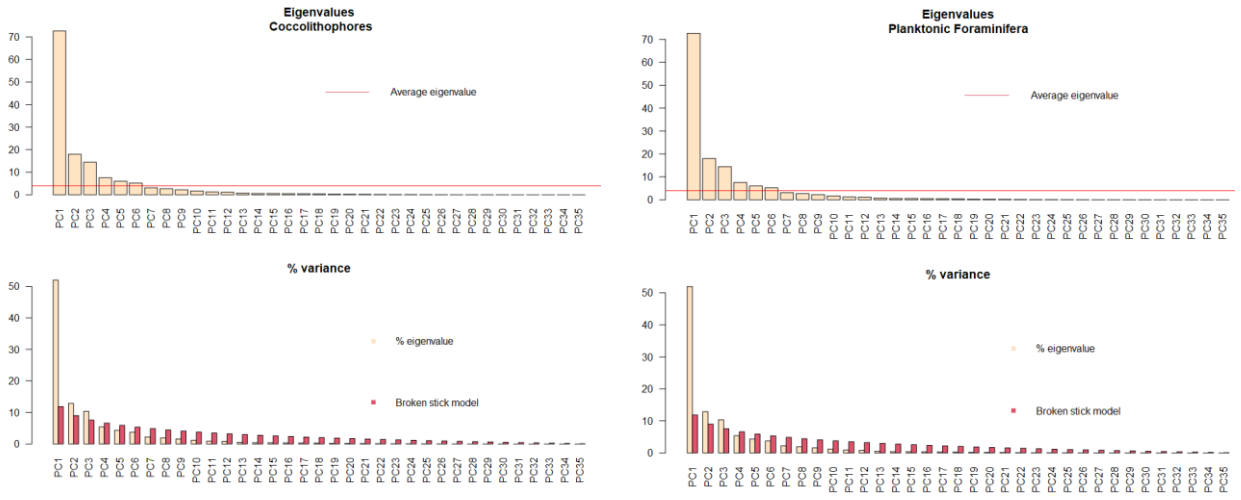

Fig. 25: Kaiser-Guttman criterion and Broken stick model for principal components analysis. Left figure: coccolithophores; right figure: planktonic foraminifera. Both analysis were computed in *R* (R Core Team 2021) utilising code after (Borcard et al. 2011a).

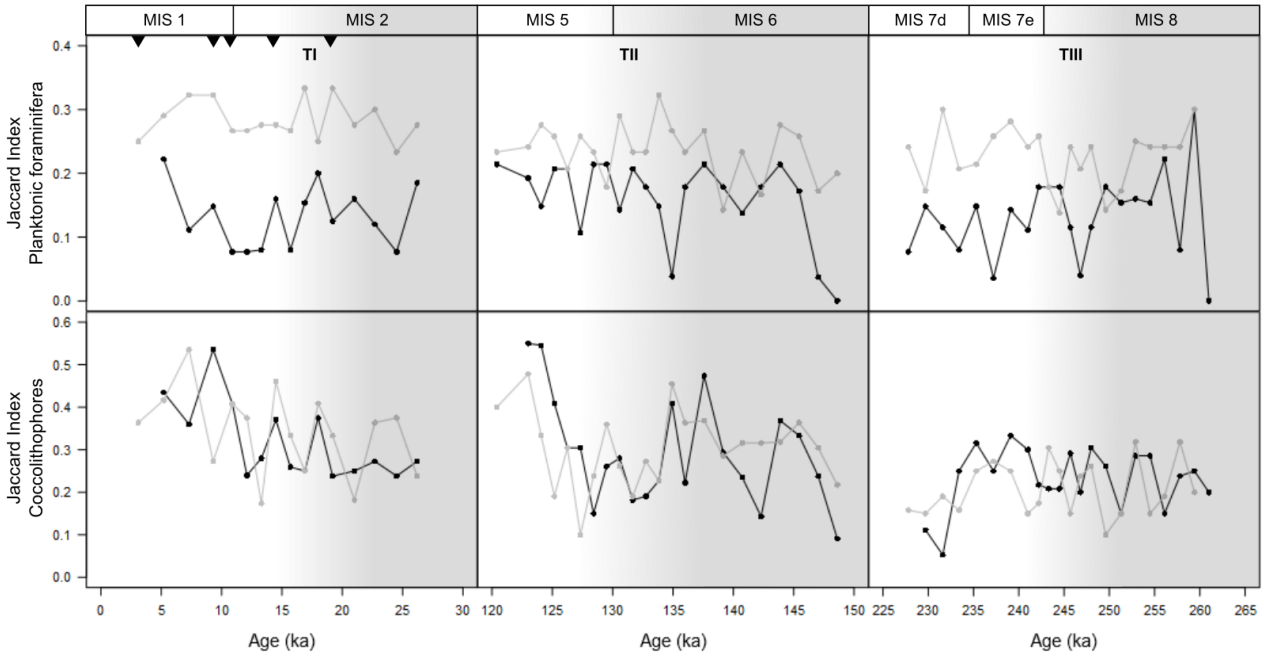

Fig. 26: Jaccard Index of planktonic foraminifera and coccolithophores. Black solid line represents sequential dissimilarity (J_{seq}) on millennial timescale and grey solid line represents individual sample versus oldest sample dissimilarity (J_{multi}) on multi-millennial timescale covering multiple glacial – interglacial cycles.

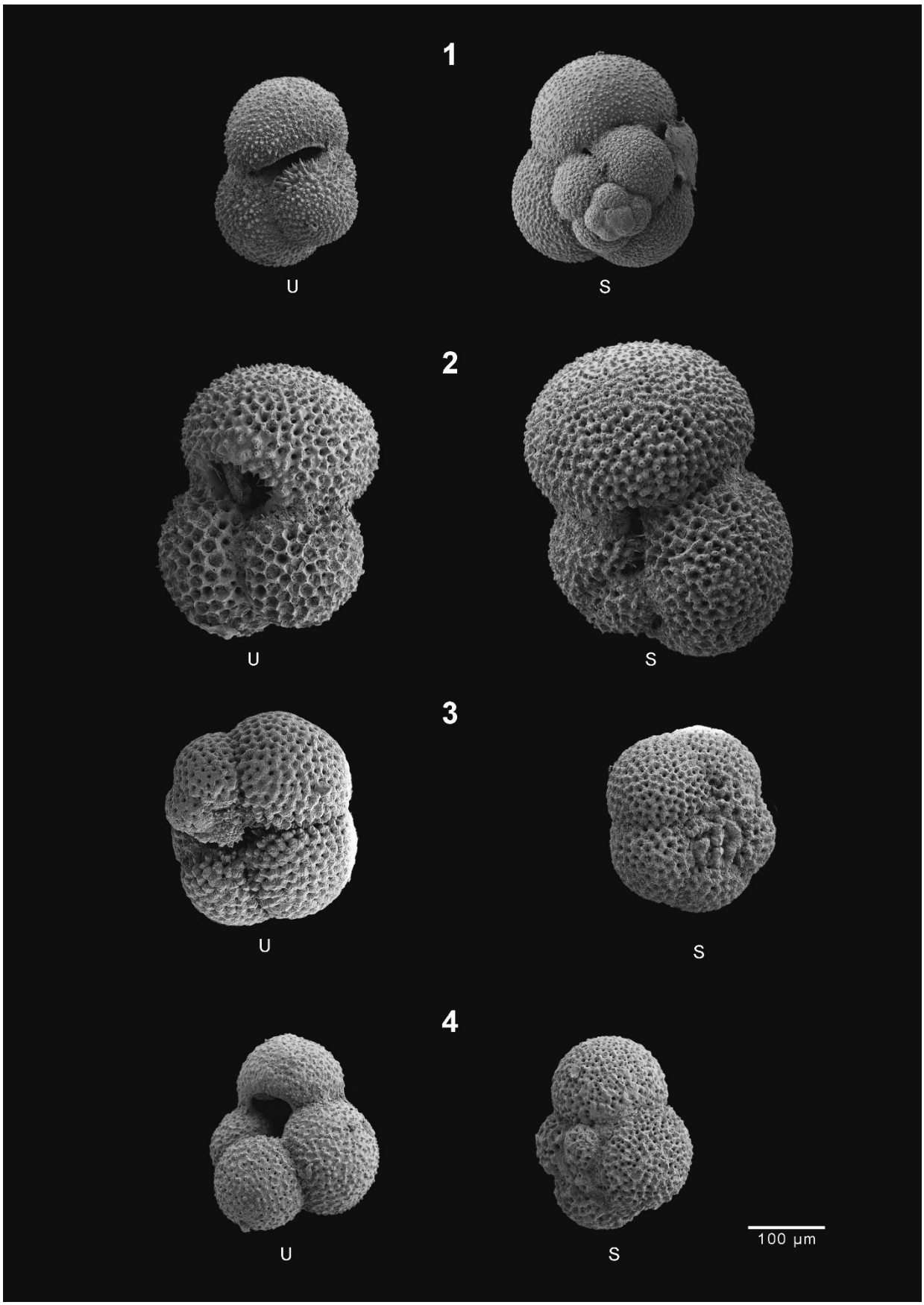

Plate V. Scanning Electron Microscope photographs of the most common planktonic foraminifera species found in the analysed core section. U = ventral view, S = dorsal view: 1) *Globigerinita glutinata*, 2) *Globigerinoides ruber* (white), 3) *Neogloboquadrina incompta*, 4) *Globigerina bulloides*.

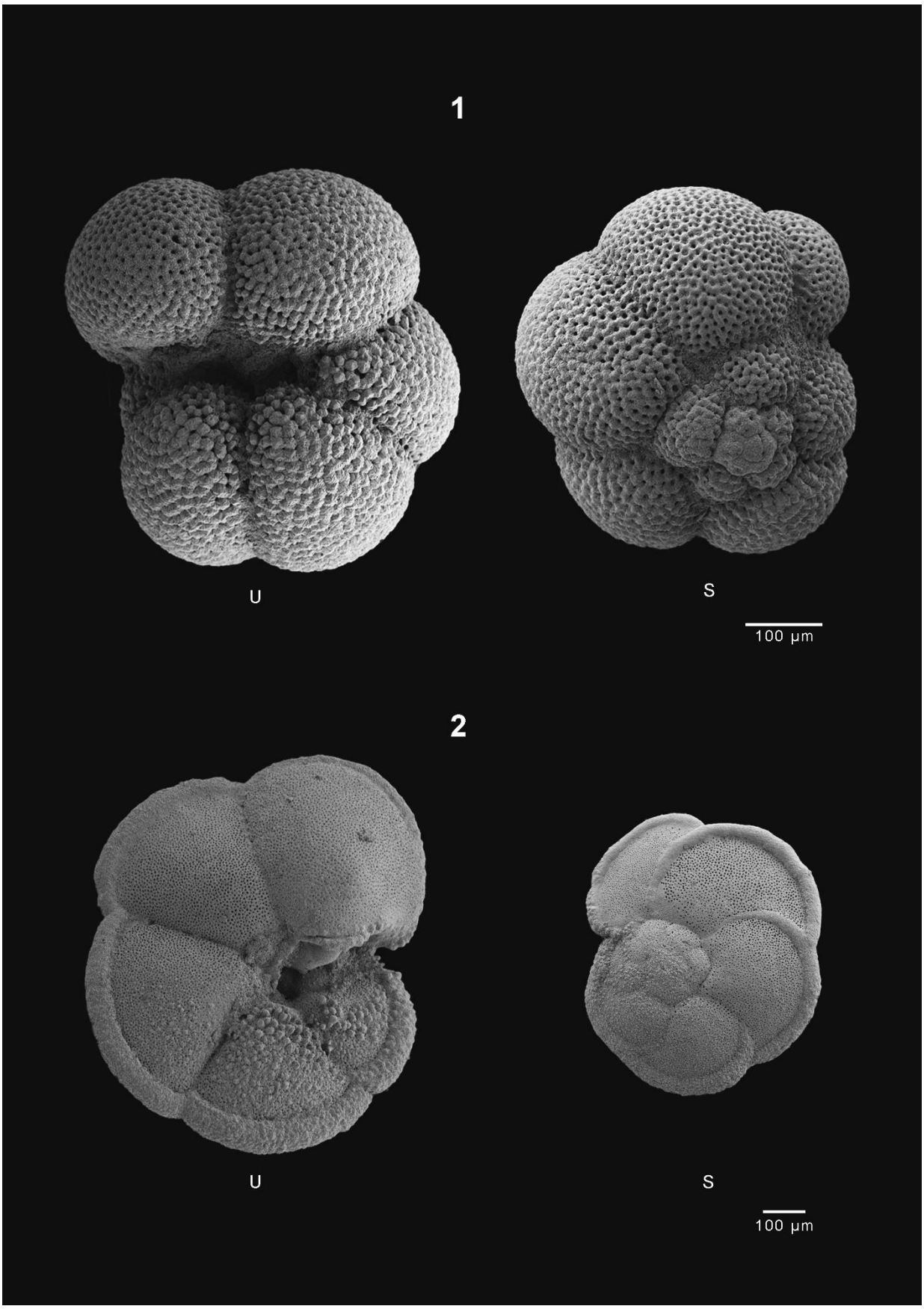

Plate VI. Scanning Electron Microscope photographs of the most common planktonic foraminifera species found in the analysed core section. U = ventral view, S = dorsal view: 1) *Neogloboquadrina dutertrei*, 2) *Globorotalia menardii*.